R005-01
Zoom meeting C ：11/1　AM1　(9:00-10:30)
09:00-09:15

# Estimation of cloud base altitude using cloud images captured by all-sky imagers

#Atsuya Nemoto[1)], Hiroyo Ohya[2)], Hiroyuki Nakata[3)], Toshiaki Takano[4)], Alessandro Damiani[5)], Tamio Takamura[5)]
[1)]Science and Engineering, Chiba University,[2)]Engineering, Chiba Univ.,[3)]Grad. School of Eng., Chiba Univ.,[4)]Chiba Univ.,[5)]CEReS Chiba Univ.

Clouds can significantly affect the Earth's radiation budget and water cycle by changing its various properties. In addition to cloud microphysical properties, cloud bottom height, which is one of the macrophysical structures of clouds, has a particularly important meaning for infrared radiation on the surface of the Earth. Cloud base height is also extremely important in air safety, airborne military operations and surveillance [Vislocky and Fritsch, 1997]. Thus, an accurate method of estimating the cloud base altitude may provide a better understanding of the effects of clouds on the Earth's radiative balance, and may provide useful information for improving aviation safety. The following ground-based instruments can be used to accurately estimate cloud base heights. Radar and lidar can be used to obtain relatively accurate cloud-bottom heights locally [Takano and Takamura, 2014]. However, they cannot provide the cloud base height information in wide area. The advantage of satellites is that high-resolution, two-dimensional distributions of the microphysical and macrophysical properties of clouds may be retrieved on a global scale [Huang et al., 2006].However, the acquisition of cloud-bottom heights is quite complex and cannot be obtained directly from satellite observations. Wilheit and Hutchison [2000] also proposed a method to retrieve the cloud base height by combining passive microwave brightness temperature and infrared cloud top temperature. However, these methods are mainly useful for special cloud types (e.g., relatively thin clouds, stratocumulus clouds, convection clouds, etc.). In this study, we propose an estimation method of the cloud base height using a pair of cloud images observed by all-sky imagers at two sites. The advantage of all-sky imagers is to be cheaper than radars and lidars. The two all-sky imagers were installed on the roofs of Engineering Research Building 1 (35.6246N, 140.1037E) and 2 (35.6266N, 140.1040E) in Nishi-Chiba campus in Chiba University, Japan. The distance between the two all-sky imagers is 216 m. The all-sky imagers have equisolid angle projection method. The estimation method of the cloud base height is described below. When the cloud base height is assumed in the range of 500-2500 m with step of 50 m, the two cloud images are projected to each map. Then we calculate cross-correlation between the two maps. The cloud base height is determined when the cross-correlation coefficients are at their maximum in all cases.　In a recent case study, the cloud base heights were estimated to be 1850 m at 11:45:13 LT on 16 March, 2020. The cloud base height was observed to be 1860 m by a lidar installed by the National Institute for Environmental Studies (NIES) in the same campus in Chiba University at 11:00 LT. The difference of cloud base height between our method and lidar was 10 m. We verified the accuracy of the cloud base height estimation by simulation. When cloud base heights of pseudo-cloud were set to be 1000 m and 2000 m, the estimated heights were higher by 100-250 m than the true one. In the session, we will show the results of verification of the accuracy of the estimation method in details.

R005-02
Zoom meeting C ：11/1　AM1　(9:00-10:30)
09:15-09:30

# レーダーインバージョン法を用いた乱流強度推定法の開発

#田村　亮祐[1)],西村　耕司[2)],橋口　浩之[1)]
[1)]京都大学生存圏研究所,[2)]国立極地研究所

# Development of measurement technique for atmospheric turbulence using radar inversion

#Ryosuke Tamura[1)], Koji Nishimura[2)], Hiroyuki Hashiguchi[1)]
[1)]Research Institute for Sustainable Humanosphere,[2)]National Institute of Polar Research

Atmospheric radar can observe the height profiles of wind velocities from the turbulent scattering of radio wave. In theory, it can also estimate turbulent intensity from the Doppler spectral width of the atmospheric radar. In order to estimate the turbulent broadening $s_{turb}$ from the observed spectral width $s_{obs}$, it is necessary to consider other broadening effects: beam ($s_{beam}$), shear ($s_{shear}$), and time ($s_{time}$) broadenings [1]. Namely, $s^2_{turb} = s^2_{obs} - (s^2_{beam} + s^2_{shear} + s^2_{time})$. However, $s^2_{turb}$ sometimes becomes negative due to the over-estimation of beam broadening. The estimation error of beam broadening is caused by the assumption that the beam pattern is rotationally symmetric and has low sidelobes. Especially, for the radar which has an asymmetric beam pattern such as the PANSY radar at Syowa Station in Antarctica, debroadening is considered remarkably difficult.
Recently, a new radar observation theory which has a potential to be able to estimate the accurate beam broadening was proposed by Nishimura et al. [2]. In this theory, if we assume that the time functions of turbulent vortex which scatter the radio wave are uncorrelated between the any different points in the observation volume and its power spectral expectation is equal, then, the correlation function (CF) of the received signal (R) is equal to the multiplication of its scattering function (F) determined by the turbulent
strength, two way beam pattern function (G) determined by the wind velocity, and window function (W) determined by sampling temporal lag [2]. That is R = FGW. It implies that when turbulent strength and wind velocity are unknown, we can theoretically estimate these parameters by solving the inverse problem.
In this study, we use the MU radar of RISH, Kyoto University to apply this new theory to real radar data analysis. As a first step, we use wind velocity obtained from Doppler Beam Swinging (DBS) method and estimate the turbulent broadening. In this case, it is relatively easy to solve inverse problem because the unknown parameter is just the turbulent strength. In practice, to avoid the affections from the noise and clutters, we estimate the parameter from the Fourier transform of CFs and optimization is conducted by the least squares method (see figure).
As the next step, we try to develop the debroadening algorithm which deals with the estimation of wind velocity and turbulent strength. It is expected to be able to analyse more precise wind velocity compared with conventional methods like DBS or Spaced Antenna (SA) method and turbulent strength.
The new way of observation algorithm can be applied not only to an atmospheric radar but also to a Doppler weather radar having the interferometer function and has a possibility to estimate the cross-radial velocities.
[1] W. K. Hocking, Measurement of turbulent energy dissipation rates in the middle atmosphere by radar techniques: A review, in Radio Science, vol. 20, no. 6, pp. 1403-1422, doi:10.1029/RS020i006p01403, 1985.
[2] K. Nishimura, M. Kohma, K. Sato and T. Sato, Spectral Observation Theory and Beam Debroadening Algorithm for Atmospheric Radar, in IEEE Transactions on Geoscience and Remote Sensing, doi: 10.1109/TGRS.2020.2970200, 2020.

大気レーダーは、放射された電波が大気乱流により散乱され、その微弱な散乱波を受信することで上空の三次元風速プロファイルを観測できるリモートセンシング技術である。原理的には、スペクトル幅から乱流強度も推定可能である。受信波のスペクトル幅( $\sigma_{obs}$) から乱流ブロードニング ( $\sigma_{turb}$) を推定するには、シアー ( $\sigma_{shear}$)、時間変動 ( $\sigma_{time}$)、ビームが有限であることに起因する平均風速成分の影響 ( $\sigma_{beam}$)(ビームブロードニング)を正確に差し引くデブロードニングを行う必要がある [1] 。すなわち、
$\sigma^2_{turb} = \sigma^2_{obs} - (\sigma^2_{beam} + \sigma^2_{shear} + \sigma^2_{time})$ 。従来手法では、ビームが回転対称でサイドローブがないという近似に基づいてデブロードニングが行われており、$\sigma^2_{beam}$ の過大評価により、$\sigma^2_{turb}$ が負になるなど、精度の問題が指摘されてきた。また、回転対称のビームパターンを持たない昭和基地の PANSY レーダーなどでは上記手法の適用が困難であった。
この問題に対し、レーダー観測理論の再検討により、乱流ブロードニングの正確な推定が可能となった [2] 。この理論によれば、観測を行う三次元空間内の異なる任意の二点間で乱流散乱効果を表す時間関数が無相関かつその二乗期待値が等しいと仮定することで、受信波の相関関数（R）が、平均風速の情報を加味した電波の伝搬パターンの相関関数（G）、乱流による電波の散乱効果を表す相関関数（F）、そしてサンプリング窓関数の相関関数（W）の積に等しいという関係式 R = FGW をえる。乱流強度は散乱効果を表す相関関数に、平均風速は電波の伝搬パターンを表す相関関数にそれぞれパラメータとして情報が含まれているので、逆問題を解くことでこれらの未知のパラメータの推定が原理的に可能である。
本研究では、京都大学生存圏研究所の MU レーダーを用いた実証を行う。初めに、平均風速はドップラービーム走査法による観測結果を用い、乱流ブロードニングのパラメータ推定を行う。この場合、平均風速が未知パラメータに

含まれないため比較的容易に逆問題を解くことができる。逆問題を解く際には、クラッターやノイズから受ける影響を検討しやすいため、相関関数を周波数空間にフーリエ変換し非線形最小二乗法により最適な乱流強度パラメータの推定を実行する。（ 図参照 ）
その後、未知パラメータに平均風速も加えた逆問題を解く手法の確立を目指す。逆問題を解く際、ドップラービーム走査法または空間アンテナ法による平均風速の結果をパラメータ初期値とすることを検討しており、結果的に従来の手法と比べ更に高精度な平均風速推定と乱流強度推定の両立を目指す。
本研究における観測手法は大気レーダーのみならず、ドップラー気象レーダーへの適用も検討している。干渉計機能を追加することでドップラー速度のクロスラジアル成分の推定が可能となり、従来さまざまな困難が指摘されてきた単一の気象レーダーによる三次元風速分布観測の実現が期待される。
[1] W. K. Hocking, Measurement of turbulent energy dissipation rates in the middle atmosphere by radar techniques: A review, in Radio Science, vol. 20, no. 6, pp. 1403-1422, doi:10.1029/RS020i006p01403, 1985.
[2] K. Nishimura, M. Kohma, K. Sato and T. Sato, Spectral Observation Theory and Beam Debroadening Algorithm for Atmospheric Radar, in IEEE Transactions on Geoscience and Remote Sensing, doi: 10.1109/TGRS.2020.2970200, 2020.

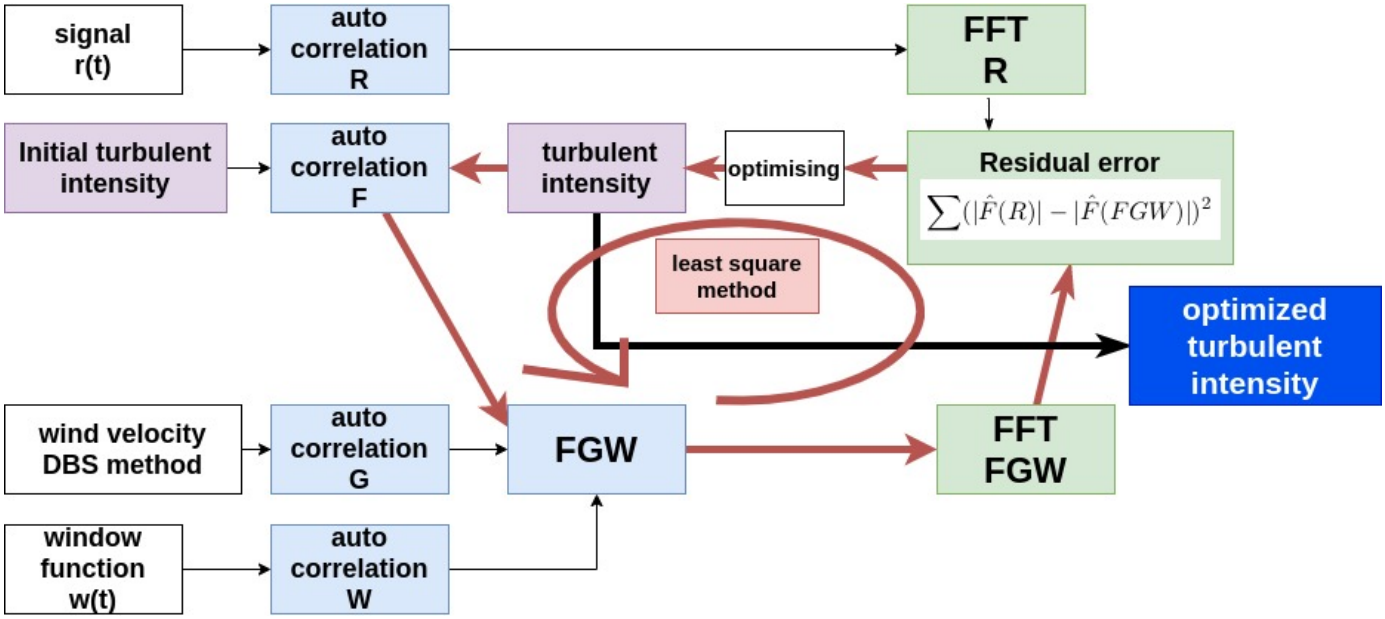

R005-03
Zoom meeting C ：11/1 AM1 (9:00-10:30)
09:30-09:45

# Estimation of location and charge amount of lightning discharges using electrostatic field observation network in Metro Manila

#Masafumi Kanno[1)], Yukihiro Takahashi[2)], Hiroyo Ohya[3)], Hiroyuki Nakata[4)], Mitsuteru SATO[5)], Purwadi Purwadi[5)], Hisayuki Kubota[6)]
[1)]Science and Engineering, Chiba Univ.,[2)]Cosmosciences, Hokkaido Univ.,[3)]Engineering, Chiba Univ.,[4)]Grad. School of Eng., Chiba Univ.,[5)]Hokkaido Univ.,[6)]Faculty of Science, Hokkaido Univ.

There are many studies on the relationship between cloud convection activity and the occurrence number of the lightning discharges. Changes in the occurrence number of lightning discharges preceded those in precipitations by approximately 5 min.[Piepgrass et al., 1982]. Variations in the occurrence number of lightning discharges preceded those in maximum wind speed of hurricanes topically by one or two days [Price et al., 2009]. Thus, it is expected that there is a relationship between cloud convection activity and the charge structure in clouds [Sakai, 2014], although that has not been investigated in detail. Based on the network of vertical electrostatic field observations, the charge structure in the cloud can be estimated. Charges of -10 to -40 C were neutralized by cloud-to-ground (CG) discharges at the altitude of 6.0-9.5 km [Jacobson and Krider, 1976]. However, it is difficult to construct a large-scale observation network with field mill senors because of the cost. The alternative instrument is plate-type capacitive antenna [Blitzer, 2013]. However, the amount of charge could not be estimated with such antenna due to the problem of calibration. In this study, we carried out a model calculation in order to estimate the horizontal location, height, and amount of neutralized charge caused by the CG and intracloud discharges using the electrostatic field observation system P-POTEKA installed in Metro Manila, Philippines under SATREPS/ULAT (Understanding Lightning and Thunderstorm) project. The P-POTEKA consists of a plate-type capacitive antenna installed at 35 sites in Metro Manila with an interval of about 5 km. The result of the model calculation suggested that the amount of neutralized charge and position of lightning can be estimated by correcting the relative sensitivities of the antenna from the changes in the electrostatic field of the CG discharges if the relative sensitivity for each observation site is within ±50 %. In this presentation, we will explain our method to estimate the charge amount and position of lightning discharges and show the results of estimation using observation data in detail.

R005-04
Zoom meeting C ：11/1　AM1　(9:00-10:30)
09:45-10:00

## 北西太平洋における熱帯低気圧の強度発達と雷放電の電気的物理量の関係性

#丹羽　俊輔[1)],佐藤　光輝[1)],久保田　尚之[1)],高橋　幸弘[1)]
[1)]北大・理・宇宙

## Estimation of the Relation of Electrical Properties of Lightning with Intensity of Tropical Cyclones in Western North Pacific

#Shunsuke Niwa[1)], Mitsuteru SATO[1)], Hisayuki Kubota[1)], Yukihiro Takahashi[1)]
[1)]Cosmosciences, Hokkaido Univ.

Prediction of the Tropical Cyclone (TC) intensity such as maximum sustained wind and minimum sea surface pressure is an important issue for a long time. Previous studies suggested that lightning activity in TCs has a possibility to improve the accuracy of intensity prediction. Although relationships between lightning frequency and TC intensity have been investigated in the previous studies, relationships of electrical properties(EPs) of lightning with TC intensity have not been studied. In this study, we investigated the relationships of EPs of lightning (peak current, charge moment change (CMC) and charge amount) with five TCs (LEEPI, category1; UTOR, category5; MAN-YI, category3, Large; WIPHA, category4, Large; HAIYAN, category5) over the Western North Pacific. We used the best track data of TCs provided by Joint Typhoon Warning Center (JTWC), time and location of lightning data provided by World Wide Lightning Network (WWLLN)　and ELF magnetic field data obtained at two stations of Global ELF Observation Network (GEON), Syowa (69.0S, 39.5E) and Kuju(33.1N, 131.2E) for calculating EPs. In order to compare TC intensity with lightning parameters, EPs of lightning in the inner core region (100 km from the center of TC, 200 km for large TCs) and in the rainband region ( 100 km ~ 500 km from the center, 200 km ~ 1000 km for large TCs), median values of the cross-correlation coefficients and lag time were calculated. In the case of UTOR and HAIYAN that were intense TCs, the correlation coefficients of peak current and charge amount of lightning in the inner core with TC intensity were relatively high. In addition, each peak of lightning parameters preceded that of TC intensity by ~ 1day. However, there was very weak correlation in TC intensity and EPs of lightning in the rainband of TCs with category 4,5 including WIPHA. The rainband region of relatively weak TCs (LEEPI and MAN-YI) had　the peak of EPs of lightning 1~2 days before the peak of maximum sustained wind. From these results, EPs of lightning in the inner core of intense TCs can be a possible indicator of TC development.

台風の中心気圧や最大風速といった強度の予報精度は長年の課題であるが、近年、台風内部の雷活動が台風の強度予報を向上させる可能性があることが示唆されている。台風の強度変化と雷放電の発生頻度を比較した先行研究は数多くあるが、雷放電の電気的物理量を用いた先行研究はほぼ皆無である。雷放電の発生頻度は、2013 だけでなく、電気的物理量も用いて台風の強度発達との関係性を調査することで、台風の強度発達と雷活動の新たな関係性が見出せる可能性がある。今回年に北西太平洋で発生した 5 個の台風（LEEPI, category1; UTOR, category5; MAN-YI, category3, 大型; WIPHA, category4, 大型; HAIYAN, category5)について、台風の強度発達と雷放電のピーク電流値、電荷モーメント変化量(CMC)、放電電荷量の時間変化を比較した。台風のベストトラックデータは米軍合同台風警報センター(JTWC)、雷放電の時刻、位置は World Wide Lightning Location Network (WWLLN)を使用した。雷放電の電気的物理量を計算するために Global ELF Observation Network（GEON）の昭和基地（69.0° S, 39.5° E）と久住(33.1° N, 131.2° E)の二地点で観測される ELF 帯磁場波形を使用した。台風の強度発達と雷放電の電気的物理量を比較する際、台風を内部コア領域(中心から 100km,大型は 200km)とレインバンド領域(中心から 100km～500km, 大型は 200km～1000km）に分け、雷放電の各指標は 6 時間ごとの中央値をとり、最大風速とラグをとりながらそれぞれの相関係数を計算した。強い台風の UTOR や HAIYAN では、内部コアにおける雷放電のピーク電流値、放電電荷量では比較的高い相関がみられ、台風の強度発達に対して同時か約 1 日先行することが確認された。しかし、WIPHA を含む category4 以上の台風のレインバンドにおける雷活動と強度発達に相関は見られなかった。比較的弱い台風である LEEPI, MAN-YI では、レインバンドにおける雷放電の電気的物理量のピークが最大風速対して約 1-2 日先行することが確認された。以上より、台風の内部コアにおける雷放電の電気的物理量は台風の強度発達をモニタリングできる可能性がある。

R005-05
Zoom meeting C ：11/1　AM1　(9:00-10:30)
10:00-10:15

## 熱帯対流圏界層における乱流による混合の観測

#橋野　桃子[1)],橋口　浩之[1)],ウィルソン　リチャルド[2)],荻野　慎也[3)],鈴木　順子[3)]
[1)]京大・生存圏研,[2)]理,[3)]海洋研究開発機構

## Observations of turbulent mixing in Tropical Tropopause Layer (TTL)

#Momoko Hashino[1)], Hiroyuki Hashiguchi[1)], richard Wilson[2)], Shinya Ogino[3)], Junko Suzuki[3)]
[1)]RISH, Kyoto Univ.,[2)]Atmospheric sciences,[3)]JAMSTEC

The Tropical Tropopause Layer (TTL) is a transitional region between the troposphere and the stratosphere peculiar to the tropical zone. In recent years, the importance of elucidating the physical and chemical processes in TTL has attracted attention, and the international TTL observation project "STRATEOLE-2" will be carried out in 2021 and 2024. The behavior of atmospheric waves in TTL is considered to affect the mass exchange between the stratosphere and the troposphere. It is said that materials are transported from the stratosphere to the troposphere along with the breaking of equatorial Kelvin wave, which is known to be predominant in the TTL, which suggest a relationship with turbulence due to breaking of the wave [e.g., Fujiwara et al., 2003]. However, no studies have shown this relationship directly from observations, and it can be said that the details of how Kelvin waves influence mass exchange have not yet been clarified. Therefore, in this study, we analyzed turbulence and mass transport near the TTL region using the data of the STRATEOLE-2 pre-observation conducted from the end of 2019 and the observation campaign conducted in synchronization with it.
The observation campaign was conducted from November 21 to December 6, 2019, and ozone/GPS sonde observations were conducted at the Equatorial Atmosphere Observatory in West Sumatra, Indonesia. The observation data from the Equatorial Atmospheric Radar (EAR) at the same station was also analyzed. In addition, from November 12, 2019 to February 28, 2020, part of the STRATEOLE-2 pre-observation data obtained using super pressure long duration balloons was used. Furthermore, analysis using ERA5 re-analysis data was performed.
The analysis results will be described below. From the sonde profile during the observation campaign, a structure thought to be equatorial Kelvin wave was found in the zonal wind field and the temperature field. It was observed that the vertical wind shear increased as the wave amplitude increased, and the shear region also moved downward as the wave phase moved downward with time. The region of increased turbulence intensity obtained from EAR observation during the same period coincides with this shear region, and it is considered that turbulence is generated due to shear instability. At this time, the vertical distribution of ozone changed from a structure with a sharp peak to a structure that spreads vertically, and it is considered that the turbulence caused vertical mixing of ozone. The figure shows the turbulence intensity (contour) calculated from the EAR data from January 23 to February 1, 2020, and the altitude trajectory of a super pressure balloon (blue line) that flew near the EAR during the same period. It is thought that the balloon was entrained in the turbulent layer and transported downward, suggesting that trace substances such as ozone in the atmosphere are also vertically diffused by turbulence. On the other hand, it was suggested from those observations that the turbulent layer is generated when equatorial Kelvin wave transitions rapidly from easterly phase to westerly phase. A similar consideration has been made in the study of equatorial Kelvin waves using re-analysis data [Nishi et al., 2007]. We analysed ERA5 data by the same method and found that the period in which rapid transitions from easterly to westerly detected using ERA5 data was consistent with the period in which the turbulence intensity observed in the EAR increased, at least at the longitude where the EAR was located. Moreover, it was confirmed that the distribution of the rapid transition zone of the zonal wind is related to the structure of equatorial Kelvin wave at all longitudes.
In this study, it was clarified from the direct observation that the turbulent flow caused by equatorial Kelvin wave transports materials. In the future, we would like to quantitatively evaluate the impact of this transportation.

熱帯対流圏界層（Tropical Tropopause Layer; 以下 TTL）は熱帯域に特有の対流圏と成層圏の遷移的領域である。近年 TTL における物理化学プロセスの解明の重要性が注目されており、2021・2024 年には国際的な TTL 観測プロジェクト「STRATEOLE-2」が実施予定である。TTL における大気波の挙動は成層圏と対流圏間の物質交換に影響すると考えられている。TTL 内で卓越することが知られる赤道ケルビン波の砕波に伴い物質が成層圏から対流圏へ輸送されると言われており、砕波による乱流との関係が示唆されている[e.g., Fujiwara et al., 2003]。しかしこの関係を観測から直接的に示した研究はなく、ケルビン波が物質交換にどのように影響するかの詳細はまだ明らかになっていないと言える。そこで本研究では TTL 領域付近における乱流と物質輸送について、2019 年末から実施された STRATEOLE-2 プレ観測とそれに同期して実施した観測キャンペーンのデータ等を用いて解析した。
観測キャンペーンは 2019 年 11 月 21 日～12 月 6 日に実施し、インドネシア西スマトラ州の赤道大気観測所においてオゾン・GPS ゾンデ観測を行った。同観測所内の赤道大気レーダー(EAR)による観測データも合わせて解析した。また 2019 年 11 月 12 日～2020 年 2 月 28 日の間、スーパープレッシャー気球を用いて行われた STRATEOLE-2 プレ観測データの一部を用いた。さらに ERA5 再解析データを用いた解析を行った。

以下、解析結果について述べる。観測キャンペーン期間中のゾンデプロファイルから東西風場と温度場に赤道ケルビン波と考えられる構造がみられた。波の振幅が増大すると東西風シアも増し、時間とともに位相が下方に進むのに伴ってシアー域も下方に移動していく様子が見られた。同期間の EAR 観測から得た乱流強度の増大領域とこのシアー域は一致しており、シアー不安定が起きて乱流が生成していると考えられる。このときオゾンの鉛直分布は鋭いピークを持つ構造から鉛直になだらかに広がった構造に変化しており、乱流がオゾンの鉛直混合を引き起こしたと考えられる。図は 2020 年 1 月 23 日～2 月 1 日の EAR データから算出した乱流強度(コンタ)に、同期間を EAR との水平距離が近い位置を飛行していたスーパープレッシャー気球の高度軌跡(青線)を重ねて示している。気球は乱流層に巻き込まれて下方に輸送されたと考えられ、大気中のオゾンを始めとする微量物質も同様に乱流によって鉛直に拡散されることが示唆される。また、乱流層は赤道ケルビン波が東風から西風へ遷移するときに生成されることが今回の観測から示唆された。再解析データを用いた赤道ケルビン波の研究[Nishi et al., 2007]でも同様の考察がされており、同様の手法で ERA5 再解析データを用いて検出した東風から西風の急速な遷移の起こる期間は、少なくとも EAR の位置する経度においては EAR で観測される乱流強度が増大する期間と一致していた。また全経度において、東西風の急速な遷移域の分布は赤道ケルビン波の構造と関連していることを確認した。
このように、本研究では赤道ケルビン波に起因する乱流が物質を輸送する様子を直接観測から明らかにした。今後はこの輸送による影響を定量的に評価していきたい。

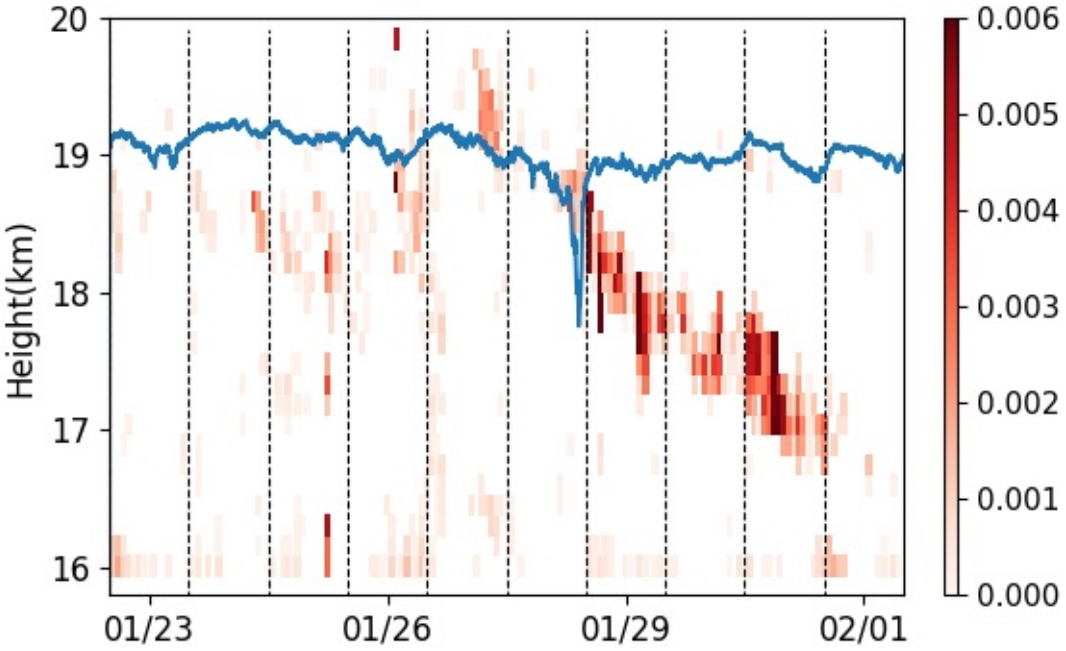

R005-06
Zoom meeting C ：11/1　AM2　(10:45-12:30)
10:45-11:00

## 多波長分光撮像・偏光観測による木星極域ヘイズ・雲活動の特徴

#横田　駿太郎[1)],佐藤　光輝[2)],高橋　幸弘[3)],高木　聖子[4)],大野　辰遼[3)],佐藤　佑樹[5)]
[1)]北大理学院,[2)]北大・理,[3)]北大・理・宇宙,[4)]北海道大学,[5)]北大院理

## Characteristics of Jovian polar atmosphere derived from multispectral and polarimetric observations

#Shuntaro Yokota[1)], Mitsuteru SATO[2)], Yukihiro Takahashi[3)], Seiko Takagi[4)], Tatsuharu Ohno[3)], Sato Yuki[5)]
[1)]Grad.Sch.Sci.Hokkaido Univ,[2)]Hokkaido Univ.,[3)]Cosmosciences, Hokkaido Univ.,[4)]Hokkaido Univ.,[5)]Grad. Sch. Sci., Hokkaido Univ.

Polarimetric observation is an effective method for determining the particle properties of the planet's surface and atmosphere. Polarimetric imaging provides information on the intensity of scattered light, which can be combined with model calculations to constrain particle properties. From this reason, many polarimetric observations of Jovian atmosphere have been performed so far. Previous studies have shown the distribution of polarization with Jupiter's latitude, confirming the effects of stripe structure and high-altitude haze [McLean et al., 2017, Schmid et al., 2011]. Polarimetric imaging at high polarization with methane absorption wavelengths is suitable for elucidating the variation of particle characteristics corresponding to cloud structure. For spectroscopic imaging observations, methane absorption wavelength have sensitivity at specific altitudes from the upper troposphere to the stratosphere due to the optical path difference of the reflected light [Karkoschka et al., 1994], and the vertical structure of Jupiter's atmosphere has been elucidated using multiple methane absorption wavelengths in ground-based telescopes and spacecraft observations. Previous studies have only observed polarization only a few times a year, and the temporal variation of particle characteristics has not been clarified. The temporal variability of particle properties in the upper troposphere and stratosphere, focusing on the spatiotemporal variability of clouds, has not been sufficiently discussed.　The purpose of this study is to observe the motion of the polar upper layer in the Jovian atmosphere and the temporal variations of the particle characteristics from the polarimetric and multispectral imaging using the 1.6 m Pirka telescope operated by Hokkaido University and to clarify the convection mechanism of the Jovian atmosphere by comparing the multispectral imaging data to polarimetric imaging data.
In this presentation, we introduce the results derived from the spectral imaging observations and the polarimetric imaging observations using the Multi Spectral Imager (MSI) (pixel scale = 0.39 "/ pix) with the band-pass filters of 619 nm, 727 nm, 756 nm, and 889 nm, which is mounted on the Pirka telescope.　We conducted the MSI observations from May 2019 to July 2020.　For this observation, we have conducted 21 nights observation and the typical seeing size was 4 arcseconds. In order to monitor the temporal variations of the cloud/haze structure and their polarimetric characteristics, it is necessary to simultaneously obtain the multispectral and polarimetric data with every few days interval.　The images at the methane absorption wavelength of 619 nm, 727 nm and 889 nm show bright clouds and haze layers in Jovian atmosphere due to the higher ratio of scattered light. The deepest methane absorption at 889 nm shows the strongest polar polarization and strong latitudinal dependence consistent with the results of Schmid et al.,[2011]. There is a correlation between the polarization and the flux intensity corrected for peripheral attenuation in the 727 nm and 889 nm imaging. This relationship is strong in the latitudinal direction and it is reflected by the zone and band structure. We can also see variation of polarization in the longitude direction, and it is possible to be reflected by the differences in cloud top height and particle composition within each structure. For the observations up to 2020, we obtained data for several consecutive days and data with intervals of more than one week.　From continuous observations on 29 May (180-260 degrees longitude), 30 May (350-0-70 degrees) and 31 May (130-210 degrees) , we found no significant temporal variation of polarization with respect to the cloud structure. At the presentation, we will show the initial results derived from the image analysis and will show the future observation plan more in detail.

偏光観測は惑星表層や大気の粒子特性の決定に有効な手法であり，木星の大気ダイナミクスと粒子種の特定を目的とした偏光観測がこれまで多く行われてきた．偏光撮像観測では散乱光強度の情報を得ることができ，モデル計算と合わせることで粒子特性に制約を与えることができる．先行研究では木星の緯度による偏光分布を示し，縞構造と高高度ヘイズの影響が確認された[McLean et al., 2017, Schmid et al., 2011] ．高い偏光度からメタン吸収波長での偏光撮像観測が雲構造と対応した粒子特性の変動の解明に適している．分光撮像観測ではメタン吸収波長を用いることで反射光の光路差から対流圏上部から成層圏までの特定高度に感度を得ることができる[Karkoschka et al., 1994]ことから地上望遠鏡，探査機による木星観測において複数のメタン吸収波長を用いて大気の鉛直構造の解明が行われてきた．これまでの先行研究では年に数回程度の頻度の偏光観測しか行われておらず，粒子特性の時間的な変動は明らかになっていない．また，雲の時空間変動に着目した対流圏上層と成層圏の粒子特性の時間的な変動は十分に議論されていない．本研究の目的は北海道大学が所有する口径 1.6 m のピリカ望遠鏡を使用し，多波長の分光撮像観測に加えて偏光撮像観測を行うことで，木星大気上層の運動と粒子特性の変化を捉え，両者の比較を行うことで大気の対流機構を調べることである．

今回, 2019 年 5 月から 2020 年 7 月までのピリカ望遠鏡に搭載された可視光マルチスペクトル撮像観測装置(MSI)(空間解像度 = 0.39"/pix)による，619 nm, 756 nm，727 nm，889 nm のバンドパスフィルターを用いた分光撮像観測，偏光撮像観測の結果とその解析結果を紹介する．今回の観測では 21 夜の観測を実施し，典型的なシーイングサイズは 4 秒角であった．本研究では分光撮像と偏光観測の同時取得と高頻度の観測による時間的な変動を追跡するために，数日おきに連続したデータの取得が望ましい．2020 年までの観測では数日間の連続したデータと 1 週間以上間の空いたデータを取得している．889 nm 727 nm, 619 nm のメタン吸収波長ではそれぞれ木星大気最上層に位置する雲やヘイズ層が明るく見え，散乱光の割合が増加するため高い偏光度を示す．メタンの吸収が深い 889 nm は最も強い偏光度を示しており, Schmid et al., [2011]の結果に矛盾しない緯度依存性と極域ヘイズの強い偏光度を示した．727 nm，889nm の撮像では周辺減光を補正したフラックス強度と偏光度には相関がある。緯度方向で強く見られるこのフラックスと偏光度の関係は縞構造を反映している．一方で経度方向にも偏光度の違いを見ることができ，各縞構造内での雲頂高度や粒子組成の違いを反映していると考えられる． 5/29(観測経度約 180-260 度)，5/30(約 350-0-70 度)，5/31(約 130-210 度)の連続した観測結果からは雲構造に対応した偏光度の目立った時間変化は見られなかった．本講演では，分光撮像観測と偏光観測の結果と比較，これらを踏まえた今後の観測計画について詳細を報告する．

R005-07
Zoom meeting C ：11/1　AM2　(10:45-12:30)
11:00-11:15

# 山岳波動の励起頻度と地形および卓越風の関係

#石井　智士[1)],鈴木　秀彦[2)]
[1)]明大・理工・物理,[2)]明治大

# Relationship between frequency of excitation of mountain waves, topography and a dominant wind

#Satoshi Ishii[1)], Hidehiko Suzuki[2)]
[1)]Dept. of Physics, Meiji Univ.,[2)]Meiji univ.

The objective of this study is to reveal the characteristics of excitation and propagation of mountain waves (MWs). Imaging observation of OH airglow had been conducted at Meiji University, Japan (35.613 °N, 139.549 °E) from Dec. 2015 to Dec. 2019. Mountainous area including Mt. Fuji locates in west side of the imager, and westerly winds predominate in the lower atmosphere throughout the year. Therefore, it has been expected that many MWs are excited in lee side and propagate to upper atmosphere. However, during the 4 years, only 8 events were identified as possible MWs. On the other hand, Criddle et al. [2011] reports 68 cases of MWs (ground phase velocity <5 m/s) which is thought to be excited by the Andes. They detected MWs by airglow imaging in Cerro Pachon, Chile (30.2 °S, 70.7 °W) from Aug. 2009 to Aug. 2010. Comparing with this event rate (68 cases/year), the number of events detected in our study (8 cases/4 years) is very small. There are two possible reasons why the number was small: (1) The frequency of MWs excitation is small in the lower layer, and/or (2) MWs do not easily propagate to the upper mesosphere. This study verified the possibility of the former case. When the over-mountain airflow exists, wavy clouds are often generated on the lee side. Since over-mountain airflow is essential for the excitation of MWs, a frequency of the wavy clouds can be considered to be a measure of the occurrence of MWs. The frequency and spatial distribution of MWs over Japan are investigated by detecting the wavy clouds from color images taken by Himawari-8 meteorological satellite for one year in 2018. The clouds are detected on more than 70 days a year around the Ou Mountains in Tohoku region, but just 20 days a year around Mt. Fuji. It is suggested that few MWs are excited around Mt. Fuji [Ishii, SGEPSS Fall Meeting, 2019]. The differences between these two regions are examined by focusing on the relationship between topography and horizontal wind in lower atmosphere. Using elevation data provided by Geospatial Information Authority of Japan and the wind data from the reanalysis data MERRA-2, the relationship between topography and wind in each area has been investigated. As a result, Tohoku region has a simple topography with the Ou Mountains running north to south, and the westerly wind blows almost perpendicular to the ridgeline. In contrast, the vast mountainous area that extends upwind of Mt. Fuji is a very complex terrain. In altitudes from 100 to 1000 m, the wind was blowing in various directions due to obstacle effects by mountains. From these results, we considered a general condition for frequent excitation of MWs in mountain area. We suggest "mountain wave hotspots", which is thought to be the frequent excitement of MWs in the world.

本研究では下層から上空に伝搬する山岳波の励起伝搬特性の解明を目的として、2015 年 12 月から 2019 年 12 月までの約 4 年間、神奈川県川崎市にある明治大学生田キャンパス（35.613 ° N, 139.549 ° E）にて OH 大気光イメージング観測を実施した。観測拠点の西方には富士山を代表とする山岳地帯が存在し、富士山の山頂高度付近（高度約 3000m）では 1 年間を通じて偏西風が卓越することから、この山岳地帯で励起された山岳波が山の風下側、つまり関東平野上空に多く伝搬していると期待した。しかし、この観測期間中、対地位相速度を持たない山岳波と思われる波動構造の検出数は 8 例に留まった。一方、Criddle et al. [2011]は、2009 年 8 月から 2010 年 8 月の約 1 年間の間に、チリのセロパチョン（30.2 ° S, 70.7 ° W）における大気光イメージング観測により、アンデス山脈によって励起されたと考えられる山岳波構造（対地位相速度＜5m/s）を 68 例報告している。この数（68 例/年）と比較すると本研究での山岳波の検出数(8 例/4 年)は非常に少ない。本研究の観測で山岳波の検出数が少なかった原因として、（1）下層での励起数が少ないこと、（2）上部中間圏への伝搬が起こりにくいことが考えられるが、本研究では（1）の可能性について検証した。
2018 年の 1 年間分の静止気象衛星ひまわり 8 号可視光観測データから、山岳波の励起に必要な山越え気流が発生した際に、風下側にしばしば発生する波状雲を検出することで日本列島上空の山岳波の励起頻度および分布を調査した。その結果、東北地方の奥羽山脈周辺では年間 70 日以上波状雲が発生していたが、富士山周辺では、最大でも年間 20 日以下の発生数にとどまっており、富士山周辺ではそもそも山岳波が励起されにくいことが示唆された［石井, SGEPSS 秋季講演会, 2019］。山岳波が頻繁に励起されている東北地方と、豊富な山岳地形を擁するにも関わらず励起数が少ない富士山周辺について、地形と風の関係に着目してその差異を考察した。国土地理院標高データを用いて各地域の地形的特徴導出し、また、再解析データ MERRA-2 を利用してそれぞれの地域における風速場の特徴を導出することで、地形と風速、風向の関係を調べた。その結果、東北地方は奥羽山脈が南北に連なる単純な地形であり、山脈の稜線に対してほぼ直交する向きに西風が吹きつけている。これに対して富士山周辺は、富士山の風上側に広大な山岳地帯が広がっていて非常に複雑な地形であり、高度 100～1000ｍにおいては山を迂回するような向きに風が吹いており複雑な風速場を形成していることが示された。以上より得られた結果から山岳波の励起特性を考察し、世

界中の山岳地域において、その地形的特徴と下層風の関係から山岳波が頻繁に励起されていると考えられる“山岳波のホットスポット"の推定を試みた。

R005-08
Zoom meeting C ：11/1 AM2 (10:45-12:30)
11:15-11:30

# The effect of heat sources response due to El Nino-Southern Oscillation on MLT solar thermal tides in GAIA model

#Masaru Kogure[1)], Huixin Liu[2)], Hidekatsu Jin[3)]
[1)]Kyushu University,[2)]None,[3)]NICT

Solar thermal tides are global-scale waves with periods of 24 hours harmonics. They are excited by three heating sources: insolation absorption of water vapor in the troposphere and ozone in the stratospheric, and latent heat release. Tidal Wavenumbers and periods are determined by the global distribution of these heating sources, which are governed by lower atmosphere processes. El Nino-Southern Oscillation (ENSO) is a well known planetary scale phenomenon and drastically changes the global distribution of water vapor insolation absorption and latent heat in tropical regions. Liberman et al. (2007) observed an enhanced amplitude of diurnal tide at 90 km altitude during the 1997/8 El Nino and attributed it to high anomalies of water vaper insolation absorption and latent heat in the tropical central and eastern Pacific during ENSO. Warner and Oberheide (2014) presented water vapor insolation absorption and latent heat during the 2010/11 La Nina and compared them to tidal wind response at 100 km altitude. They found that diurnal nonmigrating tides with wavenumbers 2 and 3 (DE3 and DE2) were the most affected. While the two pioneering works cover only one EL Nino and one La Nino events, Liu et al. (2017) covered nine ENSO events and showed that seasonal and latitudinal variation of a diurnal tidal statistical response to ENSO by using 21 years (1996-2016) data-driven from the Ground-to-topside Atmosphere-Ionosphere model for Aeronomy (GAIA). However, there is still a lack of understanding of how changes in the heat sources contribute to tidal response to ENSO.
The purpose of this study is to reveal the contribution of changes in heating sources to tidal response to ENSO by using GAIA model. From the GAIA data, diurnal components of water vaper insolation absorption and latent heat were estimated base on Yanai (1978) and their responses to ENSO are extracted for the period of 1996-2016. This is compared to tidal variations presented in Liu et al., (2017), and their correlations are examined.

R005-09
Zoom meeting C ：11/1　AM2　(10:45-12:30)
11:30-11:45

## 台風・ハリケーン・サイクロンによって励起された中間圏擾乱の ISS-IMAP/VISI による観測

#齊藤　昭則[1)],坂野井　健[2)],穂積　裕太[3)],Perwitasari　Septi[4)],中村　卓司[5)]
[1)]京都大・理・地球物理,[2)]東北大・理,[3)]電通大,[4)]国立極地研究所,[5)]極地研

## Tropical cyclone-generated mesospheric disturbances　revealed by the airglow observation of ISS-IMAP/VISI

#Akinori Saito[1)], Takeshi Sakanoi[2)], Yuta Hozumi[3)], Septi Perwitasari[4)], Takuji Nakamura[5)]
[1)]Dept. of Geophysics, Kyoto Univ.,[2)]Grad. School of Science, Tohoku Univ.,[3)]UEC,[4)]NICT,[5)]NIPR

Mesospheric disturbances associated with tropical cyclones (TC) have been investigated using the airglow observation from International Space Station (ISS). It has been widely accepted that the vertical coupling from the Troposphere to the Mesosphere and the Lower Thermosphere (MLT) region is crucial to elucidate the variations of the upper atmosphere. Especially, extreme atmospheric events in the Troposphere, such as TC and tornados, are regarded as the source of the sporadic disturbances in the MLT region. There has been a plenty of researches on the MLT disturbances associated with the Tropospheric events using the ground-based imagers, GNSS-receiver arrays, and radars. Space-borne imaging observation is idealistic to elucidate the MLT disturbances caused by the Tropospheric events because it is not blocked by the clouds in the Troposphere. Visible-light and infrared spectrum imager (VISI) of ISS-Ionosphere, Mesosphere, upper Atmosphere, and Plasmasphere mapping (ISS-IMAP) mission detected the Mesospheric airglow from the molecular oxygen in 762nm of wavelength, and the Ionospheric airglow from the atomic oxygen in 630nm of wavelength. In its three years observation, the number of TC that ISS-IMAP/VISI made the conjugate observation was 171. It was found that more than 20% of TC was associated with the mesospheric disturbances that seems to be generated by TC. The duration of these disturbances was one or two days in spite of the lifetime of TC is longer than a week. Relation between activity of TC and the Mesospheric disturbances associated with the TC will be discussed in the presentation.

R005-10
Zoom meeting C ：11/1　AM2　(10:45-12:30)
11:45-12:00

## 2019 年 9 月成層圏突然昇温時に現れた電離圏 6 日振動の励起機構

#三好　勉信[1)],山崎　洋介[2)]
[1)]九大・理・地球惑星,[2)]九大・理・地惑

## Excitation mechanism of ionospheric 6-day oscillation during the 2019 SSW event

#Yasunobu Miyoshi[1)], Yosuke Yamazaki[2)]
[1)]Dept. Earth & Planetary Sci, Kyushu Univ.,[2)]Earth and Planetary Sciences, Kyushu Univ.

A sudden stratospheric warming (SSW) event occurred in September 2019 in the Antarctic region. During the SSW event, the quasi 6?day wave (Q6DW) was enhanced in the middle atmosphere, and strong 6?day oscillations are observed in the equatorial electrojet (EEJ) and electron density. The 6?day variation in the EEJ has a westward?moving structure with the zonal wavenumber 1, indicating the influence of the Q6DW. In this study, we investigate the excitation mechanism of the 6?day variations in the EEJ and electron density b conducting numerical simulations. In this study an atmosphere-ionosphere coupled model (GAIA) is used. The main results are as follows. The 6?day variations in the ionosphere are generated not by the Q6DW, but by the tides. The amplitude of the semidiurnal tides are modulated with a period of 6 days, due to the nonlinear interaction between the Q6DW and migrating semidiurnal tide. The detailed mechanisms for the 6-da modulation of the tides and its effect on the 6-day variation in the ionosphere is shown.

2019 年 9 月に発生した南半球突然昇温時に、電離圏電子密度、赤道エレクトロジェット電流などに、顕著な 6 日振動がみられた。本研究では、電離圏 6 日振動の励起機構について、大気圏―電離圏結合モデルＧＡＩＡを用いた数値実験により調べた。中性大気中の潮汐波の日々変動を排除した実験や、6 日波（プラネタリー波）に伴う中性風変動を排除した実験などを実施することで、電離圏 6 日振動の励起機構を特定した。その結果、電離圏の 6 日振動は、プラネタリー内に伴う中性風により励起されたものではなく、潮汐波の振幅が 6 日周期で変動することが原因であることが分かった。潮汐波の 6 日周期変動は、潮汐波（主に太陽同期成分）と 6 日波との非線形相互作用により生じたことも明らかとなった。詳細な生成機構および電離圏の 6 日振動の励起機構については当日発表する予定である。

R005-11
Zoom meeting C ：11/1　AM2　(10:45-12:30)
12:00-12:15

## 大気波動による Sq-EEJ 電流系の準 6 日振動現象の解明

#高山　久美[1),]三好　勉信[2),]吉川　顕正[3)]
[1)]九大,[2)]九大・理・地球惑星,[3)]九州大学地球惑星科学専攻

## Quasi-6-day oscillation in Sq-EEJ current system by atmospheric waves

#Kumi Takayama[1)], Yasunobu Miyoshi[2)], Akimasa Yoshikawa[3)]
[1)]Kyushu Univ.,[2)]Dept. Earth & Planetary Sci, Kyushu Univ.,[3)]ICSWSE/Kyushu Univ.

Atmospheric oscillations in the Sq-EEJ current system using dense geomagnetic field observational sites along 210MM chain composed of MAGDAS (Global Geomagnetic Observation Network) and observational sites operated by Geospatial Information Authority of Japan (GIS) were analyzed for a comprehensive understanding of the three-dimensional atmosphere-ionosphere-magnetosphere coupled system. In this study, we focus on the quasi-6-day oscillation excited by atmospheric waves from below.
It is known that, the quasi-6-day wave (Q6DW), one of the atmospheric waves, is caused by atmospheric heating by moist air in the tropical troposphere [Miyoshi and Hirooka,1999] and has a seasonal dependence that strongly develops in the spring and autumn equinoxes [Liu et al.,2004]. The Q6DW in EEJ was verified with the equatorial electrojet measurements from the CHAMP and SWARM satellites and geopotential height data from the Aura satellite [Ymazaki et al., 2018]. In addition, the distribution of the quasi-6-day oscillation near the equator was clarified using the total electron content (TEC) from GPS data and the geopotential height of Aura satellite / MLS measurements. A nearly one-to-one correspondence between Q6DW activities in the ionosphere and lower thermosphere is also shown by Yamazaki et al., (2019). However, manifestation of global geomagnetic field disturbances excited by above atmospheric waves has not yet identified.
To understand global characteristic of the 6-day oscillation in Sq-EEJ current system, we analyzed H components of magnetic field data of MAGDAS and GSI during 2007 as follows.
(1)Subtract a mean value of the H component magnetic variations observed at the nightside (LT=18-06) from the H component data of each station to eliminate disturbance components by sun activities.
(2)Apply Principal component analysis for each one month to extract components of Sq-EEJ current system from H components of (1).
(3)Take the inner product between basis function of each component of (2) and H components of (1) at the same time and apply Bandpass filter in the range of 4.5-7.5 day cycle to extract components of the quasi-6-day variations.
(4)Compare with the variation of the amplitude of Q6DW to clarify the connection between the quasi-6-day oscillation and Q6DW.
Our results indicate that the quasi-6-day oscillation in the Sq-EEJ system has strong longitudinal and latitudinal dependences, although the Q6DW is a planetary-scale wave.
The excitation mechanism of the quasi-6-day oscillation in the Sq-EEJ system is examined using an atmosphere-ionosphere coupled model (GAIA).

全球的地磁気観測ネットワーク(MAGDAS)と国土地理院(GIS)の観測点からなる 210MM の高密度地磁気観測点を用いて、Sq-EEJ 電流系の大気振動を解析し、大気圏-電離圏-磁気圏の 3 次元結合系の包括的な理解を図った。本研究では、大気波動によって励起される準 6 日振動に着目した。
大気波の一つである準 6 日波(Q6DW)は熱帯対流圏の湿った空気による大気加熱によって発生することが知られており[Miyoshi and Hirooka1999]、春分点と秋分点に強く発生する季節依存性を持つ[Liu et al.,2004]。EEJ の Q6DW は、CHAMP 衛星や SWARM 衛星による赤道域の EEJ 計測や Aura 衛星によるジオポテンシャル高度データを用いて検証された[Ymazaki et al.,2018]。また、GPS データからの全電子量(TEC)と Aura 衛星によるポテンシャル高度データを用いて、赤道付近での準 6 日振動の分布を明らかにした。さらに、電離層と下部熱圏の Q6DW との間には、ほぼ一対一の対応があることが、Yamazaki et al., (2019)によって示されている。しかし、上空の大気波に励起された全球的な地磁気擾乱の顕在化はまだ確認されていない。
本研究では、Sq-EEJ 電流系の 6 日振動の全球的な特徴を理解するために、2007 年の MAGDAS と国土地理院の磁場データの H 成分を以下のように解析した。
(1)太陽活動による擾乱成分を取り除くために、各観測点の生データから夜側(LT=18~06)の変動の中央値を引く。
(2)(1)の H 成分から Sq-EEJ 電流系の成分を抽出するために、1 ヶ月毎に主成分分析をかける。
(3)(2)の各成分の基底関数と(1)の H 成分との内積を取り、4.5～7.5 日周期の範囲でバンドパスフィルタをかけ、準 6 日振動の成分だけを抽出する。
(4)準 6 日振動と Q6DW の振幅の変動と比較して、準 6 日振動と Q6DW の関係を明らかにする。
その結果、Sq-EEJ 電流系の準 6 日振動は惑星スケールの波であるにもかかわらず、強い緯度・経度依存性を持っていることがわかった。
全大気領域を包含する大気モデルと電離圏モデルとを統合した数値モデル（GAIA）を用いて、Sq-EEJ 電流系の準 6 日振動の励起メカニズムを調べる。

R005-12
Zoom meeting C ：11/1　PM1　(13:45-15:30)
13:45-14:00

# 直流電場センサーの開発と電離層 Sq 電場の直接測定

#筒井　稔
京産大　名誉教授

# Development of DC electric field sensor and direct measurement of ionosphere Sq electric fields

#Minoru Tsutsui
Prof. Emeritus of KSU

A new DC electric field sensor which is available to use in all spaces has been developed. The sensor is quite different from the mill type electric field sensor which measures electric potentials by gathering charged particles in the atmosphere. Since a key point of the new sensor is focused on electric equi-potential lines which are usually formed in orthogonal to the electric field lines everywhere, a linear dipole antenna can be applied to the new sensor.
Profiles of electric potentials around the linear dipole elements (each length of L and the gap of d), when they were set along a uniform electric field, were obtained numerically by solving the Laplace equation. The result showed that only two equi-potential lines having a distance L with each other connect to A and B on each center of the linear elements, respectively, and the potentials $V_A$ and $V_B$ of each element became the same as those of each equi-potential lines. These two potentials are led to a differential pre-amplifier. Since the output from the pre-amplifier is ($V_A$-$V_B$), an accurate electric field intensity at the position of the sensor can be obtained by ($V_A$-$V_B$)/L.
Another important point in the structure of the new sensor is that the entire dipole elements are covered with an electrical insulating jacket, because the dipole elements have to be protected from attaching of charged particles in the atmosphere.
For practical measurements on the ground, new sensors of 3-D dipole antennas were installed in an electromagnetically quiet environment where is in a mountain north of Kyoto city, and started continuous observation at the end of 2016. A typical example of one day traces of electric fields in 3-D directions is shown in the figure. From two traces of horizontal electric fields, we found a clear polarization change from south to east at about 2 hour after sunrise, and lasting with east-ward until the mid-day. After changing the polarization to westward, another large polarization change to northward appeared at about 2 hour before sunset. Since large fluctuations seen in the figure cannot be seen in rainy-days, the source of the electric fields would be above the troposphere, it is possibly in the ionosphere. The observed electric field intensity was 0.16 mV/m at maximum which is about 1/10 of those in the ionosphere which have been studied by many workers. The field intensity at the ground are consistent with the radiation effect from the ionosphere. Therefore, the observed electric field is considered to be the result of direct measurements of ionosphere Sq electric fields.
The result of this research is published in TEEE A from IEEJ as Tsutsui and Kaji, A New DC Electric Field Sensor and Direct Measurements of Ionosphere Sq Electric Field.

空間中の直流電場を測定するものとして，これまでは回転集電方式（Mill type）による対地電位を測定する方法しか無く、真空も含めた空間中の正確な直流電場を測定できるセンサーは存在しなかった。この問題を解決のために、新たな直流電場測定用センサーを開発した。この開発に当たっての着眼点は空間における 2 本の等電位線間の電位差を測定し、それを両等電位線間の距離で割る事により、空間電場を求める事にあった。開発したセンサーの構造は、2 本の線状素子（各長さ L）を短いギャップ（間隔 d）を挟んで一直線上に配置した極めてシンプルなダイポールアンテナである。
均一静電場が印加されている空間内にこのダイポールアンテナを平行に置いた場合の、その周囲の電位分布を、Laplace 方程式を数値的に解く事により求めた。その結果、L>15 d の場合は、間隔 L 離れた 2 本の等電位線のみが両ダイポール素子の中点 A 及び B にそれぞれ電気的に接続し、各々の等電位線の対地電位 $V_A$ 及び $V_B$ が両素子に現れる事が示された。この両素子に現れた電位を差動増幅器に入力し、その電位差出力（$V_A$-$V_B$）を距離 L で割れば、センサー中心位置での正確な電場を得ることが出来る。
このセンサーの構造上でもう一つ重要な点は、素子表面に大気中の荷電粒子が付着する事を防ぐための処置を施す事である。即ち、ダイポールアンテナ素子全体を電気的絶縁物で被覆する事である。またこの絶縁被覆をできる限り厚くすることにより、太陽光線に含まれている様々なスペクトルにより引き起こされるセンサー素子表面における光電効果によるショット雑音を抑制する事ができ、検出直流電場の制度を向上する事ができる。
上記知見を基に、そのプロトタイプを製作し、静電シールドボックス内に、均一電場を形成するための平行平板電極配置し、その中間点にアンテナ回転機構を備え、そこにプロトタイプを取り付け、均一電場方向に対するダイポールアンテナの角度に依存した電場強度変化を測定したところ、理論通りの 8 字特性を得る事が出来た。
上記実験結果により、この直流電場アンテナは実用可能とであると判断できたので、鉄道線路から 9 km 以上離れた電磁気的に静穏な京都市北部の山間の民家の庭に、東西・南北・および上下の各方向に長さ 5 m の直流電場測定用ダイポールアンテナを設置し、2016 年末から連続観測を開始した。

観測結果の一例を添付図に示す。これは 24 時間における 3-D 方向成分の静電場変動を示している。特に東西・南北の電場水平成分の時間的偏波を調べると、日出から約 2 時間後に南方向の電場が大きく現れ、それが短時間に東方向へ変化して、その向きのまま昼過ぎまで続き、その後西向きに変化し、日没の約 2 時間前に北方向へ大きく変化している事が見られた。これら 2 つの大きく変化する偏波の時刻を季節的に調べると、それらは日出。日没と同期して変化している事も判った。また、添付図に示した変動振幅の最大値は 0.16 mV/m であるが、雨天の時はこの振幅はほとんど現れない事から、この電場の源は対流圏より上空であり、電離層にある事を示唆している。一方、電離層研究の先人達が理論的や IS レーダや MU レーダーの観測結果で得られた電離層内での水平電場の強度は、本観測で得られ強度の約 10 倍の値であるが、Stratton の電磁界放射に関する理論により、電離層での電場強度は地上ではその約 1/10 になる事が示された。本観測におけるその他の様々な電場変動現象も電離層における電場変動現象を示唆しており、本観測で得られた電場は電離層 Sq 電場であるとの結論を得た。 またこの観測で磁気圏・電離圏結合による沿磁力線電流による効果も現れている可能性もあり、その研究にも寄与するものと思われる。
この研究成果は電気学会から共通英文論文誌(TEEE A)に Tsutsui and Kaji, A New DC Electric Field Sensor and Direct Measurements of Ionosphere Sq Electric Field として掲載予定である。

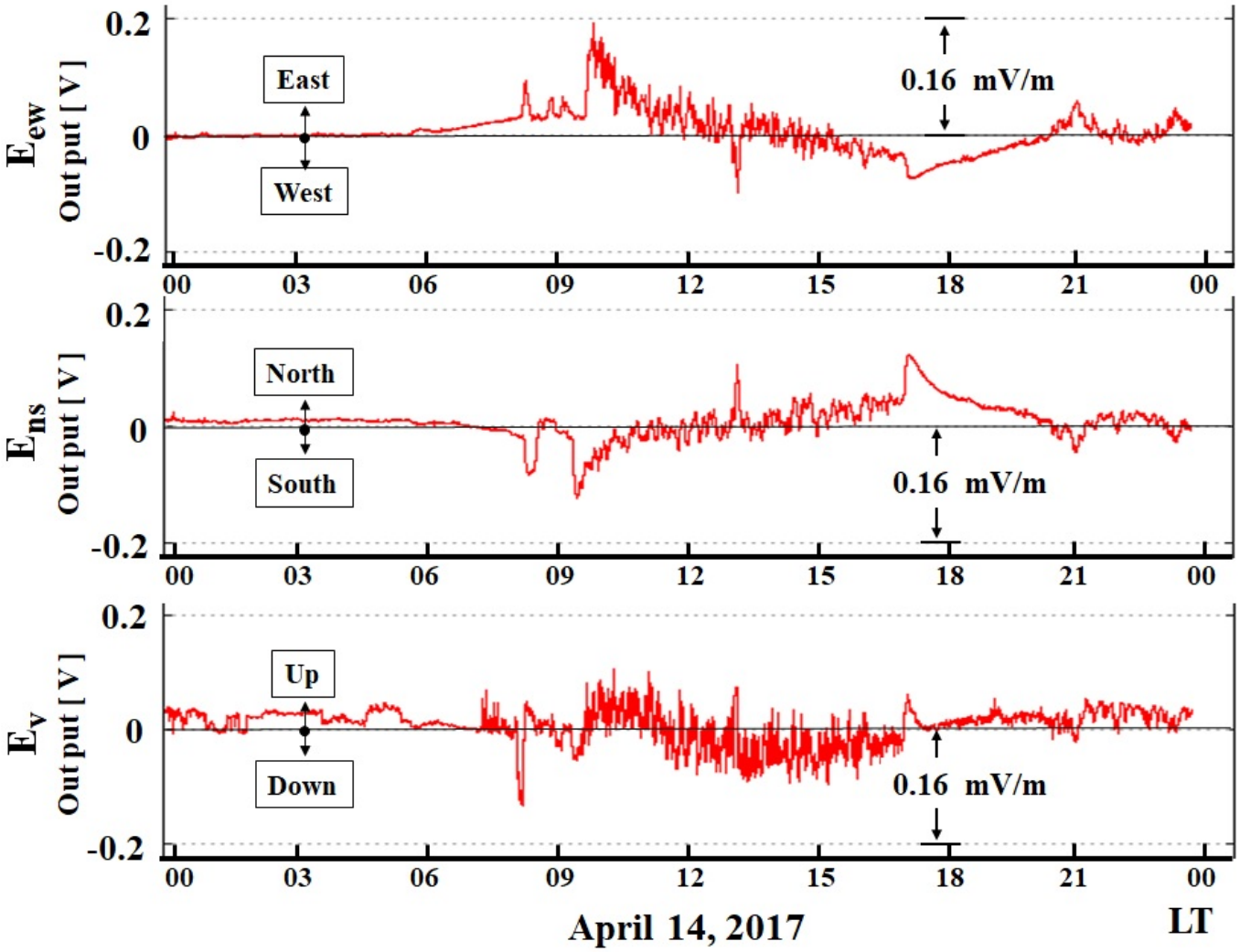

R005-13
Zoom meeting C ：11/1　PM1　(13:45-15:30)
14:00-14:15

## S-310-44 号機による Sq 電流系周辺における DC/AC 電界観測結果

#石坂　圭吾[1)],阿部　琢美[2)],熊本　篤志[3)],田中　真[4)]
[1)]富山県大・工,[2)] ＪＡＸＡ宇宙科学研究所,[3)]東北大・理・惑星プラズマ大気,[4)]東海大・情教セ

## Observation Results of DC and AC Electric Field near the Sq Current System by S-310-44 Sounding Rocket

#Keigo Ishisaka[1)], Takumi Abe[2)], Atsushi Kumamoto[3)], Makoto Tanaka[4)]
[1)]Toyama Pref. Univ.,[2)]ISAS/JAXA,[3)]Planet. Plasma Atmos. Res. Cent., Tohoku Univ.,[4)]Tokai Univ.

The Sq current system occurs in the lower ionosphere in the winter daytime. The Sq current system is appeared the specific plasma phenomenon such as electron heating, strong electron density disturbance. Therefore, it is important to measure directly the DC electric field and AC electric field (the plasma waves) in the ionosphere. The S-310-44 sounding rocket experiment was carried out at Uchinoura Space Center in Japan on January 2016 in order to investigate the unique phenomena near the Sq current focus. This rocket passed through the center of the Sq current system. In addition, scientific instruments that are equipped on the rocket also operated normally. As the results of observation, it was found that the electron temperature at the altitude from 100 km to 110 km was about 150 K larger than the background by using the fast Langmuir probe measurement. This suggests an existence of electron heating region in the Sq current focus. The Electric Filed Detector (EFD), which is one of scientific instrument onboard S-310-44 sounding rocket, was able to observe the DC electric field up to 100Hz and the waveform of the plasma waves up to 6400Hz in the altitude from 100km to 160km during the ascent. We also measured directly plasma in the ionosphere by the various scientific instruments onboard the S-310-44 sounding rocket.
In this paper, we report on the observation results on DC electric field and low frequency plasma wave spectrum by EFD onboard S-310-44 sounding rocket. Especially, it was found that the DC electric field intensity is increased at altitude of about 110km. As for this reason, it is assumed that the electric field accelerates the electrons down, and collides with the neutral atmosphere around 100 km and electrons are heated. Next, the spectrum of AC electric field in the frequency range from 2 kHz to 3 kHz look to enhance at the altitude of about 100 km. These electric field components observe during the rocket ascent only. Therefore, it is possible that the electric field component is the plasma wave related to the Sq current system. Therefore, we guess the large DC electric field and the spectrum of the VLF band electric field are related for the Sq current system.
Finally, we discuss about the generating mechanism of Sq current system using the result of the electric field and other observation result.

R005-14
Zoom meeting C ：11/1　PM1　(13:45-15:30)
14:15-14:30

# 観測ロケット搭載用イオンドリフト速度測定器の内部メッシュ構造設計および性能評価

#葉柴　隆斗[1)],尾原　咲穂[2)],阿部　琢美[3)]
[1)]北海道大学,[2)]東海大学,[3)]ＪＡＸＡ宇宙科学研究所

# Internal mesh structure design and performance evaluation of ion drift velocity analyzer for sounding rocket

#Ryuto Hashiba[1)], Sakiho Ohara[2)], Takumi Abe[3)]
[1)]Hokkaido University,[2)]Tokai University,[3)]ISAS/JAXA

In the ionosphere, the neutral particles and plasmas coexist. The momentum transfer between the neutral particle and plasma is the important process in elucidating phenomena in the lower ionosphere such as ionospheric dynamo and plasma density disturbance. However, since satellites cannot fly below 250 km altitude for a long time, the observation data are limited, and there are only a few reports based on in-situ observations. On the other hand, the sounding rocket enables in-situ observation in the lower ionosphere. In order to elucidate the phenomena in the lower ionosphere, it is necessary to observe the neutral atmosphere and ionospheric plasma using an analyzer on the sounding rocket.
We are developing an ion analyzer for the sounding rocket that enables estimation of ion drift velocity and density in the ionosphere. The analyzer is composed of a combination of RPA (Retarding Potential Analyzer) and IDM (Ion Drift Meter), which have been used for ionospheric ion observation.
The RPA section enables ion energy analysis by applying voltage to metal mesh grid, and the section is composed of five mesh grids. The ions are accelerated or decelerated by the voltage applied to the mesh grid. Inside the RPA, it is desirable that the potential distribution between the meshes is uniform in the tangential direction. However, it is concerned to be non-uniform. In the case of non-uniform potential distribution, the magnitude of acceleration or deceleration differs depending on the ion trajectory, which affects the velocity estimation error. Therefore, the potential distribution in the vicinity of grid was estimated using SIMION, which is software that can calculate the trajectories of charged particles. In this study, a variation of the potential distribution in a space between two wires and in the direction vertical to the mesh was examined by changing the wire diameter of the grid, the number of meshes, the aperture ratio, the applied voltage, and the distance. The aperture ratio is the ratio of the area of the opening to the entire mesh. The results of the voltage error estimation showed that the error changed linearly depending on the wire diameter and the number of meshes under condition for estimating the same aperture ratio and the center of the opening. In addition, on the SIMION, the transmittance of charged particles flowing into the grid was calculated and compared with the aperture ratio of the grid. The particle transmittance and particle trajectories were estimated when the wire diameter and applied voltage were changed at the same aperture ratio.
It is also necessary to generate ions that move at a specific velocity on the ground to evaluate the performance of the analyzer. Therefore, we are developing a low energy ion source. The characteristics of the ions generated by the ion source are evaluated using the Langmuir probe. Compared to the analyzer, the probe can simply measure the current caused by electrons and ions flowing into the electrode. The source and the probe were installed in the vacuum chamber, and the voltage applied to the source was changed to generate ions flow. Then, the change of the current-voltage characteristic of the probe was investigated. The electron saturation current is usually determined only by electrons, but if the ion source works properly, the current value in this region is expected to change due to the inflow of low-energy ions.
In this presentation, the estimation and verification results of the potential distribution of the mesh grid using SIMION and the electrode design will be discussed. The results of the experiments with the ion source and our future work will also be discussed.

電離圏には電離大気と中性大気が共存している．電離大気－中性大気間の運動量輸送は電離圏下部（高度約 80-300 km）において顕著であるが，人工衛星は高度 250 km 以下の領域を長時間飛行することは出来ないため観測データが限られており，直接観測した報告例は少ない．一方，観測ロケットは，人工衛星が飛行できない高度領域におけるその場観測を可能とする．電離圏下部においては中性大気とプラズマの相互作用により，電離圏プラズマ密度擾乱など様々な現象が存在するが，未解明の問題を解決するためには，観測ロケットに搭載可能な測定器を用いて電離大気と中性大気を観測する必要がある．
我々は電離圏下部においてイオンドリフト速度および密度の推定を可能にする，観測ロケット搭載用イオン測定器の開発を進めている．測定器は，電離圏イオン観測用として用いられてきた RPA (Retarding Potential Analyzer)と IDM (Ion Drift Meter) を組み合わせた構成になっている．
測定器の RPA 部では金属メッシュグリッドに電圧を印加することによりイオンのエネルギー分析を行うことが可能であり，RPA 部は 5 枚のメッシュグリッドにより構成される．メッシュグリッドにかけた電圧によりイオンは加速あるいは減速されるが，この時メッシュ間の電位分布は接線方向で均一であることが望ましいのに対し，不均一であることが予想される．不均一な電位分布の場合，イオンの軌道に応じて加速／減速の大きさが異なり，速度推定誤差

に影響を与える．そこで，荷電粒子の軌道を計算するソフトウェアである SIMION を用いて，グリッド付近の電位分布の推定を行った．特に，メッシュグリッドの線径，メッシュ数，開口率，印加電圧，配置場所を変えて，グリッド接線方向の開き目中央とグリッド鉛直方向の電位分布を推定した．開口率はメッシュ全面に対する開口部の面積の割合である．電圧誤差の推定結果から，同じ開口率かつ開き目中央を推定する条件のもとでは線径とメッシュ数の違いにより，電圧誤差は線形に変化することが分かった．想定される条件の下で，印加電圧と誤差の間に一定の関係があることが分かった．加えて，SIMION 上においてメッシュグリッドに流入させたイオンの通過率を求め，メッシュグリッドの開口率と比較した．グリッドの線径や印加電圧を変えた場合の，透過率の違いを調べたとともに，荷電粒子の軌道の変化を推定した．
また，イオン測定器の動作確認のために特定の速度で運動するイオンを地上で生成する必要があることから，低エネルギーイオン加速装置の開発を進めている．イオン加速装置によって生成されるイオンの特性を，ラングミュアプローブを用いて評価している．測定器に比べプローブは電極に流れ込む電子およびイオンによる電流を単純に測定できる．真空チャンバー内に加速装置とプローブを設置し，加速装置に印加する電圧を変更してイオンの流れを生成して，プローブで得られる電流電圧特性の変化を調べた．電子飽和電流は通常電子のみにより決まるが，イオン加速装置が正常に動作すれば低エネルギーイオンの流れ込みにより，この領域の電流値に変化が現れることが予想される．
本発表では，SIMION を用いたメッシュグリッドの電位分布の推定・検証結果，電極設計について述べる．そして，イオン加速装置により生成されたプラズマの測定により得られた結果を紹介するとともに，今後の取り組みについても述べる．

R005-15
Zoom meeting C ：11/1　PM1　(13:45-15:30)
14:30-14:45

## 超高層大気測定用圧力計の開発

#阿部　琢美[1)],渡部　重十[2)],田中　勇人[3)],三宅　亙[4)]
[1)]ＪＡＸＡ宇宙科学研究所,[2)]北海道情報大学,[3)]東海大・工,[4)]東海大・工

## Development of a pressure gauge for a study of upper atmosphere

#Takumi Abe[1)], Shigeto Watanabe[2)], Yuto Tanaka[3)], Wataru Miyake[4)]
[1)]ISAS/JAXA,[2)]Hokkaido Information University,[3)]Tokai Univ.,[4)]Tokai Univ.

We are developing a pressure gauge for installing the sounding rocket to estimate the number density of neutral atmospheric particles in the lower thermosphere. A brief overview of this instrument development will be presented in this paper.
Charged and neutral particles co-exist in the lower ionosphere. The former tends to move in a direction different from the latter, because of a difference in those behaviors against the electromagnetic force. The ionospheric current and ambipolar electric field existing in this region are attributed to a difference in a collision frequency between ion and electron with neutral particles. Characteristic phenomena such as traveling ionospheric disturbance and electron density irregularity are significantly generated due to the diversity of the particles in this region. Sounding rocket is only the platform which enables us to make in-situ measurement at altitudes from 60 to 250 km because the atmospheric drag prevents low-altitude satellite from staying in orbit for a long time period. It is desirable to develop an instrument which provides information on local quantities about charged and neutral particles.
We have started developing a pressure gauge for the sounding rocket to estimate the neutral atmospheric density in the lower thermosphere. The pressure gauge has two sensor elements; 1) crystal gauge for the relatively higher-pressure region and 2) B-A (Bayard-Alpert) gauge for the lower-pressure region. The B-A gauge will be turned on under the pressure below 4 Pa while the crystal gauge is responsible for the measurement at pressures above this threshold. In our measurement, two identical pressure gauges will be stored in two different shaped containers. The first container is designed on the basis of Patterson probe, which is known as a closed spherical container with a long tube, from which gases flow in. In the Patterson probe, incoming gas first collide with inner wall of the tube and lose translational kinetic energy, and the pressure gauge inside can measure static pressure due to thermal motion of atmospheric particles. The second one is an open-type cylindrical container. This container is newly developed in this study and has a small inlet for gas inflow. The internal structure was designed so that it can have high sensitivity in the direction of the incoming gas flow.
Both of the pressure gauges are expected to install on the top side of payload section of the sounding rocket. Detailed design of the sensor, container, and electronics will be made within one year. Laboratory experiment to evaluate the instrument performance will be made afterwards. In addition, numerical simulation to verify the instrumental response to gas inflow is planned to carry out. The latest status of our instrument development will be described in the presentation.

R005-16
Zoom meeting C ：11/1 PM1 (13:45-15:30)
14:45-15:00

## Development of new receivers for HF Doppler sounding utilized by Software-Defined Radio device

#Hiroyuki Nakata[1)], Yuhei Oki[1)], Kenro Nozaki[2)], Keisuke Hosokawa[2)], Ichiro Tomizawa[2)], Kumiko Hashimoto[3)], Ryo Matsushima[2)], Hiroyo Ohya[1)]
[1)]Grad. School of Eng., Chiba Univ.,[2)]UEC,[3)]KIU

HF Doppler sounding system has been utilized to examine the behaviors of the ionosphere. To maintain and develop the system of this sounding system, the knowledge of the analog circuit's hardware is necessary. Recently, on the other hand, the Software-Defined Radio (SDR) techniques, which can implement various wireless communication methods using software instead of traditional hardware, has been developed. We can easily establish the equipment for HF Doppler sounding system by utilizing the SDR devices without the knowledge of the analog circuits. In this study, therefore, new receivers of the HFD sounding system were developed using SDR devices (USRP N210). The operation of USRP can be performed by the free software, GNU Radio. The former receivers can observe radio waves at four different frequencies (5006 kHz, 6055 kHz, 8006 kHz, and 9595 kHz) with 100 Hz sampling. The new receivers were constructed with comparable specifications. Since the transmission of 9595 kHz has stopped, the new receivers receive 3.925 MHz instead. In the new system, the signal flows into four filters from the source (the signal from the antenna), and each signal decimated to a 100 sampling/sec rate. By simultaneous observations of the previous analog receiver and the new digital receiver, the performance of the new digital receiver was confirmed. It was found that the SN ratio of new digital receivers is much better (about 20dB) than the former analog receivers. I/Q detection and sharp edge filter brought SDR receivers improved characteristics on interference. We also checked the frequency accuracy of the observations by examining the Doppler frequency offsets of the SDR radio reception. In most SDR, the offsets of the Doppler frequency are within about 0.01 Hz. By using the rather low-spec PC for data acquisition, on the other hand, the offset becomes worse (about 0.09 Hz). Therefore, the spec of PC for data acquisition must be high enough to receive the four radio waves.
As the future of the HFD observation system, we are now planning to replace the analog receivers to the new digital receivers, and install the receivers at Sarobetsu and Kyushu area. In addition to the improvement of the transmission system, we also plan the ranging of the reflection heights by the new system.

R005-17
Zoom meeting C ：11/1　PM1　(13:45-15:30)
15:00-15:15

## USRP 高周波受信ユニットを活用した中緯度 SuperDARN イメージング受信機の構築に向けて

#西谷　望[1),]濱口　佳之[1),]堀　智昭[1)]
[1)]名大 ISEE

## Approach for the construction of SuperDARN imaging receivers using USRP units

#Nozomu Nishitani[1)], Yoshiyuki Hamaguchi[1)], Tomoaki Hori[1)]
[1)]ISEE, Nagoya Univ.

The latest status of the development of the SuperDARN imaging receiver for the Hokkaido East radar using the USRP units is presented. So far we constructed a 4-channel prototype system (out of the whole 20 channels), which was tested at the radar site in early July. The full 20-channel receiver system is planned to be attached to the radar and supposed to be able to simultaneously record the data, both by the original HF radar system and the imaging receiver. Installation of the imaging receivers will significantly improve the spatial-temporal resolution of the radar data, and make it possible to monitor several phenomena such as Pc3 pulsation and coseismic ionospheric disturbances, which were not captured with sufficient spatial- temporal resolution with the preexisting receiver set.

名古屋大学宇宙地球環境研究所では、USRP 高周波受信ユニットを活用した中緯度 SuperDARN イメージング受信機の構築を進めている。現在全 20ch の内 4ch のプロトタイプが完成し、7 月初旬に現地において　4 日間の試験運用を実施した。現在受信データの解析を進めているところである。
この試験運用の結果を見て、全 20ch の試験結果の運用を進めようとしている。フルシステムが完成した暁には、現状より時間分解能および空間分解能が格段に向上し、従来のシステムの通常観測モードではとらえられなかった Pc3 や Pi2 の時間空間分布、地震を始めとする地表面や下層大気における擾乱による電離圏擾乱の詳細特性をとらえられることが期待される。
同様の SuperDARN イメージングシステムは日本を含む世界数カ国で構築が進められ、すでに稼働しているものもあるが、廉価な装置である USRP を活用したシステムは他にはカナダのグループのものしか存在せず、既存のシステムに取り付けて運用することで既存のデータ取得も継続して行えるものは我々のグループのものが唯一のシステムである。講演では最新の解析結果について報告する予定である。

R005-18
Zoom meeting C ：11/1 PM1 (13:45-15:30)
15:15-15:30

## Reassessment of SuperDARN/SENSU near range echoes (3)

#Akira Sessai Yukimatu
NIPR/SOKENDAI

SuperDARN is a unique international HF radar network originally designed for and primarily contributed to space weather research by providing global (high to mid-latitude) ionospheric plasma convection and electric field potential map in high temporal resolution of typically 1 to 2 minutes in quasi real time with its global coverage of international HF radar's FOVs. It also contributes to vertical coupling of ionised and neutral atmosphere in middle and upper atmosphere by observing TIDs (traveling ionospheric disturbances), neutral winds, and PMSE/PMWE related echoes in MLT (mesosphere and lower thermosphere) or MTI (mesosphere, thermosphere and ionosphere) regions.
SuperDARN near range echoes are important targets especially for lower altitude echoes like those in ionospheric D and E regions and those in MLT region. As typical range resolution of SuperDARN radars is rather coarse and HF ray paths bend in ionosphere, obtaining precise height/altitude information is key to understand the physics in the region correctly.
These years SuperDARN community has tried extensively to improve and re-establish the method of interferometer calibration mostly in success. Some radars have also started to try higher range resolution observation with imaging (SDI/FDI) and pulse coding technique etc. Some issues for these challenges still remain and have also become clearer for further improvement for near future.
We here try to re-calibrate the interferometer and elevation angles measured with our SENSU Antarctic Syowa SuperDARN radars and to reassess the altitude information of the near range echoes.
Some recent papers related to this issue proposed near range echoes in summer midday obtained with SuperDARN radars seem not from mesopause region altitude but from rather slightly higher altitude so those echoes might not be PMSEs. Results of reassessment of near range echoes in Syowa SENSU radars in more detail and possible potential origins of the echoes will be discussed.

R005-19
Zoom meeting C ：11/1　PM2　(15:45-17:30)
15:45-16:00

## 衛星＝地上間の電離圏全電子数観測の開発状況

#山本　衛[1),]斎藤　享[2)]
[1)]京大・生存圏研,[2)]電子航法研

## Development of satellite-ground ionospheric total electron content (TEC) observation instruments and methods

#Mamoru Yamamoto[1)], Susumu Saito[2)]
[1)]RISH, Kyoto Univ.,[2)]ENRI, MPAT

This paper gives an overview of the development status of the observation instruments and methods of ionospheric total electron content (TEC) by using radio wave propagation from satellites to the ground. The radio wave propagation in plasma shows higher phase velocity and lower group velocity than those in the vacuume. Since the amount of such velocity variation is inversely proportional to the square of the frequency, TEC can be obtained by measuring the phase variation of dual-band radio wave propagation or the propagation velocity of the modulated wave. We have developed a digital receiver that receives radio waves from a dual-frequency beacon satellite. The observations were carried out by using dual-band beacon from satellites and the GNU Radio Beacon Receiver (GRBR) that supports frequencies of 150MHz and 400MHz. We have also developed a new digital receiver GRBR-2 which measures the new beacon signal (401MHz/966MHz) from FORMOSAT-7/COSMIC-2 satellites launched in 2019. Observations with GRBR-2 have already been continued in Indonesia, Thailand, Vietnam, etc. since September 2019. On the other hand, recently, TEC observations using GNSS (Global Navigation Satellite System, satellite positioning, that is, a general term for GPS and similar systems) have been widely implemented. The deployment of GNSS satellites by the United States, China, Russia, and the EU is progressing, while the price of receivers is dropping dramatically. The price of a dual-fr equency receiver dropped down to 20,000-30,000 yen. This situation helps development of multiple-points measurement of the ionospheric TEC. We are now developing a TEC observation system with a receiver board using F9P (a dual frequency GNSS consultation chip developed by Ublox). In the lecture we will discuss the current status of instrument development and observations.

衛星から地上までの電波伝搬を用いた電離圏全電子数（Total Electron Content; TEC）の観測手法の開発状況について概観する。電波はプラズマ中において真空中に比して電波の位相速度は速くなり、一方で群速度は低下する。その変化の程度は周波数の二乗に反比例するため、同じ経路に複数の周波数の電波を伝搬させ、その位相変化あるいは変調波の伝搬速度を測定することによって、TEC が測定できる。これまで我々は、2 周波ビーコン衛星からの電波を受信するディジタル受信機を開発してきた。初期には 150MHz と 400MHz の周波数に対応した GNU Radio Beacon Receiver（GRBR)によって、通常のビーコン衛星を用いた観測を行ってきた。また 2019 年に打上げられた FORMOSAT-7/COSMIC-2 衛星に搭載された 401MHz/966MHz の電波を用いた新しい 2 周波ビーコン観測に対応した新しいディジタル受信機 GRBR-2 を開発してきた。GRBR-2 による観測は、2019 年 9 月からインドネシア・タイ・ベトナムなどにおいて開始され、現在まで継続されている。一方、最近では、GNSS (Global Navigation Satellite System、衛星測位つまり GPS とその類似システムの総称）を用いた TEC 観測が広く実施されている。米国・中国・ロシア・EU による GNSS 衛星の配備が進んでおり、一方では受信機の価格が劇的に下がりつつある。ついに 2-3 万円の 2 周波受信機が現れたため、これを利用することで、電離圏 TEC の多点観測が容易になってきた。我々は、Ublox 社が開発した 2 周波 GNSS 受信 LSI である F9P を用いた受信ボードによる TEC 観測システムを開発中である。講演では現在の機器開発と観測の状況について述べる。

R005-20
Zoom meeting C ：11/1　PM2　(15:45-17:30)
16:00-16:15

# ロケット GNSS-TEC 観測搭載用アンテナシステムの構築

#奥村　誠[1),]芦原　佑樹[2)]
[1)]奈良高専,[2)]奈良高専・電気

# Design of antenna system for rocket GNSS-TEC observation

#Makoto Okumura[1)], Yuki Ashihara[2)]
[1)]NITNC,[2)]Elec. Eng., NIT Nara

Earth's upper atmosphere is ionized due to X-rays and ultraviolet rays contained in sunlight and it forms cold plasma region which is called ionosphere. Ionospheric disturbances causes satellite-based communication failure and positioning error of GNSS. Spatial structure observation of ionospheric electron density is indispensable for elucidating the generation process.
In ionospheric observations, Ionosonde, GNSS-TEC, and other remote sensing methods are generally used. Ionosonde can observe altitudes below the electron density peak in the F region, and GNSS-TEC can observe the total electron content on the propagation path between satellite to receiver. However, these do not obtain the spatial structure of the ionosphere.
At present, we proposed rocket GNSS-TEC tomography method as a new approach to the ionospheric observation. To evaluate this method,　S-520-32 sounding rocket is equipped with a GNSS-TEC receiver and fly over the boundary between the E and F regions of the ionosphere. Then we can obtain TEC data separated in F region and E region.
S-520 sounding rocket spins at a rotation speed of approximately 1 to 2 Hz to maintain the flight attitude. Generally, since the antenna has directivity, it is difficult to cover all directions with a single antenna while the rocket body spins. Therefore, this antenna system prevents the signal lock-off by a way of combining RF signals using multiple antennas. In this research, we made a ground-based experimental rocket model so that it would not be affected by ground reflected waves. This presentation shows GNSS-TEC observation results when the number of antennas is 4 or more.

地球の上層大気は、太陽光線に含まれる X 線や紫外線などにより電離され、電離圏と呼ばれる弱電離プラズマを形成する。電離圏擾乱は衛星通信障害や GNSS の測位誤差を引き起こすが、その生成過程の解明には電離圏電子密度の空間構造観測が不可欠である。
電離圏観測は、Ionosonde、GNSS-TEC 等をはじめとしたリモートセンシング手法で行われるのが一般的である。Ionosonde は F 領域の電子密度ピーク以下の高度について、GNSS-TEC は伝搬経路上の全電子数について観測できるが、電離圏の空間構造は得られない。そのため、空間構造観測にはパルスレーダや GNSS-TEC のトモグラフィ解析などが用いられる。
本研究では電離圏観測手法の新たなアプローチとしてロケット GNSS-TEC トモグラフィ法を提案する。観測ロケット S-520-32 号機に GNSS-TEC 受信機を搭載し、電離圏 E 領域と F 領域の境界を飛翔することで、E 領域、F 領域を分離した TEC データを取得する。
S-520 観測ロケットは飛翔姿勢維持のため 1～2Hz 程度の速度でスピンする。一般的にアンテナは指向性を持つため、ロケット機体がスピンする中で、全方位を単一アンテナひとつでカバーすることは難しい。そのため、複数アンテナを用いて RF 信号を合成する手法でロックオフを防止する。昨年までに、アンテナが 2 つの場合は追尾ロックが外れてヌルが発生しまい、全方位をカバーするには不十分であることがわかった。
本研究では、地上反射波の影響を受けないように配慮したモデルを作成し、アンテナの数を 4 以上にしたときの GNSS-TEC 測定結果を示す。

R005-21
Zoom meeting C ：11/1　PM2　(15:45-17:30)
16:15-16:30

## 観測ロケットに搭載する TEC 観測のための 2 周波ビーコン送信機・アンテナの開発

#黒川　浩規[1)],山本　衛[1)]
[1)]京都大学生存圏研究所

## Development of transmitter and antenna on board of sounding rocket for the TEC measurement

#Koki Kurokawa[1)], Mamoru Yamamoto[1)]
[1)]RISH, Kyoto University.

A sounding rocket experiment is planned by JAXA in 2022 for the study of medium-scale traveling ionospheric disturbance (MSTID). By transmitting dual-band radio beacon with a frequency ratio of 3: 8 from the rocket and measuring the phase difference between the two signals on the ground, the total electron content (TEC) over the radio wave path from the rocket to the ground can be measured. To realize this observation, we are now developing the observation equipment onboard of this rocket. The instruments are a dual-band beacon transmitter of 150MHz and 400MHz and a set of antennas that are installed on the rocket skin. The transmitter needs to output two phase-coherent radio waves at the same time. As the signal source, we selected Si5338 which is a high-performance, low-jitter clock generator capable of synthesizing at most four signals with different frequencies. The antenna system consists of four elements that can transmit both frequencies. The elements must fit the harsh environment (high temperature, intense vibration, etc.) that is expected at the outside of the sounding rocket at launch. We use inverted-L antenna for 150MHz with the parasitic element for 400MHz. The antenna material is high dielectric-constant material to reduce the size of the antenna. This antenna is designed by using electromagnetic-field simulation software called CST. We plan to verify the error between actual antenna and the simulation model, and conduct the environmental tests.

中規模伝搬性電離圏擾乱（MS-TID）の研究のために、JAXA によって 2022 年打上げの観測ロケット実験が計画されている。ロケットから周波数比 3：8 の 2 つの信号を送信し地上の受信機で 2 つの信号間の位相差を測定することにより、ロケットから地上への電波経路上の全電子数（TEC）を測定できる。この観測を実現するために、ロケットに搭載する観測装置の開発を行っている。観測装置は、150MHz と 400MHz の 2 周波ビーコン送信機と、ロケット壁面に取り付けるアンテナの二つで構成される。2 周波ビーコン送信機は、2 つの位相制御された電波を同時に出力する必要がある。信号源として、異なる周波数で最大 4 つの信号を合成できる高性能、低ジッターのクロックジェネレーターである Si5338 を選定した。アンテナは、150 MHz と 400 MHz の周波数の信号を同時に送信し、小型にする必要がある。また、アンテナ素子は、打上げ時にロケットの外側で予想される環境（高温、激しい振動など）に適合する必要がある。現在までのところ、逆 L 型アンテナの形状と寄生エレメントによって両方の周波数の送信を可能にし、アンテナ材質に高誘電体を使用することで小型に成功した。設計には、CST と呼ばれる電磁界解析シミュレーションソフトウェアを使用している。今後、実際の材料での観測装置の作製とシミュレーションとの誤差の検証を行い、環境試験を行う予定である。

R005-22
Zoom meeting C ：11/1 PM2 (15:45-17:30)
16:30-16:45

# Variations in the D-region ionosphere observed in fireballs using VLF/LF transmitter signals.

#Takeru Suzuki[1)], Hiroyo Ohya[2)], Fuminori Tsuchiya[3)], Kazuo Shiokawa[4)], Hiroyuki Nakata[2)]
[1)]Science and Engineering, Chiba University,[2)]Engineering, Chiba Univ.,[3)]Planet. Plasma Atmos. Res. Cent., Tohoku Univ.,[4)]ISEE, Nagoya Univ.

Meteors and fireballs are known to ionize the D-region and lower E-region ionospheres at 80-120 km heights [Davies, 1966]. The fireballs are meteors that the magnitude of brightness is larger than -4 based on the IAU (International Astronomy Union) definition. TID (traveling ionospheric disturbance) associated with the Chelyabinsk meteoroid in Russia was reported based on GPS-TEC (total electron content) observations [Perevalova et al., 2015]. The amplitude of the TEC variations was 0.07-0.5 TECU, and the period was 10 minutes. The epicenter of the TID was airburst point at 20-30 km heights of the meteoroid, and the velocities were 250-660 m/s. However, few quantitative studies for the D-region ionosphere associated with meteors and fireballs have been reported. In this study, we investigate the variations in the D-region ionosphere during a fireball occurred in Hokkaido, using VLF (very low frequency, 3-30 kHz) / LF (low frequency, 30-300 kHz) transmitter signals. The VLF/LF transmitter signals are reflected in the D-region ionosphere and are sensitive for variations in electron density in the lower ionosphere. The transmitters used in this study were JJY40kHz (Fukushima, Japan, 37.37° N, 140.85° E), JJY60kHz (Saga, Japan, 33.47° N, 130.18° E), and JJI (Miyazaki, Japan, 22.2 kHz, 32.05° N, 130.82° E). The receiver was located at RKB (Rikubetsu, Japan, 43.45° N, 143.77° E). Periodic variations of 100-200 s were identified by a wavelet transformation of the signal intensities for the JJY40kHz-RKB, JJY60kHz-RKB, and JJI-RKB paths at about five minutes (12:01 UT) after the fireball. The phases of the JJY40kHz-RKB and JJY60kHz-RKB paths had similar periods of 100-200 s at that time. We consider that these variations of intensity and phase were caused by the D-region variations due to acoustic waves in the atmosphere excited by the fireball. If the acoustic waves were excited at the luminous point (118 km altitude), the VLF/LF reflection point (90 km altitude) or vanishing end point (25 km altitude) of the fireball, the propagation times of the acoustic waves from the exited point to the LF reflection point at 90 km height over RKB were calculated to be 138 s, 126 s, or 311 s, respectively. The arrival time (311 s) of the acoustic waves excited from the vanishing point at the 25 km altitude was in good agreements with the onset of the VLF/LF variations with the period of 100-200 s. The acoustic waves excited at the vanishing end point propagate upward and may cause the variations in electron density in the D-region ionosphere. We will also show results of another fireball event over Kanto region, Japan, at 17:32:02 UT on 1 July, 2020, and discuss the fireball effects on the D-region ionosphere.

R005-23
Zoom meeting C ：11/1 PM2 (15:45-17:30)
16:45-17:00

## Solar flare effects on the D-region ionosphere using VLF/ LF transmitter signals

#Kodai Yamanobe[1)], Hiroyo Ohya[1)], Fuminori Tsuchiya[2)], Kozo Yamashita[3)], Yukihiro Takahashi[4)], Kazuo Shiokawa[5)], Hiroyuki Nakata[1)]
[1)]Engineering, Chiba Univ.,[2)]Planet. Plasma Atmos. Res. Cent., Tohoku Univ.,[3)]Engineering, Ashikaga Univ.,[4)]Cosmosciences, Hokkaido Univ.,[5)]ISEE, Nagoya Univ.

It has been known that intensity and phase of very low frequency (VLF, 3-30 kHz)/low frequency (LF, 30-300 kHz) transmitter signals significantly change due to intense ionization by solar flares [e.g., Mitra, 1974; Thomson et al., 2005]. The duration of the D-region enhancements due to X-ray is easier to be estimated using the VLF/LF waves, because the relaxation time for recombination in the D-region ionosphere is short to be within ~100 s [e.g., Ohya et al., 2015]. In this study, we investigate solar flare effects on the D-region ionosphere using VLF/LF transmitter signals. The transmitters used in this study were NWC (21.817S, 114.167E, 19.8 kHz), JJI (32.05N, 130.82E, 22.2 kHz), JJY40kHz (37.37N, 140.85E), JJY60kHz (33.47N, 130.18E), and BPC (34.63N, 115.83E, 68.5 kHz). The receivers were PTK (Pontianak, Indonesia, 0.003N, 109.367E), SGR (Sasaguri, Japan, 33.632N, 130.505E), RKB (Rikubetsu, Japan, 43.45N, 143.77E), and SRB (Saraburi, Thailand, 14.528N, 100.910E). The analyzed 16 M-class solar flares occurred in 2015. The changes in the VLF/LF phase had a weak correlation with the maximum X-ray flux of solar flares. Based on wave-hop method, there were three kinds of sky waves for each propagation path. By the wave-hop method, the resulting electric field strength of the ground wave (direct wave of LF signals) and sky waves of 1-hop, 2-hop, 3-hop, ..., and 10-hop can be calculated. For the three kinds of propagations, the largest electric field strengths of the sky waves were 1-hop, 2-hop, and equivalent 1- and 2-hop one. If the D-region height uniformly decreased along whole propagation paths during solar flares, the amplitude of the phase variations for the 2-hop sky waves would be larger by two times than that for 1-hop one. We corrected the differences of the phase due to the hop number. In the session, we will show the results in detail and discuss the solar flare effects on the D-region ionosphere.

R005-24
Zoom meeting C ：11/1　PM2　(15:45-17:30)
17:00-17:15

# 大規模太陽フレアによる中間圏オゾン短期変動の検出可能性に関する研究

#長濱　智生[1)],水野　亮[1)],中島　拓[1)]
[1)]名大・宇地研

# Study on a possible detection of short-term variations in mesospheric ozone caused by large solar flares

#Tomoo Nagahama[1)], Akira Mizuno[1)], Taku Nakajima[1)]
[1)]ISEE, Nagoya Univ.

We report on the short-term variability of mesospheric ozone, which may be due to the radiation of a large solar flare. The chemical composition of the Earth's atmosphere is affected by a variety of events related to solar activity. The mesosphere, in particular, is a neutral atmospheric region that is most likely to be affected by solar activity due to its near-space environment. Among the various solar activities, solar flares are intense bursts of radiation that come from the release of magnetic energy associated with sunspots, typically within a few minutes to hours. During the event, the solar X-ray and UV radiation largely varies, which is expected to have an impact on the chemical composition of the Earth's atmosphere. To assess the impact on the chemical composition, short-term variations of mesospheric ozone during solar flare effects (SFEs) listed by Observatori de l'Ebre, Spain, were investigated by using the data of a ground-based millimeter-wave radiometer, which is operated by ISEE, Nagoya University, at Rikubetsu, Hokkaido since 1999, and we found two possible events (June 4, 2004 and May 5, 2015) of ozone variation in upper stratosphere and lower mesosphere that may be associated with SFEs. The maximum variability of the ozone was estimated as -4% at 45 km altitude in June 4, 2004 and +13% at 61 km in May 5, 2015, respectively, and they are about the detection limit of the measurement. However, to confirm these events, we performed the same analysis using the global AURA/MLS ozone data (version 4.2) and did not detect any significant variation for either event. This result suggests that a typical large solar flare of M to X class is unlikely to have a significant impact on the chemical composition of the middle atmosphere. In the presentation, we report on the detailed characteristics of the temporal variation of mesospheric ozone and solar X-ray and UV fluxes during the event as well as analysis methods including event selection.

大規模太陽フレアの放射に起因すると考えられる中間圏オゾンの短期変動について報告する。地球大気の化学組成は太陽活動に関連した様々な事象の影響を受け、大きく変動することが知られている。特に、中間圏は宇宙空間に最も近い中性大気の領域であるため、太陽活動の影響を最も受けやすい領域である。様々な太陽活動の中でも、太陽フレアは太陽黒点に関連した磁気エネルギーの放出により発生するバースト現象で、その継続時間は典型的には数分から数時間以内である。この間に太陽 X 線や紫外線の放射量は非常に大きく変動するため、地球大気の化学組成に何らかの影響を与える可能性が考えられる。そこで、本研究では大きな太陽フレア発生時の大気組成変動を評価するために、Observatoratori de l'Ebre がリストアップした地磁気の太陽フレア効果（SFE）発生時における中間圏オゾンの短期変動を、1999 年から北海道陸別町に設置されている名古屋大学宇宙地球環境研究所の地上ミリ波放射分光計によるオゾン高度分布データを用いて調べた。その結果、SFE と関連している可能性のある上部成層圏と下部中間圏のオゾン変動イベントを 2 つ（2004 年 6 月 4 日と 2015 年 5 月 5 日）見出した。検出されたオゾンの最大変動率はそれぞれ高度 45 km で－4%、高度 61 km で+13%で、装置の検出限界程度の変動である。しかしながら、これらの事象を確認するために、AURA/MLS による全球オゾンデータ（Version 4.2）を用いて同様の解析を行ったところ、いずれのイベント時についても有意なオゾンの変動は確認できなかった。この結果は、典型的な M～X クラスの大型太陽フレアの X 線や紫外線によって中間圏大気組成環境に大きな影響を受ける可能性は低いことを示唆している。発表ではイベント中の中間圏オゾンと太陽 X 線・紫外線フラックスの時間的変動の特徴やイベントの選択を含めた解析手法について報告する。

R005-25
Zoom meeting C ：11/2　AM1　(9:00-10:30)
09:00-09:15

## 全球降雨分布と磁気リップルおよびF層電子密度波状構造振幅分布の比較

#家森　俊彦[1)],青山　忠司[1)2)],横山　佳弘[3)]
[1)]京大,[2)]エフ・ファクトリー,[3)]京大理

## A comparison of global rainfall distribution with amplitude of magnetic ripples and wavy structure of electron density

#Toshihiko Iyemori[1)], Tadashi Aoyama[1),2)], Yoshihiro Yokoyama[3)]
[1)]Kyoto Univ.,[2)]F-Factory,[3)]Grad school of Science, Kyoto Univ.

The magnetic structure with amplitude less than a few nT and spatial scale of around 100 ? 200 km commonly observed by low-altitude satellites along their orbit is named as "magnetic ripples" (Aoyama et al., 2017). They are mainly observed on the dayside in low or middle latitudes, and they are expected to be the results of lower atmospheric disturbance such as cumulous convection. Not only the magnetic ripples but also the wavy structure of electron density fluctuations is observed by the Swarm satellites. Although the magnetic ripples and electron density fluctuations do not necessarily appear at the same location on the satellite orbit, preliminary results suggest that some of them are caused by the vertically upward propagating atmospheric waves, i.e., acoustic mode waves. If the atmospheric waves are generated by the strong cumulous convection, we expect a correlation with the region of strong rainfall. In this presentation, we shall show a comparison of global distribution of magnetic ripples and that of electron density fluctuations with the global rainfall distribution obtained by the JAXA/GSMaP project.
[Acknowledgment] The Swarm satellite data have been provided by the Swarm Science and Validation Opportunity Project (ID: 10230) under the ESA. The global rainfall data have been provided by the JAXA/GSMaP project.

電離圏 F 層高度を飛翔する低軌道衛星が昼間側中低緯度でほぼ常時観測する波長がおおよそ 100km-200km で振幅が数 nT 以下の微細な磁場の構造(磁気リップル)は、それらの振幅の季節および地理的分布から、下層大気現象に由来すると推測される。Swarm 衛星による電子密度観測データ(注 1)を磁気リップル検出同様な手法で解析することにより、磁気リップルと位置や波長は必ずしも一致しないが、同様な変動(以下では電子密度波状構造と呼ぶ)が存在することが明らかになってきた。この発表では、磁気リップルと電子密度波状構造の分布と、GSMaP プロジェクト(注 2)により提供された衛星観測による降雨の全球的分布を比較し、それらの類似点あるいは相違点について議論する。
(注 1) ESA/Swarm 衛星観測データは The Swarm Science and Validation Opportunity Project under the ESA (ID:10230)により提供された。
(注 2)全球降雨観測データは、JAXA/GSMaP プロジェクトにより提供された。

R005-26
Zoom meeting C ：11/2　AM1　(9:00-10:30)
09:15-09:30

## H-IIA ロケット打ち上げに伴う電離圏変動の解析

#山崎　淳平[1)],中田　裕之[2)],大矢　浩代[3)],鷹野　敏明[4)],細川　敬祐[5)]
[1)]千葉大,[2)]千葉大・工・電気,[3)]千葉大・工・電気,[4)]千葉大・工,[5)]電通大

## Examination of the ionospheric perturbations propagation associated with H-IIA rocket launchings

#Junpei Yamazaki[1)], Hiroyuki Nakata[2)], Hiroyo Ohya[3)], Toshiaki Takano[4)], Keisuke Hosokawa[5)]
[1)]Chiba Univ.,[2)]Grad. School of Eng., Chiba Univ.,[3)]Engineering, Chiba Univ.,[4)]Chiba Univ.,[5)]UEC

It is reported that passage and exhaust plumes associated with rocket launches generate TEC perturbations observed by GEONET data (e.g., Furuya and Heki 2008; Lin et al., 2014, 2017). The ionospheric perturbations associated with rocket launches were caused by the shock waves and the delayed waves. The delayed waves are referred to as the acoustic waves reflected on the ground, but the mechanism of the delayed waves is still incompletely understood. Using HF Doppler sounding, therefore, we analyzed ionospheric perturbations associated with H-IIA launches (No.25 and 26) whose trajectories are relatively far from the Japanese islands. The Doppler sounding system is utilized by the University of Electro-Communications (UEC). In this system, the radio waves of 5.006 MHz and 8.006 MHz are transmitted from Chofu campus of UEC were observed at Sugadaira, Oarai, Kakioka, and Fujisawa were used. In those data, the perturbations of Doppler shifts were observed about 35 minutes after the launches. It is confirmed that this delay corresponds to the propagation time of the infrasound wave from the rockets to observation points once reflected on the ground. In both events, the periods of the disturbance of Doppler shift were 100~200 s (5~10 mHz). The amplitude of Doppler shift perturbations were clear when the infrasound wave reached the observation point after reflection on the ground as compared to the case where the infrasound wave reached the observation point directly. The Doppler shift perturbations could divide two packets. One is the packet A that the perturbations observed faster. The other is the packet B that the perturbations follow the packet A. In case of packet A, the perturbations of Doppler shifts at high altitude were reached earlier than that at low altitude. Therefore, it denoted that the infrasound waves propagated from high altitude to low altitude. In case of packet B, the perturbations of Doppler shifts at both high and low altitudes were observed at almost the same time. It can be considered that the infrasound waves propagated the observation points horizontally.

テポドンなどのロケット打ち上げに伴う大気波動や排気煙により TEC 変動が発生することが GEONET データによる解析結果として報告されている(e.g., Furuya and Heki 2008; Lin et al., 2014, 2017)。大気波動による変動は衝撃波によるものと遅延波によるものに分けられる。遅延波は地面で反射し電離圏に到達する音波と考えられているが、具体的なメカニズムはまだ解明されていない。そこで、本研究では HF ドップラー観測と GPS-TEC 観測を用いて、H-IIA ロケット(25, 26 号)打ち上げに伴う、ロケットの軌道から比較的離れた位置での電離圏の変動を解析した。本研究で使用した HF ドップラー観測システムは電気通信大学で運用されているもので、送信点は電気通信大学調布キャンパス(5.006 MHz, 8.006 MHz)である。また、本研究では、送信された電波をそれぞれ、菅平、大洗、柿岡、藤沢の各観測点で受信した際のドップラーデータを用いた。その結果、ロケット打ち上げから約 35 分後にドップラーシフト変動が確認された。この時刻はロケットにより生じた音波が地面で 1 回反射後に観測点に到達した時刻と一致したことが、音波のレイトレイシングより確認された。また、これらの変動は 100～200 秒(5～10 mHz)の帯域で変動強度が上昇していることが、どちらのイベントでも確認された。ドップラーシフトの振幅は、ロケットからの音波が直接観測点に到達した変動よりも、1 回地面に反射して観測点に到達した変動のほうが大きかった。ドップラーシフトの変動は大きく 2 つに分けられ、先に変動するパケット A と後に変動するパケット B が存在する。また、パケット A に関して変動の到達時間から、低高度のよりも高高度の変動のほうが、約 20 秒早いことが確認できた。このことから、パケット A は、ロケットに伴う変動は高高度から低高度へ伝搬していると考えられる。パケット B に関しては、どちらの高度もほぼ同時に変動を確認できた。このことより、変動は地面に平行に伝搬していると考えられる。

R005-27
Zoom meeting C ：11/2　AM1　(9:00-10:30)
09:30-09:45

## HFD を用いた地震に伴う電離圏擾乱の空間分布の解析

#堀切　友晃[1)],中田　裕之[2)],大矢　浩代[3)],細川　敬祐[4)]
[1)]千葉大学院融合理工学府,[2)]千葉大・工・電気,[3)]千葉大・工・電気,[4)]電通大

## Analysis of spatial distributions of coseismic ionospheric disturbances using HFD

#Tomoaki Horikiri[1)], Hiroyuki Nakata[2)], Hiroyo Ohya[3)], Keisuke Hosokawa[4)]
[1)]Chiba University Graduate School of Science and En,[2)]Grad. School of Eng., Chiba Univ.,[3)]Engineering, Chiba Univ.,[4)]UEC

It is known that ionospheric disturbances are caused by acoustic waves or atmospheric gravitational waves generated by ground motions or tsunamis that propagate to the ionosphere altitude after large-scale earthquakes. The propagation characteristics of ionospheric disturbances associated with earthquakes have been studied by using GPS observations. The horizontal propagation of ionospheric disturbances, is examined . On the other hand, its vertical propagations sre little reported. Since HF Doppler sounding system, which is operated by the University at Electro-Communications, is enable to receive the four radio waves simultaneously, three-dimentional distributions of rarious ionospheric disturbances can be examined by this system. In this study, we examined the 3-dimentional distribution of ionospheric disturbances associated with earthquakes by using the HF Doppler sounding system.
The HF Doppler observation (HFD) used in this study enables us to observe variations at several altitudes using different transmission frequencies (5.006, 6.055, 8.006 and 9.595 MHz). At first, we examined the ionospheric disturbances associated with the earthquake occurred at Hamadori, Fukushima Prefecture on April 11, 2011.
In the data observed at Iitate, where the HFD reflection point is the closest to the epicenter, the largest fluctuations of Doppler frequencies about 1.5Hz at 5.006MHz and 2.6Hz at 8.006MHz were observed. At Kakioka, where 6.055 MHz data was available, the frequency variation was about 1.2Hz. The ionospheric reflection altitudes for each frequency were calculated using the International Reference Ionosphere (IRI), and the reflection altitudes of the radiowaves received at Sugadaira were found to be about 193 km at 5.006 MHz, 230 km at 6.055 MHz, and 240 km at 8.006 MHz.
From these results, is is confirmed that the fluctuation in association with the earthquake whose magnetude is 7.0 spreads over 240 km from the epicenter. By examining the other events, we will study the relation ship between the magnetude of the earthquake and the spread of the coseismic ionospheric disturbances.

大規模な地震の発生後に地面変動や津波により生じた音波や大気重力波が電離圏高度まで伝搬し電離圏擾乱が発生することが知られている。地震に伴う電離圏擾乱の伝搬特性は GPS 観測等を用いた研究により、水平方向の伝搬については詳細に調べられてきたが、鉛直方向の伝搬に関する解析はきわめて少ない。現在電気通信大学を中心に行われている、HF ドップラー観測(HFD)では、日本全国に広がる観測点で複数の電波が受信できる観測システムであり、様々な電離圏変動の空間的な広がりを調べることが可能である。そこで本研究では地震に伴う電離圏擾乱の鉛直方向の伝搬特性に特に注目し解析を行った。
本研究で用いる HF ドップラー観測では、異なる送信周波数(5.006, 6.055, 8.006, 9.595 MHz)の電波を用いることで複数の高度で変動を観測できる。本研究ではまず地震は福島県浜通りで 2011 年 4 月 11 日に発生したマグニチュード 7.0 の地震に伴う変動について解析を行った。
HF 波の反射点が地震源に一番近い飯舘で取得されたデータでは、他の受信局と比べドップラー周波数の変動が大きく、5.006MHz で 1.5Hz、8.006MHz では 2.6Hz の変動が確認された。また、6.055MHz のデータの中で震源に近い柿岡では 1.2Hz 程度の変動であった。さらに、国際標準電離圏モデル(IRI)を用いて各周波数の電離圏反射高度を求めたところ、菅平では 5.006MHz で 193km、6.055MHz で 230km、8.006MHz で 240km 程度の反射高度となった。この結果から、M7 の地震では震源を中心に約 240km にわたる範囲に変動が伝搬していることが確認できた。今後事例を追加し、マグニチュードと変動の広がりについての関係を明らかにしていく。

R005-28
Zoom meeting C ：11/2　AM1　(9:00-10:30)
09:45-10:00

## GPS 電波掩蔽観測を用いた東北沖地震に伴う津波による電離圏擾乱の高度分布解析

#伏見　亮祐 [1)],中田　裕之 [2)],大矢　浩代 [3)]
[1)]千葉大・融合理工,[2)]千葉大・工・電気,[3)]千葉大・工・電気

## Vertical profiles of ionospheric disturbances caused by the tsunami of the Tohoku earthquake using GPS occultation observation

#Ryosuke Fushimi[1)], Hiroyuki Nakata[2)], Hiroyo Ohya[3)]
[1)]Science and Engineering, Chiba Univ.,[2)]Grad. School of Eng., Chiba Univ.,[3)]Engineering, Chiba Univ.

It is reported that ionospheric disturbances are caused by large earthquakes. One of the causes is the infrasound wave excited by surface waves and tsunami. The characteristics of the ionospheric disturbances horizontally propagating after large earthquakes have been examined by using a network of ground-based GPS receivers. On the other hand, the vertical propagation of ionospheric disturbances especially due to tsunamis is rarely reported. In this study, to examine the vertical propagation of the ionospheric disturbances due to tsunamis, we have examined electron density profiles observed by GPS radio occultation measurements of FORMOSAT-3/COSMIC satellites. We analyzed the ionospheric disturbances caused by a tsunami associated with Tohoku Earthquake (M9.0) occurred at 5:46:18 on 11th March 2011 (UTC). We analyzed density profiles observed within 3 hours after the passage of the tsunami focusing on the north Pacific Ocean. Extracting the fluctuation components from observed values of ionospheric electron densities using Chapman model, Short-wavelength fluctuations were observed compared to those observed on land. Fluctuation was also seen in the data observed near the Hawaiian Islands. However, the fluctuation is similar to the data observed on quiet days, further detailed analysis is necessary.

大規模な地震の発生後に電離圏擾乱が発生することが報告されている。これは、地面変動や津波により生じた音波や大気重力波が電離圏高度まで伝搬するためである。地震発生後の電離圏変動の水平方向の伝搬特性は、TEC 観測などを用いて明らかにされつつあるが、鉛直方向の伝搬を捉えた例は少ない。さらに、津波に伴う電離圏擾乱の鉛直方向伝搬の解析例は全くないと言ってよい。そこで、本研究では、東北沖地震により発生した津波に伴う電離圏擾乱の高度方向の変化について解析を行った。用いたデータは FORMOSAT-3/COSMIC 衛星による GPS 電波掩蔽観測で得られる電子密度の高度プロファイルデータである。2011 年 3 月 11 日 5 時 46 分 18 秒（協定世界時）に東北沖で発生した M9.0 の東北地方太平洋沖地震による津波の第 1 波到達後 3 時間以内に取得されたデータを抽出し、チャップマンモデルを用いてフィッティングを行い、観測データから変動成分の抽出を行った。北太平洋で得られたデータを中心に調べたところ、地上で見られる変動に比べ、波長の小さな変動が観測された。また、ハワイ諸島付近の観測データにおいても変動が観測された。ただし、静穏日における変動とも類似した点があるため、今後詳細な解析を行っていく予定である。

R005-29
Zoom meeting C ：11/2　AM1　(9:00-10:30)
10:00-10:15

## 赤道大気レーダーによる 2019 年 12 月の金環日食時の電離圏観測

#高木　理絵子[1)],横山　竜宏[1)],山本　衛[1)],Hozumi　Kornyanat[2)]
[1)]京大・生存圏研,[2)]NICT

## Ionospheric observations by Equatorial Atmosphere Radar during annular eclipse in December 2019

#Rieko Takagi[1)], Tatsuhiro Yokoyama[1)], Mamoru Yamamoto[1)], Kornyanat Hozumi[2)]
[1)]RISH, Kyoto Univ.,[2)]NICT

The area of the Earth's atmosphere above an altitude of about 80 km is called the ionosphere, where molecules and atoms are partially ionized. Since the electron density varies depending on altitude, time, and location, radio waves passing through the ionosphere are delayed or refracted, which cause satellite communication failures and degrade GPS positioning accuracy. It is required to monitor and predict ionospheric conditions accurately. A phenomenon called 150-km echoes is VHF radar backscatter echoes observed in the daytime near 150 km of the equatorial ionosphere. Although the generation mechanism of 150-km echoes is not yet clear, two types of echoes are known to exist: one from a naturally enhanced incoherent scattering (NEIS) process, which has a low SNR and SNR-dependent Doppler spectral width, and the other from the unstable growth of field-aligned irregularities (FAIs), which has a high SNR and SNR-independent Doppler spectral width. We study the equatorial ionospheric variations during the annular solar eclipse on Decembrer 26, 2019. It is known that a solar eclipse reduces the amount of sunlight when the moon passes in front of the sun in the daytime and affects the electron density distribution. We observed ionospheric irregularities in the E region with the Equatorial Atmosphere Radar (EAR) in West Sumatra, Indonesia, and the background ionospheric conditions with the ionosonde network in Southeast Asia. The annular solar eclipse occured above the EAR between 10:18 and 14:08 local time, with the maximum obscuration at 12:11.
We conducted a special ionospheric observation by the EAR from December 25 to 27, 2019 with high time resolution by focusing on the ionospheric E region. 150-km echoes were observed on the 25th and 27th, but not on the 26th, the day of the eclipse. The eclipse might suppress the occurrence of 150km echoes. The E-region echoes were observed on all three days at around 100 km altitude. Echoes were seen over a wide range of times around 90 km, and sometimes echoes were observed around 110 km. The Doppler velocity of the E-region echoes fluctuated about thirty minutes before the beginning of the eclipse. Doppler velocities became lower from about 9:30 to 11:30, increased from about 11:30 to 13:30, and then decreased again after about 13:30. Scatterplots of SNR and spectral widths for 150-km echoes show a population with a high SNR and SNR-independent Doppler spectral width on the 25th and 27th when 150-km echoes occurred. This suggests that the 150-km echoes observed by the EAR are produced by FAIs. Echoes from the NEIS could not be detected due to the lack of sensitivity of the EAR. The results of ionosonde observations show that the critical frequency of the F layer fluctuated with about an hour delay from the variation of the obscuration at all sites. Taking advantage of what we observed with two beams during the eclipse, we will synthesize the beams and analyze the east-west and north-south components of Doppler velocities. In addition, we will comprehensively analyze the results of previous EAR observations.

地球の大気の高度約 80km 以上の領域は電離圏と呼ばれ，分子や原子が一部電離した状態で存在している．電子密度は高度や時間，場所によって異なり，電離圏を通過する電波の遅延や屈折が発生し，衛星通信障害や GPS 測位精度低下の原因となるため，電子密度分布を正確に把握し予測することが求められている．150km エコーとは，日中に赤道電離圏の 150km 付近で観測される VHF レーダー後方散乱エコーである．150km エコーの発生原理はまだ明らかになっていないが，SNR が低く SNR に依存したドップラースペクトル幅を持つ NEIS（naturally enhanced incoherent scattering）過程によるものと，SNR が高く SNR に依存しないドップラースペクトル幅を持つ沿磁力線不規則構造（FAI: field-aligned irregularities）の不安定な成長によるものの 2 種類が存在することが知られている [Chau and Kudeki, 2013]．本研究では，2019 年 12 月 26 日の東南アジア付近における金環日食時の赤道域の電離圏の変動を解析した．日食期間中は，日中に太陽の前を月が通過することで日照量が低下し，電子密度分布に影響を与えることが知られている．インドネシア共和国西スマトラ州の赤道上にある赤道大気レーダー（EAR: Equatorial Atmosphere Radar）で E 地域の電離圏不規則構造を観測し，東南アジアのイオノゾンデネットワークで背景電離圏の状態を観測した．金環日食は，EAR 上空では現地時刻の 10:18 から 14:08 にかけて発生し，12:11 に最大食を迎えた．
EAR では，2019 年 12 月 25 日から 27 日にかけて電離圏 E 領域に焦点を当てた高時間分解能の電離圏特別観測を実施した．150km エコーは 25 日と 27 日には観測されたが，日食当日の 26 日には観測されなかった．日食が 150km エコーの発生を妨げた可能性がある．また，E 領域のエコーは 3 日とも高度 100km 付近で観測された．E 領域のエコーは 90km 付近で広範囲に観測され，110km 付近でエコーが観測されることもあった．また，26 日のドップラー速度と日照量の時間変化を比較したところ，ドップラー速度は日照量よりも 30 分程度早く変動していることがわかった．朝は 0 付近の値を取っていたドップラー速度は 9:30 から 11:30 にかけて減少し，11:30 から 13:30 にかけて

増加し，13:30 頃から再び減少して 0 付近の値を取った．最大食を迎えた 12 時過ぎのドップラー速度は 0 付近の値を取っていた．さらに，150km エコーについて SNR とスペクトル幅を比較したところ，150km エコーが発生した 25 日と 27 日に，SNR が高く SNR に依存しないドップラースペクトル幅を持つ集団が現れたため，EAR で観測された 150km エコーは FAI によるものであると思われる．NEIS からのエコーは，EAR の感度が低いために検出できなかった．イオノゾンデの観測結果からは，どの地点でも F 層の臨界周波数が日照量の変化から約 1 時間遅れて変動していたことがわかった．今後は，金環日食中に 2 ビームで観測したことを活かして，ビームの合成を行いドップラー速度の東西・南北成分を解析する．また，過去の EAR の観測結果を総合的に解析する．

R005-30
Zoom meeting C ：11/2　AM2　(10:45-12:30)
10:45-11:00

## 太陽放射スペクトルの変動による熱圏・電離圏の応答

#陣　英克[1)],三好　勉信[2)],垰　千尋[1)],品川　裕之[1)],藤原　均[3)]
[1)]情報通信研究機構,[2)]九大・理・地球惑星,[3)]成蹊大・理工

## Response of ionosphere and thermosphere to solar irradiance variations

#Hidekatsu Jin[1)], Yasunobu Miyoshi[2)], Chihiro Tao[1)], Hiroyuki Shinagawa[1)], Hitoshi Fujiwara[3)]
[1)]NICT,[2)]Dept. Earth & Planetary Sci, Kyushu Univ.,[3)]Faculty of Science and Technology, Seikei University

Solar flares cause its irradiance variations, which result in increase of ionospheric electron density as well as thermospheric heating and expansion. One of the aims of PSTEP project is to construct a hazard map of space weather effects on human activities in space. For this purpose, we have changed the solar irradiance model used in a whole atmosphere-ionosphere coupled model GAIA so it can treat temporal solar irradiance variations in X to EUV bands. In this presentation, we present several simulation results of solar flare events to discuss validation of physical and chemical processes in the ionospheric and thermospheric responses to flares, and their effects on atmospheric drag and radio propagation.

太陽フレアの発生時には幅広い波長域の太陽放射光強度が増加し、電離圏イオン・電子密度の一時的な増加、熱圏の加熱と膨張を引き起こす。こうした超高層大気の変化は、電波の減衰や大気抵抗の増加など宇宙利用に影響をもたらす。PSTEP プロジェクトでは実際どの程度影響するかをハザードマップとして調査することを一つの目的としている。我々は全地球大気圏電離圏モデル GAIA について、これまで F10.7 を唯一のパラメータとする EUV 帯の太陽放射モデルを入力していたところ、今回太陽放射モデルを変更し、X 線～EUV 領域のスペクトルの時間変化に対する超高層大気の応答を GAIA で扱えるようにした。本発表では、幾つかの太陽フレアによる熱圏・電離圏の応答を GAIA でシミュレーションを行い、観測との比較により物理・化学過程を検証するとともに、大気抵抗など宇宙利用への影響について議論する。

R005-31
Zoom meeting C ：11/2　AM2　(10:45-12:30)
11:00-11:15

## GAIA モデルとの結合に向けた赤道プラズマバブルシミュレーションの改良

#古元　泰地[1)],横山　竜宏[1)]
[1)]京大生存研

## Upgrade of equatorial plasma bubble simulation toward coupling with GAIA model.

#Taichi Komoto[1)], Tatsuhiro Yokoyama[1)]
[1)]RISH, Kyoto Univ.

In recent years, as space development has advanced, high-precision, high-reliability communication, positioning, and navigation using GPS etc. are being put to practical use. The ionosphere is a transition region that connects the lower atmosphere and space, in which many artificial satellites orbit, and at the same time, that affects satellites radio waves and causes delays. The effect of radio wave delay due to the ionosphere becomes large relative to the required accuracy, and in order to correct it, there is a strong demand for understanding of the physical process of the ionosphere, the current situation, and its prediction. However, the observation means of the ionosphere are limited, and only limited temporal and spatial information can be obtained. Therefore, simulation is an effective means. Plasma bubbles are phenomena that occurs at low-latitude ionosphere. Low density region rises like bubbles due to the instability of the density stratification. Since the inside of the bubbles is very unstable and contains irregular structures, it has a great influence on the radio waves propagation. The purpose of this study is to connect the local ionospheric numerical model and the global ionospheric numerical model in a hierarchical manner, using their strength and making up for their shortcomings, and to develop a numerical model that can predict the plasma bubbles generation self-consistently. This is expected to be useful for understanding the relationship between various spatial scale phenomena and plasma bubbles generation. At this stage, we succeeded in converting the local ionospheric numerical model to whole longitude and confirmed the convergence of the calculation of electrostatic potential. The boundary condition at the top boundary is modified by giving a sine wave (a wavelength per day) that is considered to be similar to real longitudinal electric field variation. The obtained electric field distribution is in good agreement with the vertical drift velocity that could be calculated from the IRI model.

昨今、宇宙開発が進み GPS 等を利用した高精度、高信頼度の通信、測位、航法が実用化されつつある。電離圏は、下層大気と宇宙空間を繋ぐ遷移領域であり、 多くの人工衛星が周回する領域であると同時に、衛星電波が遅延等の影響を受ける伝搬経路でもある。電離圏による電波遅延の影響は、要求される精度に対して相対的に大きくなってきており、その補正のために、 電離圏の物理過程の理解、現状把握(ナウキャスト)、 そしてその予測が強く求められている。しかし、電離圏の観測手段は限られており、時間的、空間的に断片的な情報しか得ることができない。そのため、シミュ レーションが有効な手段となる。プラズマバブルは電離圏下部の密度成層が不安定化し、低密度領域が泡のように上昇する現象である。泡の内部は非常に不安定で不規則な構造をしているため、周辺を通過する電波に大きな影響を及ぼす。本研究の目的は、局所電離圏数値モデルと、全球電離圏数値モデルを階層的に結合させることで、それぞれの長所を活かし、短所を補った、プラズマバブルの発生を自己無撞着に予測できる数値モデルの開発である。これにより、様々な空間スケールの現象とプラズマバブル発生の関連の解明に役立つことが期待される。現段階では、局所モデルの全経度化に成功し、ポテンシャルの計算の収束を確認することができた。この際の境界条件の変更として、上空側の経度方向に、現実に比較的近いと考えられる正弦波(1 日を 1 波長)のポテンシャルを与えて計算を行ったところ、得られた電場分布は、IRI モデルから計算できる鉛直ドリフト速度によく一致した結果を得ることができた。

R005-32
Zoom meeting C ：11/2　AM2　(10:45-12:30)
11:15-11:30

## 赤道プラズマバブルの急速な発達と中緯度帯への影響

#横山　竜宏[1)],品川　裕之[2)],陣　英克[2)],大塚　雄一[3)]
[1)]京大生存研,[2)]情報通信研究機構,[3)]名大宇地研

## Effect of rapidly growing equatorial plasma bubbles on midlatitude region

#Tatsuhiro Yokoyama[1)], Hiroyuki Shinagawa[2)], Hidekatsu Jin[2)], Yuichi Otsuka[3)]
[1)]RISH, Kyoto Univ.,[2)]NICT,[3)]ISEE, Nagoya Univ.

Equatorial plasma bubble (EPB) is a well-known phenomenon in the equatorial ionospheric F region. As it causes severe scintillation in the amplitude and phase of radio signals, it is important to understand and forecast the occurrence of EPB from a space weather point of view. In order to simulate the instability in the equatorial ionosphere, a 3D High-Resolution Bubble (HIRB) model has been developed. It provides a unique opportunity to study the development of EPBs under various conditions. During a severe space weather event, intense penetration electric fields are expected even in the equatorial ionosphere. If the penetration electric fields enhance the pre-reversal enhancement of the eastward electric field in the dusk sector, the growth rate of the Rayleigh--Taylor instability is greatly intensified to force EPBs to reach very high apex altitude. Such EPBs can reach midlatitude regions along the flux tubes with very high apex altitude and cause communicaton/navigation outage in midlatitude. We will expand the simulation domain of the HIRB model to cover the midlatitude region, for example the latitude of Tokyo area, and estimate the background conditions under which EPBs can reach and affect the midlatitude ionosphere. $H^+$ ion should be included in addition to the original $NO^+$ and $O^+$ ions. Previous observations of such extreme events will be compared with the simulation results.

赤道電離圏においては、赤道スプレッド F/プラズマバブルと呼ばれる現象の研究が古くから行われている。プラズマバブルに伴う局所的なプラズマ密度の不規則構造が発生した場合には、電波の振幅、位相の急激な変動、すなわちシンチレーションが生じるため、GPS 等による電子航法に深刻な障害を及ぼすことが知られている。現在までに開発を進めてきた High-Resultion Bubble (HIRB)モデルは、プラズマバブルの成長・発達過程の様々な側面を明らかにすることを可能とした。太陽フレア等に伴う強い磁気嵐が発生した場合、極域に印加された電場が赤道域にまで侵入する場合がある。この侵入電場が日没付近の東向き電場に重畳した場合、非常に高高度まで到達するプラズマバブルが発生する可能性がある。実際、強い磁気嵐時に日本の緯度付近にまで到達するプラズマバブルの報告例が存在する。そこで、HIRB モデルのシミュレーション領域を中緯度域、例えば東京付近の緯度までを含むように拡張する。具体的には、$NO^+$と $O^+$のみであったイオン種に $H^+$を追加し、上部電離圏までのシミュレーションを行えるよう修正を加える。強い電場が印加された場合にさらに高高度へプラズマバブルが成長する様子を再現し、プラズマバブルの影響が中緯度域にまで及ぶ可能性について検討する。

R005-33
Zoom meeting C ：11/2 AM2 (10:45-12:30)
11:30-11:45

# GPS Total Electron Content Observation of Plasma Bubbles Surviving in the Daytime during Recovery Phase of Geomagnetic Storm

#Yuichi Otsuka[1)], Atsuki Shinbori[1)], Takuya Sori[2)], Takuya Tsugawa[3)], Michi Nishioka[3)]
[1)]ISEE, Nagoya Univ.,[2)]ISEE, Nagoya Univ.,[3)]NICT

Plasma bubble is a localized plasma density depletion in the ionosphere. The plasma bubble is generated at the magnetic equator through the Rayleigh-Taylor instability and extend to higher altitudes and latitudes with a structure elongating along the magnetic field line. For the generation of plasma bubble, eastward electric field pay an important role. In general, plasma bubbles are generated at the evening terminator, survive during nighttime, and disappear after sunrise due to the plasma production by solar EUV radiation. During magnetic storms, the plasma bubbles can be generated around midnight and/or near sunrise. In this study, we found that plasma bubbles generated near sunrise reached middle latitudes during a recovery phase of geomagnetic storm, and survived until noon.
We have analyzed GPS data in Japan to investigate temporal variation of horizontal two-dimensional distribution of total electron content (TEC) during a geomagnetic storm on May 28 2017. Dst index reached -125 nT at 08 UT on May 28, 2017. TEC depletions extending up to approximately 38° N in the meridional direction appeared sequentially over Japan around 20 UT on May 28 (05 JST on May 29), when TEC rapidly increased at sunrise due to the solar EUV radiation. The TEC depletions could be caused by plasma bubbles. The TEC depletions disappeared around noon on May 29. In this event, the plasma bubbles over Japan survived for approximately 7 hours in the sunlit condition. The background TEC was approximately 15 TECU at 20 UT on May 28 (05 JST on May 29) when the plasma bubble appeared over Japan, and approximately 12 TECU during 00-04 UT (09-13 JST) on May 29. In this event, the plasma density in the ionosphere did not increased after the plasma bubble appearance over Japan so that the plasma density during daytime would not be large enough to fill the plasma depletions caused by the plasma bubbles. This could be a reason why the plasma bubbles survived during the daytime in this event.

R005-34
Zoom meeting C ：11/2 AM2 (10:45-12:30)
11:45-12:00

# Occurrence feature of plasma bubbles during geomagnetic storms using long-term GNSS-TEC data

#Takuya Sori[1)], Atsuki Shinbori[2)], Yuichi Otsuka[3)], Takuya Tsugawa[4)], Michi Nishioka[5)]
[1)]ISEE, Nagoya Univ.,[2)]ISEE, Nagoya Univ.,[3)]ISEE, Nagoya Univ.,[4)]NICT,[5)]NICT

Plasma bubbles are generated in the bottomside F region of the nighttime equatorial ionosphere after sunset by the Rayleigh-Taylor instability (RTI) mechanism [e.g., Farley et al., 1970; Kelley, 2009]. The growth rate of RTI depends on an intensity of eastward electric fields and an ionospheric altitude, and enhances with an increase of both parameters. The pre-reversal enhancement in the evening sector of the equatorial ionosphere, that is, an eastward electric field intensified at sunset, is believed to be the major contributor to a significant enhancement of the RTI growth rate [Rezende et al., 2007]. On the other hand, during a geomagnetic storm, the two main disturbance electric fields responsible for changes in the equatorial plasma drifts and current perturbations are the prompt penetration electric fields and the ionospheric disturbance dynamo electric fields, respectively. Although each electric field is believed to contribute to the generation of the equatorial plasma bubbles in the dusk and dawn sectors, respectively, the statistical view of the response of the plasma bubble generation to the storm-time electric fields has not yet been established. In this study, we analyzed total electron content (TEC) and rate of TEC index (ROTI) [Pi et al., 1997] data obtained from global navigation satellite system (GNSS) receivers over the world during 2000?2018 to investigate temporal and spatial variations of storm-time plasma bubbles and clarify causes of them.
We defined the SYM-H variations with the minimum value of less than -40 nT as a geomagnetic storm event, and identified 652 events during 2000?2018. For these storm events, we investigated the relationship between temporal and spatial variations of ROTI and other parameters (solar wind and geomagnetic indexes) in these events with a superposed epoch analysis. In this analysis, we defined the time of minimum value of SYM-H index as the zero epoch. As a result, an enhanced ROTI region appeared within 20o in geomagnetic latitude (GMLAT) between 19.5 and 0.5 MLT (magnetic local time) under the geomagnetically quiet conditions before the onset of the geomagnetic storms. During the main phase of the geomagnetic storms, the enhanced ROTI region expanded to the higher latitude. The upper limit of the latitude tended to increase with an increasing intensity of the geomagnetic storms. After that, the enhanced ROTI region moved to the post-midnight sector with time and another enhanced ROTI region appeared in the post -midnight to dawn sectors between 2 and 5 MLT during the recovery phase. On the other hand, the enhanced ROTI region in the dusk sector weakened within 15o (GMLAT) and was confined only between 20 and 22.5 MLT during the recovery phase.
Averaged ROTI values at the magnetic equator increased between 19 and 20.5 MLT during the late main phase of geomagnetic storms, corresponding to the enhancement of an averaged dawn-to-dusk component of interplanetary electric field. During the recovery phase of geomagnetic storms, the averaged ROTI values at the magnetic equator increased between 1 and 6 MLT while those at the magnetic equator decreased between 19.5 and approximately 1 MLT. Fejer et al. [2008] reported that the prompt penetration electric field is directed westward between the midnight and dawn sectors (0?7 h local time) and eastward between the dusk and midnight sectors (18?24 h local time). The disturbance dynamo electric field is directed eastward between the dusk and dawn sector (21?7 h local time) and westward in the dusk sector (18?21 h local time).
From these results, the plasma bubbles can be generated in the dusk sector due to the under-shielding prompt penetration electric field (eastward electric field) during the main phase of geomagnetic storms. Due to the over-shielding prompt penetration electric field or disturbance dynamo electric field, they can be generated in the post-midnight and dawn sectors (eastward electric field) and suppressed in the dusk sector (westward electric field) during the recovery phase.

R005-35
Zoom meeting C ：11/2　AM2　(10:45-12:30)
12:00-12:15

## 機械学習を用いたイオノグラムにおけるスプレッド F 自動検出

#清水　淳史[1)],中田　裕之[1)],大矢　浩代[1)],鷹野　敏明[1)]
[1)]千葉大・工・電気

## Automatic detection of Spread-F on ionogram using Machine Learning

#Junji Shimizu[1)], Hiroyuki Nakata[1)], Hiroyo Ohya[1)], Toshiaki Takano[1)]
[1)]Grad. School of Eng., Chiba Univ.

Ionospheric irregularities referred to as equatorial spread-F are very significant phenomena in radio wave propagation because their spatial scales are from centimeters to tens of kilometers, and they affect wide-band radio waves. Therefore, they influence the reliability of satellite-ground communications, navigation systems,　and so on.　The ionozonde is one of the important observation systems of the ionosphere. The spread F is the scattered traces in the ionogram, which is a visualization plot of the received data by ionosonde. Convensionally, the detection of spread-F in the ionogram is done manually by naked eye.　If spread-F in the ionogram is detected automatically by developing an excellent machine learning system, real time detection of spread-F could be replaced with automatic detection by developing an unique machine learning system.　Therefore, we have developed an automatic detection of spread-F in the ionogram using machine learning.
In this study, we used ionograms observed at Okinawa throughout 2018 utilized by National Institute of Information and Communications Technology.　In this presentation, as learning images, we prepared 100 images of frequency type spread F, 100 images of range type spread F.　As traces other than spread F, we also utilized 50 images of normal E region traces and 50 images of F region traces. These data were increased by adding noise in 8 ways.　These images were trained for each class using an object detection method called YOLO (You Only Look Once).
Using the trained data to detect spread-F in the nest of ionograms of Okinawa in 2018 which are not used as learning data, we confirmed identifying about 80% of frequency type and about 70% of range type.

赤道スプレッド F と呼ばれる電離圏の不規則性は、電波の伝播という観点から非常に重要な現象である。スプレッド F に伴う電離圏擾乱の空間スケールはセンチメートルから数十キロメートルであり、極めて広帯域の電波に影響を与える。したがって、それらは衛星地上通信、ナビゲーションシステムなどの信頼性にも影響を与える。
イオノグラムは、スプレッド F の重要な観測システムの 1 つである。従来イオノグラム内のスプレッド F の検出は手動で行われているので、優れた機械学習システムを開発することによってスプレッド F の検出を自動検出に置き換えることができれば、リアルタイムのスプレッド F の検出も可能になる。そこで、機械学習を用いてイオノグラム中のスプレッド F を自動検出する手法を開発した。
本研究では、情報通信研究機構が沖縄の大宜見で運用している観測所で観測されたイオノグラムから周波数型とレンジ型のスプレッド F が現れているイオノグラムを用意した。今回の発表では、2018 年を通して沖縄にて観測された周波数型スプレッド F を 100 枚、レンジ型スプレッド F を 100 枚、スプレッド F 以外の主なトレースとして E 層トレースを 50 枚、拡散していない F 層トレースを 50 枚用意し、8 通りのノイズ付加をすることによりデータ拡張したものを学習画像として用いた。この画像群に対して YOLO(You Only Look Once)と呼ばれる物体検出手法を用いて各クラス学習させた。この学習データを用いて学習に用いなかった 2018 年の沖縄のイオノグラムに対して検出を行ったところ周波数型は 8 割程度、レンジ型は 7 割程度のスプレッド F の識別が確認できた。

R005-36
Zoom meeting C ：11/2　AM2　(10:45-12:30)
12:15-12:30

## O/X モード分離のイオノグラムを用いた電離圏パラメータ自動抽出手法の改善

#西岡　未知[1)],前野　英生[1)],津川　卓也[1)],石井　守[1)]
[1)]情報通信研究機構

## Improvement of automatic scaling technique of ionospheric parameters using O/X separated ionograms

#Michi Nishioka[1)], Hideo Maeno[1)], Takuya Tsugawa[1)], Mamoru Ishii[1)]
[1)]NICT

National Institute of Information and Communications Technology (NICT) has been observing ionosphere by ionosondes for over 70 years in Japan in order to monitor ionospheric conditions. Currently, four ionosonde systems are routinely operated at four stations at Wakkanai (Sarobetsu, Hokkaido), Kokubunji (Toykyo), Yamagawa (Kagoshima), Okinawa (Ogimi, Okinawa). Automatic scaling of an ionogram, which is a diagram of time-of-flight against transmitted frequency, is one of the important techniques for real-time monitoring. The automatic scaling technique has been developed and implemented since the late 1980s. It has developed through trails and errors, however, the complexity of the ionospheric echoes which both Ordinary mode (O-mode) and Extra-ordinary mode (X-mode) exist makes it difficult to scale them properly. In 2016-2017, we replaced our ionosonde system with a new system, Vertical Incidence Pulsed Ionospheric Radar 2 (VIPIR2) ionosonde. One of the advantages of VIPIR2 is a receiving antenna array, which makes it possible to separate O-mode from X-mode by utilizing in-phase and quadrature data. The O/X mode separated ionograms are used for automatic scaling with artificial intelligence (AI) technique. The AI model is trained using manually scaled data and the corresponding ionograms for four stations. The method was validated with one-year foF2 data in 2018 for four stations. The scaling accuracy is improved from 80.0% to 99.8%. The successful rate of scaling is also improved from 0.26MHz to 0.12MHz for foF2. The new auto-scaling method is applied from Jan. 2020. The auto-scaled parameters are provided through our web site in real-time: http://wdc.nict.go.jp/IONO/HP2009/ISDJ/auto_txt.html. In presentation, we will overview the new automatic scaling procedure and give some example which is now possible to detect automatically using the new automatic scaling tool.

R005-37
Zoom meeting C ：11/2 PM1 (13:45-15:30)
13:45-14:00

## Complementing regional ground GNSS-STEC computerized ionospheric tomography (CIT) with ionosonde data assimilation

#Nicholas Ssessanga[1)], Mamoru Yamamoto[1)], Susumu Saito[2)], Akinori Saito[3)], Michi Nishioka[4)]
[1)]RISH, Kyoto Univ.,[2)]ENRI, MPAT,[3)]Dept. of Geophysics, Kyoto Univ.,[4)]NICT

The accurate probing of the three-dimensional (3-D) structure of the ionosphere endures a unique set of challenges that include, for example, high campaign costs, poor distribution of instruments and collected data, and geometric limitations. To remedy these challenges, over the East-Asian sector (covering 110?160 E and 10 ?60 N, and extending from 80 to 20,000 km in altitude) a near-realtime regional 3-D computerized ionospheric tomography (CIT) technique has been developed using a plethora of GNSS (Global Navigation Satellite System) observations of total electron content. Prior to in-operation applications, studies validated the CIT results using ionosonde, middle-upper atmosphere radar and occultation data and found the technique to adequately reconstruct the regional ionosphere vertical structure, however, with room for improvement in estimating the peak height and avoiding physically unrealistic negative densities in the final solution. We present preliminary results from a technique that addresses these issues by incorporating CIT results into a data assimilation (DA) technique. The DA technique adds ionosonde bottomside measurements into CIT results, thereby improving the accuracy of the reconstructed bottomside 3-D structure. More specifically, on average CIT NmF2 and hmF2 get an above 60% improvement. Further, during analysis, ionosphere electron densities are assumed to be better described by probability log-normal distribution, which introduces the positivity constraint that is mandatory in ionospheric imaging.

R005-38
Zoom meeting C ：11/2　PM1　(13:45-15:30)
14:00-14:15

## 全球 GNSS-TEC とあらせ衛星観測による中緯度トラフとプラズマ圏界面の位置関係

#新堀　淳樹[1)],大塚　雄一[2)],津川　卓也[3)],西岡　未知[3)],熊本　篤志[4)5)],土屋　史紀[5)],松田　昇也[6)],笠原　禎也[7)],松岡　彩子[8)]
[1)]名大・宇地研,[2)]名大宇地研,[3)]情報通信研究機構,[4)]東北大・理・地球物理,[5)]東北大・理・惑星プラズマ大気,[6)]ISAS/JAXA,[7)]金沢大,[8)]京都大学

## Relationship between the locations of the mid-latitude trough and plasmapause by global GNSS-TEC and Arase satellite measurements

#Atsuki Shinbori[1)], Yuichi Otsuka[2)], Takuya Tsugawa[3)], Michi Nishioka[3)], Atsushi Kumamoto[4),5)], Fuminori Tsuchiya[5)], Shoya Matsuda[6)], Yoshiya Kasahara[7)], Ayako Matsuoka[8)]
[1)]ISEE, Nagoya Univ.,[2)]ISEE, Nagoya Univ.,[3)]NICT,[4)]Dept. Geophys, Tohoku Univ.,[5)]Planet. Plasma Atmos. Res. Cent., Tohoku Univ.,[6)]ISAS/JAXA,[7)]Kanazawa Univ.,[8)]Kyoto University

The equatorial plasma density structure in the vertical direction above the F-region of the ionosphere shows a gradual decrease with an increasing L-value and the plasma density sharply decreases around L = 4-6. This boundary and the inner region with a high plasma density has been called the plasmapause and plasmasphere, respectively (Carpenter, 1966). The plasmapause is formed at the location of counteraction of corotation and dawn-to-dusk convection electric fields in the magnetosphere (Nishida, 1966). Therefore, when the convection electric field is intensified associated with geomagnetic disturbances, the plasmapause moves toward the Earth. On the other hand, the mid-latitude trough is characterized by a significant plasma depletion in the F-region of the ionosphere at sub-auroral and mid-latitudes below the auroral oval. The structure of the mid-latitude trough shows a latitudinally narrow density depletion with a wide longitudinal extent. The mid-latitude trough is believed to be formed by four processes: flow stagnation (Kelley, 2009), transportation and frictional heating by SAID/SAPS (Spiro et al., 1979), auroral particle precipitation and the replenishment of plasma from the nighttime plasmasphere (Roger et al., 1986). These two structures in between the ionosphere and inner magnetosphere are generally believed to appear on the same magnetic field line. Recently, Shinbori et al. (2018) also reported that the location of the plasmapause almost agrees with that of the mid-latitude trough minimum during a geomagnetic storm that occurred on April 4 2017 from a comparison between the electron density in the inner magnetosphere obtained from the Arase satellite and global navigation satellite system (GNSS) ? TEC observations. In this study, we analyze long-term observation data of global GNSS-TEC and electron density in the inner magnetosphere obtained from the Arase satellite with high time and spatial resolutions to clarify the relationship between the locations of the plasmapause and mid-latitude trough minimum during geomagnetically quiet times, main and recovery phases of geomagnetic storms. In this analysis, we identify the mid-latitude trough minimum as a minimum value of GNSS-TEC at sub-auroral and mid-latitude regions, and determine the plasmapause as an electron density decrease by a factor of 3-5 or more within ?L < 0.5 in the inner magnetosphere. As a result, the position of the plasmapause does not always coincide with the mid-latitude trough minimum in all magnetic local time (MLT) sectors under all geomagnetic conditions. During the geomagnetically quiet periods, the mid-latitude trough minimum is located at a lower geomagnetic latitude (GMLAT) of the plasmapause except for the evening sector (16?19 h, MLT). This implies that the mid-latitude trough and plasmapause may not be on the same magnetic field line. On the other hand, during the main phase of geomagnetic storms, the mid-latitude trough minimum and plasmapause move toward a low-latitude region with day-night and dawn-dusk asymmetries and the correlation becomes highest, compared with other geomagnetic conditions. This suggests that the formation of the mid-latitude trough and erosion of the plasmasphere occur on almost the near magnetic field line due to an enhancement of convection electric field and sub-auroral polarization stream during the main phase of geomagnetic storms.

R005-39
Zoom meeting C ：11/2　PM1　(13:45-15:30)
14:15-14:30

# ハワイで得られた大気光画像に見られる大気重力波と MSTID の相関及びこれらの波動と対流圏上昇流の相関

#内藤　豪人[1)],塩川　和夫[1)],大塚　雄一[1)],藤波　初木[1)],坂野井　健[2)],齊藤　昭則[3)],中村　卓司[4)]
[1)]名大宇地研,[2)]東北大・理,[3)]京都大・理・地球物理,[4)]極地研

# Correlation between AGWs and MSTIDs in airglow images obtained in Hawaii and their relation with the tropospheric upward flow

#Hideto Naito[1)], Kazuo Shiokawa[1)], Yuichi Otsuka[1)], Hatsuki Fujinami[1)], Takeshi Sakanoi[2)], Akinori Saito[3)], Takuji Nakamura[4)]
[1)]ISEE, Nagoya Univ.,[2)]Grad. School of Science, Tohoku Univ.,[3)]Dept. of Geophysics, Kyoto Univ.,[4)]NIPR

Atmospheric gravity waves (AGWs) and medium-scale traveling ionospheric disturbances (MSTIDs) are important wave phenomena in the upper atmosphere, since they can control global dynamics of the atmosphere and affect GNSS positioning. These waves can be visualized through nighttime airglow imaging. Matsuda et al. [JGR, 2014] proposed a method of deriving the horizontal phase velocity of the power spectral density of waves found in images using three-dimensional Fast Fourier transform. Matsuda et al. [JGR, 2017] applied this method to the airglow images obtained at Syowa (69oS, 40oE), Davis (69oS, 78oE), McMurdo (78oS, 167oE), and Halley (76oS, 27oW), the Antarctic. Takeo et al. [JGR, 2017] applied the method to the airglow images obtained at Shigaraki, Japan (35oN, 136oE). Perwitasari et al. [AnnGeo, 2018] applied the method to the airglow images obtained at Syowa, Shigaraki, and Tomohon, Indonesia (1oN, 122oE). Tsuchiya et al. [JGR, 2018, 2019, 2020] applied the method to the airglow images obtained at Rikubetsu, Japan (44oN, 144oE), Athabasca, Canada (55oN, 247oE), and Magadan, Russia (60oN, 151oE). However, there have been no study of using this method for airglow images obtained at Hawaii whose latitude, longitude, and orography are greatly different from the above observation points. In this study, we applied the analysis method of Matsuda et al. [2014] to the airglow images obtained at wavelengths of 557.7 nm and 630.0 nm during the three years from 2013 to 2016 at Haleakala (21oN, 156oW) in Hawaii. The purpose of this study is to clarify the characteristics and generation mechanism of AGWs and MSTIDs.

We investigated the source of AGWs from the tropospheric upward flow using seasonal averages of reanalysis data in the troposphere. As a result, the upward flow in the troposphere was not strongly observed in the area where the wave source was expected. This is probably due to significant day-to-day variabilities of the tropospheric upward flow which are averaged if we take the seasonal averages. Thus we also used the tropospheric upward flow for each event which is obtained every 4 hours. As a result, the correspondence rate between the upward flow in the troposphere and AGWs was ~70%. This is because of active convection in Hawaii which is located in the subtropical zone. Dependences of the correspondence on season and propagation direction are not discernible in the statistics. These results are consistent with the result reported by Perwitasari et al. [AnnGeo, 2018] that AGWs above Tomohon do not have a specific propagation direction and were caused by upward flow. In the presentation we will also report the correspondence between the upward flow in the troposphere and the power spectral density of AGWs.

The power spectral density of MSTIDs was strongest in winter and the waves propagate mainly in the east-west direction. We consider the possibility of generating these MSTIDs by AGWs in the thermosphere. We investigated the source of the AGWs in the thermosphere from the upward flow in the troposphere using seasonal averages of the reanalysis data. The upward flow in the troposphere was not strongly observed in the east-west direction of Hawaii. Thus we also used the tropospheric upward flow for each event which is obtained every 4 hours. The correspondence rate between the upward flow in the troposphere and MSTIDs was about 68%. This is because of active convection in Hawaii which is located in the subtropical zone. Dependences of the correspondence on season and propagation direction are not discernible in the statistics. We will also report the correspondence between the upward flow in the troposphere and the power spectral density of MSTIDs and the relation between the power spectral density of mesospheric AGWs and MSTIDs.

超高層大気の波動現象である大気重力波や中規模伝搬性電離圏擾乱（MSTID）は、大気のグローバルな循環や衛星測位に大きな影響を与えることが知られている。夜間大気光の撮像を通して、これらの波動を可視化することができる。Matsuda et al. [JGR, 2014]は、3 次元高速フーリエ変換を用いて大気光画像中に見られる波のパワースペクトル密度の水平位相速度分布の導出手法を提案した。この手法は、Matsuda et al. [JGR, 2017]によって南極大陸の昭和基地（69oS, 40oE)及びデイビス基地（69oS, 78oE)及びマクマード基地（78oS, 167oE)及びハリー基地（76oS, 27oW)、Takeo et al. [JGR, 2017]によって滋賀県の信楽（35oN, 136oE)、Perwitasari et al. [AnnGeo, 2018]によって昭和基地及び信楽及びインドネシアのトモホン（1oN, 122oE)、Tsuchiya et al. [JGR, 2018, 2019, 2020]によって北海道の陸別（44oN, 144oE)及びカナダのアサバスカ（55oN, 247oE)及びロシアのマガダン（60oN, 151oE)で得られた大気光画像に適用された。しかし、この手法を上述の観測点と緯度・経度・地形が大きく異なるハワイのハレアカラ観測点(21oN, 156oW)で得られた大気光画像の解析に用いた例はない。ハワイは周りが海に囲まれていて、高い山

が点在するという他とは異なる地形を持つ。本研究は、ハレアカラ観測点で 2013 年から 2016 年の 3 年間に得られた波長 557.7 nm と 630.0 nm の大気光画像に Matsuda et al. [JGR, 2014]の解析方法を適用し、ハワイ上空の大気重力波と MSTID の特徴と生成機構を明らかにすることを目的としている。

大気重力波の波源について、対流圏の再解析データの季節平均を用いて、対流圏の上昇流から季節ごとに考察を行った。その結果、大気重力波の波源が期待される方向に対流圏の強い上昇流は見られなかった。これは季節平均を取った際に、日々の変動が激しい対流圏の上昇流が平均化されたことが原因である可能性があるため、4 時間ごとに得られたイベントごとに対流圏の上昇流との比較を行った。この結果、対流圏の上昇流と大気重力波の対応率がおよそ 70%であった。これはハワイが亜熱帯に位置し対流が活発であるためだと考えられる。また、対応率の季節依存性や伝搬方向依存性は統計誤差の範囲内であり、統計的に有意な差ではなかった。これらの結果は Perwitasari et al. [AnnGeo, 2018]によって報告されたトモホン上空の大気重力波の伝搬方向が特定の方向に決まっておらず、それらが対流によって生成されると考えられることと一致している。講演ではさらに、対流圏の上昇流と大気重力波の対応をさらに詳しく考察するために、上昇流の速度と大気重力波のパワースペクトル密度の相関解析を行った結果も発表する。

MSTID においては、パワースペクトル密度に関しては冬が最も強く、主に東西方向に波が伝搬していたことから、その生成機構は熱圏の大気重力波によるものだと考えられる。この MSTID の生成に関わる、熱圏の大気重力波の波源を調べるために、同様に対流圏の再解析データの季節平均を用いて、対流圏の上昇流から季節ごとに考察を行った。その結果、波源が期待される東西方向に強い対流圏の上昇流は見られなかった。これは季節平均を取った際に、日々の変動が激しい対流圏の上昇流が平均化されたことが原因である可能性があるため、4 時間ごとに得られたイベントごとに対流圏の上昇流との比較を行った。その結果、MSTID と対流圏の上昇流の対応率がおよそ 68%であることがわかった。これもハワイが亜熱帯に位置し対流が活発であるからだと考えられる。また、対応率の季節依存性や伝搬方向依存性は統計誤差の範囲内であり、統計的に有意な差ではなかった。講演ではさらに、対流圏の上昇流と MSTID の対応をさらに詳しく考察するために、上昇流の速度と MSTID のパワースペクトル密度の相関解析、中間圏の大気重力波と MSTID のパワースペクトル密度の相関解析を行った結果も発表する。

R005-40
Zoom meeting C ：11/2　PM1　(13:45-15:30)
14:30-14:45

## 高緯度の大気光画像とあらせ衛星を用いた中規模伝搬性電離圏擾乱の複数例解析

#川合　航輝[1)],塩川　和夫[1)],大塚　雄一[1)],大山　伸一郎[1)2)11)],門倉　昭[2)],田中　良昌[2)],笠羽　康正[3)],中村　紗都子[1)],笠原　禎也[4)],熊本　篤志[3)],小路　真史[1)],土屋　史紀[3)],松岡　彩子[5)],今城　　峻[1)],風間　洋一[6)],Wang Shiang-Yu[6)],Tam Sunny W. Y.[7)],Chang Tzu-Fang[7)],Wang B.-J.[6)],浅村　和史[8)],笠原　慧[9)],横田　勝一郎[10)],桂華　邦裕[9)],堀　智昭[1)],田　采祐[1)],Miyoshi Yoshizumi[1)]
[1)]名大 ISEE,[2)]国立極地研究所,[3)]東北大,[4)]金沢大,[5)]京都大,[6)]Academia Sinica,[7)]国立成功大,[8)]JAXA,[9)]東京大,[10)]大阪大,[11)]University of Oulu, Finland

## Multi-event analysis of MSTIDs using airglow images at high latitude and the Arase satellite

#Kouki Kawai[1)], Kazuo Shiokawa[1)], Yuichi Otsuka[1)], Shin-ichiro Oyama[1),2),11)], Akira Kadokura[2)], Yoshimasa Tanaka[2)], Yasumasa Kasaba[3)], Satoko Nakamura[1)], Yoshiya Kasahara[4)], Atsushi Kumamoto[3)], Masafumi Shoji[1)], Fuminori Tsuchiya[3)], Ayako Matsuoka[5)], Shun Imajo[1)], Yoichi Kazama[6)], Shiang-Yu Wang[6)], Sunny W. Y. Tam[7)], Tzu-Fang Chang[7)], B.-J. Wang[6)], Kazushi Asamura[8)], Satoshi Kasahara[9)], Shoichiro Yokota[10)], Kunihiro Keika[9)], Tomoaki Hori[1)], ChaeWoo Jun[1)], Yoshizumi Miyoshi[1)]
[1)]ISEE, Nagoya Univ.,[2)]National Institute of Polar Research,[3)]Tohoku Univ.,[4)]Kanazawa Univ.,[5)]Kyoto Univ.,[6)]Academia Sinica,[7)]National Cheng Kung University, Taiwan,[8)]JAXA,[9)]Tokyo Univ.,[10)]Osaka Univ.,[11)]University of Oulu, Finland

Additional co-author: Iku Sjinohara (Institute of Space and Astronautical Science, Japan Aerospace Exploration Agency)

Medium-scale traveling ionospheric disturbance (MSTID) is the electron density fluctuation in the ionosphere, which can have a big influence on the satellite positioning errors. The spatial scale of MSTID is ~100-1000 km. The MSTIDs generated by the E-region?F-region coupling and Perkins instabilities show mirrored structures at magnetically conjugate points in both the hemispheres [e.g., Otsuka et al., GRL, 2014]. If the electric field variation associated with the MSTID propagates along the magnetic field lines to the opposite hemisphere, it can be measured by a satellite situated on its way of propagation in the inner magnetosphere. The simultaneous observations of MSTID by airglow imagers and ionospheric satellite has been reported by Shiokawa et al. [JGR, 2003]. However, there are few studies on the plasma and field measurements of MSTIDs at magnetospheric altitudes, except for one event reported by our previous study (Kawai et al., JpGU-AGU2020, 2020). In this study, we give multiple examples of simultaneous observations of MSTID made by airglow imagers being operated at Gakona (62.39 N, 214.78 E), Alaska, and Husafell (64.67 N, 338.97 E), Iceland, and the Arase satellite in the inner magnetosphere. We investigate the MSTIDs observed by the airglow imager at Gakona on November 3, 2018 and February 26, 2019 and at Husafell on January 26, 2019 in detail. We find that the electric field and electron density variations observed by the Arase satellite are related to the structure of the MSTID observed in the 630.0-nm images. We discuss characteristics of plasma and electric and magnetic fields in the inner magnetosphere based on the observations by the airglow imagers and Arase.

追加共著者: 篠原 育 (宇宙航空研究開発機構)

中規模伝搬性電離圏擾乱(MSTID)は、電離圏の電子密度の擾乱であり、衛星の測位誤差に大きな影響を与える。MSTID の空間スケールは約 100-1000 km である。E・F 領域が結合した電離圏のプラズマ不安定性により生成された MSTID は、磁気共役点において鏡像構造を持つ[e.g., Otsuka et al., GRL, 2014]。この場合、MSTID に関連する電場変動が磁力線に沿って伝搬するならば、内部磁気圏を飛行する衛星でも測定することができることが期待される。大気光イメージャ、電離圏高度の衛星により MSTID を同時観測した例[Shiokawa et al., JGR, 2003b]は報告されているが、磁気圏高度で MSTID に伴う電場を観測した例は、我々が春の JpGU-AGU2020 学会で報告した 1 例（Kawai et al., JpGU-AGU2020, 2020）のみであった。そこで本研究では、アラスカ州にある Gakona (62.39 N, 214.78 E)とアイスランドにある Husafell (64.67 N, 338.97 E)に設置された大気光イメージャと内部磁気圏衛星あらせにより MSTID を同時観測した例を複数例調べた結果を報告する。Gakona の大気光イメージャでは 2018 年 11 月 3 日、2019 年 2 月 26 日、Husafell の大気光イメージャでは 2019 年 1 月 26 日に観測された MSTID について、詳しい解析を行った。その結果、波長 630.0 nm の画像中に見られる MSTID の構造に関連して、あらせ衛星で観測された電場や電子密度に変動がみられた。講演では MSTID の大気光変動に伴い、内部磁気圏の環境・粒子の状態をあらせ衛星に搭載された機器を用いて、両者を比較しながら議論する。

R005-41
Zoom meeting C ：11/2 PM1 (13:45-15:30)
14:45-15:00

## Statistical analysis of seasonal and solar activity dependences of MSTID occurrence using the SuperDARN Hokkaido pair of radars

#Wataru Hazeyama[1)], Nozomu Nishitani[1)], Tomoaki Hori[1)]
[1)]ISEE, Nagoya Univ.

We presented the latest results of the statistical analysis of medium-scale traveling ionospheric disturbances (MSTIDs) using the SuperDARN Hokkaido pair of (HOP) radars data. We applied the three-dimensional fast Fourier transform algorithm developed by Matsuda et al. (2014) to the dataset and studied diurnal and seasonal variations of propagation directions of MSTIDs and solar activity dependence of the MSTID power spectrum density (PSD). The nighttime MSTIDs propagate mainly southwestward whereas some of them propagate northward, and the daytime MSTIDs propagate mainly southward. On the other hand we also found the negative correlation between the PSD of MSTIDs and solar activity. However, our result of daytime MSTIDs propagation direction seems to be affected by radar field-of-view boundary effects. Attempt to remove these effect is now in progress.

R005-42
Zoom meeting C ：11/2 PM1 (13:45-15:30)
15:00-15:15

## Propagation direction analysis of MSTIDs observed with TEC map using 3D spectral analysis method over North America

#SEPTI PERWITASARI, Takuji Nakamura[2),3)], Takuya Tsugawa, Michi Nishioka, Yoshihiro Tomikawa[2),3)], Mitsumu, K. Ejiri[2),3)], Masaru Kogure[4)], Hidekatsu Jin, Chihiro Tao
NICT,[2)]NIPR,[3)]SOKENDAI,[4)]Kyushu University

We applied a novel three-dimensional spectral analysis method to GPS-TEC map over North America to study the propagation direction of daytime and nighttime MSTIDs. This method automatically calculates phase velocity spectrum and directionality of MSTIDs. We focus on the period of high MSTIDs occurrence, June-July 2006 for nighttime and November-December 2006 to study daytime MSTIDs. We divided the North America into west (100-130 deg W, 25-55 degN) and east (70-100 deg W, 25-55 deg N) part. Our results show MSTIDs propagations exhibit strong longitudinal variation as a function of local time and daily variation for both daytime and nighttime MSTIDs. The daytime MSTIDs dominant propagation direction is southward in the west and southeastward in the east part, respectively, with an average speed of 50-300 m/s. The local time variation shows that the MSTIDs activity peaks around 10-16 LT in west and 10-14 LT in east part. The combination of wind filtering and source location likely controls the propagation direction seen in longitudinal and local time variation. For nighttime MSTIDs, the nightly average of the spectrum in the west part shows that the propagation is shifted westward with a phase speed of 50-200 m/s. The magnetic declination (~20 deg E) seems affecting the orientation of the phase fronts, resulting in westward motion. In the east part, the average nightly spectrum shows that the dominant propagation is southwestward with a phase speed of 50-150 m/s. We do not see significant effect of magnetic declination (4 deg E-16 deg W) to propagation direction. The MSTIDs activity peaks around 20-02 LT and 20-00 LT for west and east part, respectively. We will discuss the results more in details during the presentation.

R005-43
Zoom meeting C ：11/2 PM2 (15:45-17:30)
15:45-16:00

# Propagation characteristics of Sporadic-E and MSTIDs: Statistics using HF Doppler and GPS-TEC data

#Ryo Matsushima[1)], Keisuke Hosokawa[1)], Jun Sakai[1)], Mitsumu K. Ejiri[2)], Michi Nishioka[3)], Takuya Tsugawa[3)]
[1)]UEC,[2)]NIPR,[3)]NICT

Sporadic-E (Es) is a thin layer in the E-region ionosphere (~100 km) composed of dense metallic ions and electrons. Es is known to appear in the mid-latitude region during summer months. Extremely high electron density within Es sometimes reflects radio waves in VHF frequency range, especially above 100 MHz. Such a Es-related reflection of radio waves causes anomalous long-distance propagation of waves leading to radio interferences of commercial/navigation signals. Thus, Es is one of the important ionospheric phenomena which should be studied in the framework of space weather applications. Recent theoretical studies and numerical simulations have suggested that Es plays an important role in generating wave-like structures at F-region altitudes in summer nighttime, which are known as Medium-Scale Traveling Ionospheric Disturbances (MSTIDs). However, there have been only a few studies investigating the simultaneous observations Es and MSTIDs appearing in the E and F regions, respectively. Such a situation is primarily due to the lack of instruments that can directly observe Es in summer night time. To overcome this limitation, we employed data from HF Doppler (HFD) sounder network in Japan to detect Es and tried to evaluate the E-F coupling, i.e., Es in the E-region and MSTIDs in the F-region. The HFD system is composed of a transmitting station in Chofu, Tokyo (35.7N, 139.5E) and receiving stations at ~10 places in Japan. Based on such multi-point observations, we can derive the dynamical characteristics of Es layer, for example, its moving speed and direction.
In this paper, we carried out a statistical analysis of the propagation characteristics of Es and MSTIDs observed in the nighttime by combining HFD and Total Electron Content (TEC) obtained from the GPS receivers of GEONET (GPS-TEC) data for 4 years from 2014 to 2017. We made use of Es reflection data from the HFD receivers in Sugito, Saitama (36.0N, 139.7E), Fujisawa, Kanagawa (35.3N, 139.5E) and Sugadaira, Nagano (36.4N, 138.3E). By using this triangle observation, we succeeded in deriving the horizontal speed and direction of the motion of Es. In addition, we estimated the phase velocity of MSTIDs seen in the simultaneously obtained maps of GPS-TEC with the same triangle observation procedure. The speeds of Es and MSTIDs were commonly less than 100 m/s in most cases and the propagation direction of most of Es and MSTIDs was southwestward. This result is consistent with the statistical characteristic of nighttime MSTIDs in the previous studies. More importantly good correspondence between the propagation characteristics of the two phenomena confirms that Es and MSTIDs move in tandem with each other, further suggesting that Es plays an important role in the generation process of MSTIDs.

R005-44
Zoom meeting C ：11/2　PM2　(15:45-17:30)
16:00-16:15

## 中緯度スポラディック E 層の発生に及ぼす電気力学的影響に関する数値シミュレーシ ョン

#安藤　慧 [1)],齊藤　昭則 [1)],品川　裕之 [2)]
[1)]京大・理,[2)]情報通信研究機構

## Numerical simulation of electrodynamic effects on occurrences of the mid-latitude sporadic E layer

#Satoshi Andoh[1)], Akinori Saito[1)], Hiroyuki Shinagawa[2)]
[1)]Graduate School of Science, Kyoto Univ.,[2)]NICT

The effect of the electric field on the structure of the mid-latitude sporadic E (Es) layers is investigated by a three-dimensional local ionospheric model combined with the neutral wind and electric fields from the whole atmospheric global model GAIA. Es layers are high-density metallic ion layers appearing in the lower ionosphere. It is widely accepted that vertical shears of the horizontal neutral winds play a key role to the formation of Es layers. On the other hand, the effect of the electric fields on the Es layer structures has been extensively studied especially in the equatorial and low-latitude ionosphere. However, effects on the Es layers in the mid-latitude ionosphere has not been investigated because the electric fields there are weaker than that in the other latitudes.
In this study, Es layer simulations in two cases are conducted by using the three-dimensional local ionospheric model; the neutral winds are used as inputs for Case 1 and the neutral winds and the electric fields for Case 2. The neutral winds and electric fields are obtained from GAIA model. The simulations show that the occurrence rate of the Es layers, especially in the morning, increases due to the electric fields. Heights of the simulated Es layers are compared to those of the Es layers observed by ionosonde to investigate the relation between the Es layer structures and the electric fields.

３次元領域電離圏モデルに対し、全球モデル GAIA の中性風場と電場を入力として用いることで、中緯度域スポラディック E 層(Es 層)の構造に対する電場の影響を調査した。Es 層は電離圏 E 領域に発生する高密度の金属イオン層であり、防災無線や航空通信で利用される VHF 帯の電波の異常伝播の原因となることが知られている。Es 層の発生機構は Wind Shear 理論が通説となっており、水平方向中性風の鉛直シアが Es 層の形成には重要である。一方で、Es 層の構造に対する電場の影響も赤道域・低緯度域電離圏で盛んに研究されている。しかし、中緯度域における電場は他の緯度帯の電場に比べて弱いということから、Es 層への影響は調査されてこなかった。
今回、我々の開発した３次元領域電離圏モデルに対して、中性風場のみを入力とした数値計算と、中性風場と電場の両者を入力とした数値計算の２つの場合における Es 層発生について調査した。中性風場と電場は GAIA モデルのものを使用した。結果として、電場の影響によって Es 層の特に朝方の発生率が上昇することを見出した。本発表では、数値計算結果をイオノゾンデで観測された Es 層発生高度の変動と比較しつつ、中緯度域 Es 層の発生率と電場の関係性について考察する。

R005-45
Zoom meeting C ：11/2 PM2 (15:45-17:30)
16:15-16:30

# Characteristics of calcium ion layer observed with resonance scattering lidar at Syowa in Antarctic

#Mitsumu K. Ejiri[1),6)], Takanori Nishiyama[1),6)], Takuo Tsuda[2)], Katsuhiko Tsuno[4)], Makoto Abo[3)], Takuya Kawahara[5)], Takayo Ogawa[4)], Satoshi Wada[4)], Takuji Nakamura[1),6)]
[1)]NIPR,[2)]UEC,[3)]System Design, Tokyo Metropolitan Univ.,[4)]RIKEN, RAP,[5)]Faculty of Engineering, Shinshu University,[6)]SOKENDAI

Layers of metal ions in the mesosphere and lower-thermosphere (MLT) are produced by meteoric ablation. The meteoric metal ions have relatively long chemical life time in the MLT region and behave as plasma affected by neutral atmosphere dynamics. In the mid-latitude, the meteoric metal ions in the MLT region are generally accepted as key species for generation of sporadic E ($E_s$) layer in the wind shear theory. Calcium ion ($Ca^+$) is one of meteoric metal ion and only one ion, which can be measured its vertical profile from the ground by a lidar sounding. The close link between the $E_s$ layer and metal ion layer has been shown also by simultaneous observations of the $Ca^+$ lidar and radars [Raizada et al., 2012; Ejiri et al., 2019]. Annual variation of the Ca+ vertical distribution observed at Kuhlungsborn in 1997-1998 showed existing a permanent $Ca^+$ layer between 90 and 100 km through the year though it was sometimes rather weak [Gerding et al., 2000]. Recently, the Whole Atmosphere Community Climate Model incorporated a large database of neutral and ion?molecule reaction kinetics of calcium (Ca) species (WACCM-Ca) simulated the seasonal $Ca^+$ layer globally [Plane et al., 2018]. However, the results cannot be verified well yet because observation lacks except at the mid-latitude in the northern hemisphere.
A new resonance scattering lidar system with frequency-tunable alexandrite laser was developed by the National Institute of Polar Research (NIPR) and installed at Syowa Station (69S, 40E) by the 58th Japan Antarctic Research Expedition (JARE 58). Density profiles of $Ca^+$ in the MLT region over Antarctic were successfully observed 6 nights in total in September and October, 2017 and 2018. The $Ca^+$ layers observed at Syowa showed similar altitude of peak (~94 km) and layer width (~7 km) with Kuhlungsborn (54N, 12E) in spring while $Ca^+$ density at Syowa seems slightly smaller than that at Kuhlungsborn. Sporadic $Ca^+$ ($Ca^+_s$) layer with higher density than several hundred $cm^{-3}$ was not seen in our observations at Syowa in spring while the $Ca^+_s$ layer is often observed at the mid-latitude in the northern hemisphere. $Ca^+$ column abundance observed at Syowa was one order smaller than that predicted by WACCM-Ca. This is qualitatively consistent with Plane et al. [2018] that WACCM-Ca tends to overestimate $Ca^+$ measurements made by lidar.

R005-46
Zoom meeting C ：11/2 PM2 (15:45-17:30)
16:30-16:45

# Sporadic Fe layer event simultaneously observed by a resonance scattering lidar and an MF radar at Syowa station (69.0S, 39.6E)

#Takanori Nishiyama[1),2)], Mitsumu K. Ejiri[1),2)], Takuo Tsuda[3)], Katsuhiko Tsuno[4)], Takuji Nakamura[1),2)], Makoto Abo[5)], Takuya Kawahara[6)], Masaki Tsutsumi[1),2)], Takayo Ogawa[4)], Satoshi Wada[4)]
[1)]NIPR,[2)]The Graduate University for Advanced Studies, SOKENDAI,[3)]UEC,[4)]RIKEN,[5)]System Design, Tokyo Metropolitan Univ.,[6)]Faculty of Engineering, Shinshu University

Metallic layers, which ablate from meteoroids, are known to be formed between 80 and 105 km in the terrestrial mesopause region. Meteoric species such as Fe, Mg, and Na exist as atoms in the layers and their dynamical and chemical variability have been investigated by resonance scattering lidars [Plane et al., 2015 and references therein] and satellite-borne measurements [e.g., Fan et al., 2007; Dawkins et al., 2014; Langowski et al., 2015; Tsuda et al., 2017]. Sporadic E layer, Es layer, is characterized as a thin layer with enhanced electron density and mainly observed by incoherent scatter radars and ionosondes. $Mg^+$ and $Fe^+$ ions are regarded as dominant ion components in Es layers due to their long lifetime [Kopp, 1997] and, therefore, sporadic metallic layers are believed to play important roles in forming Es layers. Suggested generation mechanisms of sporadic metallic layers in polar regions are as follows: vertical ion converge and neutralization due to wind shear [e.g., Nygren et al., 1984] and ionospheric electric field [e.g., Kirkwood and von Zahn, 1991], convergent vertical neutral wind associated with atmospheric gravity waves, and sputtering from meteor smoke particle layers [von Zahn et al., 1987].
We identified sporadic Fe, hereafter FeS, event on June 5, 2018 at Syowa station (69.0S, 39.6E), Antarctic, that was observed by a resonance scattering lidar [Ejiri et al., 2019]. This FeS event can be summarized as follows: a center altitude and FWHM of the FeS layer are 90 km and 5 km, respectively. Duration was about 3 hours. Geomagnetic activity was quiet during this event and co-located ionosonde demonstrated intermittent Es activity. Apparent growth rate, which is defined in Alpers et al. [1994], is 1.5 %/min implying that development of the FeS is quite slow. During the FeS event, neutral wind data with from an MF radar at Syowa is available. Meridional and zonal wind profiles at the moment of FeS peak density around 17 UT show strong horizontal wind shear (du/dz is positive and dv/dz is negative), which is consistent with Es layer forming in the southern hemisphere [Chu et al., 2014]. We tried to explain the observed FeS by wind shear theory since ionospheric electric field (less than 10 mV/m) during the FeS can be neglected. Ion-neutral collision frequency for $Fe^+$ was estimated by an empirical model of Voiculescu and Ignat [2002], NRLMSISE-00, and IGRF-13. In addition, vertical ion velocity and its temporal variations were calculated in consideration of magnetic declination [Yu et al., 2019]. Magnetic declination angle at Syowa station is -51 degree and, therefore, should be taken into account. Estimated vertical ion velocity, $w_i$, and vertical gradient of $w_i$, $dw_i/dz$, were both negative near 12 UT. In particular, $dw_i/dz$ reached at -0.012 m/s/km, that is comparable to simulation result of Yu et al. [2019]. It is also consistent with strong Es (foEs ~ 5 MHz) observed by ionosonde at the moment. However, near 17 UT when FeS peak density was observed, both $w_i$ and $dw_i/dz$ were positive and favorable for vertical ion divergence. This implies that FeS peak was not caused by vertical ion velocity shear at this moment. Our analysis suggests that $Fe^+$ converge associated with negative $dw_i/dz$ might take place about 4 hours earlier than FeS appearance and subsequently neutralization of $Fe^+$ led to the observed FeS forming. Above 90 km $Fe^+$ lifetime ranges from a few minutes to $10^5$ s with altitudes [e.g., Plane et al., 2015]. It seems to be roughly consistent with the delayed appearance of FeS. We will examine this scenario based on wind shear theory by further analysis and a simple 1-D numerical simulation.

R005-47
Zoom meeting C ：11/2 PM2 (15:45-17:30)
16:45-17:00

## Statistical study of Sporadic Sodium Layers (SSLs) above Tromsoe (3)

#Satonori Nozawa[1)], Takuo Tsuda[2)], Norihito Saito[3)], Takuya Kawahara[4)], Satoshi Wada[3)], Yasunobu Ogawa[5)], Hitoshi Fujiwara[6)], Toru Takahashi[7),8)], Tetsuya Kawabata[1)], Chris Hall[9)], Asgeir Brekke[9)]
[1)]ISEE, Nagoya Univ.,[2)]The University of Electro-Communications,[3)]RIKEN Center for Advanced Photonics,[4)]Shinshu University,[5)]NIPR,[6)]Seikei University,[7)]University of Oslo,[8)]ENRI,[9)]UiT The Arctic University of Norway

This study is the first statistical study of Sporadic Sodium Layers (SSLs) differentiating in-situ generated SSLs from advected SSLs at high latitudes, and has evaluated conditions necessary for generating a SSL. Based on about 3000 hours of sodium density data obtained with the Tromsoe sodium LIDAR over 7 seasons (October-March) between 2012 and 2018, we have identified 36 events of SSL in the polar mesosphere and lower thermosphere (MLT) region (80 ? 110 km). By using an advantage of five directional simultaneous measurements, we have derived movement velocities of SSLs using detection times (i.e., arrival times) at five positions by assuming that a SSL has a linear front perpendicular to the movement direction and moving at a constant speed. Then, we have compared the movement velocities with wind velocities obtained with the sodium LIDAR. The movement directions of SSLs are dominantly from south-eastward to south-westward except for 3 events: Most SSLs moved southward in the meridional direction. No wind data are available for four events out of the 36 events. Based on comparison of the velocities, we have found that 28 out of 32 events (88%) are likely classified to be advection events, while 4 events are left for candidates of in-situ generation events.
We have evaluated generation mechanisms for “in-situ" events. The event observed on January 21, 2015 is categorized as such an “in-situ" event. The SSL for the night appeared around 21.3 UT and lasted for about 3 hours at the five directions. Time-height development of the SSL is similar at five directions: A high sodium density region gradually moved down from 103 km to 97 km as time went by. Favoured wind directions are observed where the SSL appeared: Westward/northward winds can derive sodium ions downward. Furthermore, southward E-field existed for the interval, and could drive sodium ions downward. The winds and the E-field must play a major role to generate the SSL. We will summarize observational results, and discuss generation mechanisms of SSLs.

R005-48
Zoom meeting C ：11/2　PM2　(15:45-17:30)
17:00-17:15

## トロムソナトリウムライダーデータを用いた極域 MLT 領域の大気安定度の研究

#前田　咲穂[1)],野澤　悟徳[1)],川原　琢也[2)],斎藤　徳人[3)],津田　卓雄[4)],和田　智之[3)],高橋　透[5)7)],川端　哲也[1)],Hall Chris[6)]
[1)]名大・宇地研,[2)]信州大・工,[3)]理化学研究所・光量子工学研究センター,[4)]電通大,[5)]オスロ大学物理学科,[6)]トロムソ大・TGO,[7)]電子航法研究所

## Study of atmospheric stability in the polar MLT region by using Tromsoe sodium LIDAR data

#Sakiho Maeda[1)], Satonori Nozawa[1)], Takuya Kawahara[2)], Norihito Saito[3)], Takuo Tsuda[4)], Satoshi Wada[3)], Toru Takahashi[5),7)], Tetsuya Kawabata[1)], Chris Hall[6)]
[1)]ISEE, Nagoya Univ.,[2)]Faculty of Engineering, Shinshu University,[3)]RIKEN Center for Advanced Photonics, RIKEN,[4)]UEC,[5)]Department of physics, UiO,[6)]TGO, UiT,[7)]ENRI

We have studied the atmospheric stability in the polar upper Mesosphere and Lower Thermosphere (MLT) region (80-105 km) above Tromsoe, Norway (69.6 degrees north, 19.2 degrees east) based on 2500 hours of sodium LIDAR data. To investigate the atmospheric stability, we have evaluated the convective instability and shear instability using temperature and velocity data (3 min and 0.5 km resolutions) obtained over 8 seasons from October 2012 to March 2019. For the quantitative evaluation, we have introduced the probability of instability [Zhao et al., JASTP, 65, 219-232, 2003]. By using this probability, we have investigated these instabilities and discussed the characteristics and factors of the instability region.

ノルウェー・トロムソ上空の冬季上部中間圏・下部熱圏(MLT)領域の大気安定度についてナトリウム(Na)ライダーデータを用いて調べた結果を報告する。高度 85？95 km では平均的に対流不安定は 9.7 %、シアー不安定は 11.3 %の確率で起きており、合わせると、20 %以上の確率でこの領域の大気は不安定であること、またこの不安定は日々大きく変動することが分かった。
中間圏界面領域は下層大気からの大気波動伝搬により、大気温度および風速が大きく変動する領域である。例えば、大気重力波はその振幅を増しながら上方へ伝搬し、MLT 領域で砕波する。この過程によって大気へ運動量とエネルギーを供給し、ときおり大気は不安定となる。中間圏界面付近の大気安定度について、これまでアメリカ・ニューメキシコ州(35° N、106.5° W)やコロラド州(41.1° N、105.1° W)、ブラジル・サン・ジョゼ・ドス・カンポス(23.1° N、25.9° W)において観測研究が行われており[Zhao et al., JASTP, 65, 219-232, 2003; Sherman et al., JASTP, 68, 1061-1074, 2006; Andrioli et al., JGR, 122, 4500-4511, 2017]、それぞれの地域での大気安定度の変化とその要因についての報告がされてきた。しかし、極域ではこのような研究は行われておらず、太陽風エネルギー流入がある北極域 MLT 領域でのこの種の研究は、非常に興味深いものである。
本研究では、トロムソに設置されたナトリウムライダーにより得られた 2012 年から 2019 年までの 8 年分の冬季の温度・風速データを使用し(高度分解能、時間分解能はそれぞれ 3 分および 500 m)、この期間中の MLT 領域における静的安定度および動的安定度について調べた。静的安定度(対流不安定度)を評価するためにブラントバイサラ周波数、動的安定度（シアー不安定度）を評価するためにリチャードソン数を計算し、不安定確率[Zhao et al., JASTP, 65, 219-232, 2003]を導入し、大気安定度を定量的に評価した。その結果、大気安定度の日々変動は大きく、高度 85 km から 95 km の間では対流不安定確率は最大 20.6 %から最小 0.5 %、シアー不安定確率は最大 14.0 %から最小 1.4 %まで変化することが分かった。また、全期間において対流不安定確率は観測高度のうち 95 km より上、および 85 km より下の高度で高く、シアー不安定確率は 95 km より上の高度で高いという結果が得られた。この要因として、半日大気潮汐波、太陽活動およびオーロラ活動による大気加熱への影響が考えられる。太陽活動およびオーロラ活動による影響を、F10.7 指数および Kp 指数との相関により調べた結果、両者の相関は低く、これらの大気不安定度への影響は、支配的でないことが分かった。半日潮汐波の振幅と不安定確率の相関を調べたところ、シアー不安定確率との相関では相関係数 0.6 以上の相関が得られたこととから、半日潮汐波は比較的大きな影響を与えているが、支配的要因ではないと推測される。これらを踏まえてさらに安定度を変化させる要因を明らかにし、また先行研究との比較の結果を報告する。

R005-49
Zoom meeting C ：11/3 AM1 (9:00-10:30)
09:00-09:15

## Real-time monitoring of polar mesospheric clouds utilizing Himawari-8 full disk images

#Takuo Tsuda[1)], Yuta Hozumi[1)], Yoshiaki Ando[1)], Keisuke Hosokawa[1)], Hidehiko Suzuki[2)], Takuji Nakamura[3)], Ken T. Murata[4)]
[1)]UEC,[2)]Meiji univ.,[3)]NIPR,[4)]NICT

Polar mesospheric clouds (PMCs) or noctilucent clouds (NLCs) consist of water-ice particles, which can be produced in summer at the mesopause region, mainly at high latitudes. Since the first report on PMCs in 1885, various methods have been used to perform PMC observations. Optical observations by ground-based cameras, imagers, or lidars are often limited by weather conditions because a clear sky is required for such observations. Hence, satellite observations from space are valuable for more continuous observations, which enable significant systematic data coverage. Thus, many PMC observations have been done by low Earth orbit (LEO) satellites. By contrast, there are only few reports of PMC observations by geostationary Earth orbit (GEO) satellites, which includes Meteosat First Generation (MFG) and Meteosat Second Generation (MSG). These GEO satellites can provide full-disk images including the Earth's limb, which would give valuable opportunities for PMC observations by continuous limb-viewing from its almost fixed location relative to the Earth.
In this presentation, we will introduce PMC observations by the Japanese GEO meteorological satellite Himawari-8, that has been in the regular operation since 7 July 2015. In particular we will show our PMC detection method for application to the Himawari-8 data, which consists of two-step detections. The first detection is as follows. We calculate positions in each pixel of Himawari-8 full-disk image, as tangential points in the limb viewing. Then, based on the calculated position, we produce spatial averaged emission intensity data for each bin with 1? latitude and 1-km altitude, and thus height profiles in the averaged emission intensity are obtained at each latitude. We define a threshold based on a dark level determined from the the emission intensity above 90 km, and extract PMCs which have significant emission intensity compared with the threshold. In the second detection, in order to extract weaker PMC emissions, we remove emission profiles only due to atmospheric scattering (i.e., Rayleigh scattering) using polynomial approximation. After that, by setting a smaller threshold, weaker PMCs are extracted. This method is currently applied to real-time Himawari-8 data, and a website showing real-time PMC activity will be opened to the public shortly. This kind of data product would be of benefit for research on various PMC science.

R005-50
Zoom meeting C ：11/3 AM1 (9:00-10:30)
09:15-09:30

## Polar mesospheric cloud structure tracking with data from the meteorological satellite Himawari-8

#Yuta Hozumi[1)], Takuo Tsuda[1)], Yoshiaki Ando[1)], Keisuke Hosokawa[1)], Hidehiko Suzuki[2)], Takuji Nakamura[3)], Ken T. Murata[4)]
[1)]UEC,[2)]Meiji univ.,[3)]NIPR,[4)]NICT

A cloud tracking technique is applied to polar mesospheric cloud (PMC) data from the Geostationary-Earth-Orbit (GEO) meteorological satellite Himawari-8 to examine the diurnal PMC variations. While previous PMC observations from the ground and Low-Earth-Orbit (LEO) satellites have a limitation on local time coverage, observations from the GEO satellite provide a great opportunity to study the PMC variability with all local time coverage and a wide field of view. The band 1 (the blue band, 0.47 $\mu$m) data of the Advanced Himawari Imager (AHI) onboard Himawari-8 is resampled to the horizontal versus vertical grids data on the Earth-s limb with the grid-box size of 10 km (horizontal) and 5 km (vertical). A pattern matching technique is applied to the PMC peak radiance of the resampling data, and the horizontal movement of PMC along the transverse direction to the line of sight is derived. The horizontal movement shows diurnal and semi-diurnal variations with a mean westerly movement of about 10 m/s. The westerly mean movement is consistent with the horizontal wind derived from PMC images taken with the Cloud Imaging and Particle Size instrument (CIPS) on the Aeronomy of Ice in the Mesosphere (AIM) satellite, and the wind of HWM14. The horizontal movement of PMC observed by Himawari-8 is likely to be subjected to wind advection.

R005-51
Zoom meeting C ：11/3 AM1 (9:00-10:30)
09:30-09:45

## Numerical simulation of polar mesospheric cloud emissions observed by Himawari-8

#Yoshiaki Ando[1)], Takuo Tsuda[1)], Yuta Hozumi[1)], Keisuke Hosokawa[1)], Hidehiko Suzuki[2)], Takuji Nakamura[3)], Ken T. Murata[4)]
[1)]UEC,[2)]Meiji univ.,[3)]NIPR,[4)]NICT

Recently, we reported that polar mesospheric cloud (PMC) emissions can be observed by Himawari-8, the Japanese geostationary earth orbit (GEO) meteorological satellite. The full disk images of Himawari-8 provide PMC emissions in the Earth's limb region, which allows us to perform continuous PMC monitoring from a fixed point, the GEO orbit, more routinely. It is noted that the intensity of the measured PMC emissions does not indicate directly the number density of PMC particles because the emission intensity captured by the sensor is the sum of PMC emissions along the satellite line of sight and the scattering cross section of PMC particles depends on the size and the scattering angle due to configuration of the sun, the earth, and the satellite. Therefore, a numerical simulation is necessary to identify PMC parameters such as number density, radius distribution, and their spatial distribution, from Himawari-8 observation data.
In this study, we develop a numerical simulation method to reproduce the emission intensity observed by the Himawari-8 with a given PMC distribution. In the proposed method, the PMC particles are assumed to be lossy dielectric spheres because the size of PMC particles is considerably smaller than the observation wavelengths, which are three visible bands: blue (0.47 um), green (0.51 um), and red (0.64um). For this case, the exact solution of scattering cross section is given by Mie theory. We use the common assumption regarding particle size distribution, which is given as a log-normal form. The light traveling in the atmosphere is attenuated due to scattering by air molecules and PMCs, which is also considered in the proposed method. The attenuation due to the air molecules (described by Rayleigh scattering) is calculated from number density and temperature of the air molecules, which are given by the NRLMSISE-00 atmospheric model.
The developed simulation method shows a good agreement with observed data. It is demonstrated that number density and particle size distribution can be uniquely identified by using data observed with multiple wavelengths. The developed method enables us to retrieve spatial distribution and particle size distribution of PMCs from Himawari-8 data.

R005-52
Zoom meeting C ：11/3　AM1　(9:00-10:30)
09:45-10:00

## 極中間圏雲の発生と磁気圏からの高エネルギー電子降下の関連について

#細川　敬祐[1)],津田　卓雄[1)],穂積　裕太[1)],安藤　芳晃[2)],鈴木　秀彦[3)],中村　卓司[4)],村田　健史[5)]
[1)]電通大,[2)]電通大,[3)]明治大,[4)]極地研,[5)]情報通信研究機構

## Relationship between polar mesospheric clouds and energetic electron precipitation from the magnetosphere

#Keisuke Hosokawa[1)], Takuo Tsuda[1)], Yuta Hozumi[1)], Yoshiaki Ando[2)], Hidehiko Suzuki[3)], Takuji Nakamura[4)], Ken T. Murata[5)]
[1)]UEC,[2)]The Univ. of Electro-Comms.,[3)]Meiji univ.,[4)]NIPR,[5)]NICT

Polar Mesospheric Clouds (PMCs) are optical phenomena produced through scattering of solar illumination by icy particles formed at altitudes of 82-85 km during summer months. Since PMCs are composed of icy particles, the frequency of their occurrence varies depending on both the temperature and the water vapor concentration at the mesospheric altitudes. In recent years, there have been a few studies demonstrating a decrease in the frequency of PMCs during the Solar Proton Event (SPE) associated with large flares (e.g., von Savigny et al., 2007). Although the mechanism linking SPE and PMCs still remains unclear, these studies have suggested that energetic particles released through short-term variations at the Sun (e.g., flares) may modify the mesosphere environment (possibly through low-altitude ionization and subsequent chemical processes) and suppress the development of PMCs (Winkler et al., 2012). In this study, we focus on the Energetic Particle Precipitation (EPP) as an another agent causing low-altitude ionization and discuss its effect on the activity of PMCs. We statistically analyzed the occurrence of PMCs derived from the continuous optical observations from the Himawari-8 satellite at the geostationary orbit (Tsuda et al., 2018), and then examined the correlation between EPP and PMCs. Recent studies have shown that sub-relativistic electron precipitations from the magnetosphere, that is the main part of EPP, are often observed in the morning sector, well synchronized with the appearance of pulsating aurora (PsA) (Miyoshi et al., 2015). It has also been suggested that such low-altitude ionization caused by EPP can lead to the destruction of mesospheric ozone (Turunen et al., 2017). In the presentation, we discuss whether a similar causal relationship exists between EPP and PMCs.

極中間圏雲（Polar Mesospheric Clouds: PMCs）は，夏季に寒冷化した中間圏の 82-85 km 高度に生成された氷粒子が太陽光を散乱することによって生じる（観測される）現象である．PMCs は氷粒子によって構成されているため，その発生頻度は，中間圏の「温度」と「水分子の量」の双方を反映して変動する．近年，大規模なフレアに伴う太陽プロトンイベント（Solar Proton Event: SPE）に伴って，PMCs の発生頻度が減少しているという報告がいくつかなされている（e.g., von Savigny et al., 2007）．SPE と PMCs 発生頻度の間をつなぐメカニズムはいまだに明らかになっていないが，フレアに代表される太陽の短期的な変動に伴う高エネルギー粒子の降下が（おそらくは大気の電離とそれに続く化学過程を介して）中間圏の環境を変え， PMCs の発生を抑制している可能性が指摘されている（Winkler et al., 2012）．本研究では，SPE と同じように低高度の電離を引き起こすエージェントである EPP（Energetic Particle Precipitation）に着目し，PMCs の発生頻度との関連性を調べた結果を報告する．PMCs の検出には，ひまわり 8 号による静止軌道からの光学観測（Tsuda et al., 2018）を使用した．近年の研究によって，EPP のメインパートである磁気圏からの準相対論的電子降下が，脈動オーロラ（Pulsating Aurora: PsA）の発生と同期する形で朝側のローカルタイムにおいて観測されることが分かってきている（Miyoshi et al., 2015）．EPP と中間圏オゾンの間の関連性はこれまでにも指摘されているが（Turunen et al., 2017），類似の因果関係が PMCs との間にもあるかどうかを議論する．

R005-53
Zoom meeting C ：11/3　AM1　(9:00-10:30)
10:00-10:15

## 地磁気静穏時に発生した pseudo breakup における熱圏応答のイベント解析

#大山　伸一郎[1)2)3)],新堀　淳樹[1)],小川　泰信[3)],Kellinsalmi　Mirjam[4)],Raita　Tero[5)],Rietveld　Michael[6)],Aikio　Anita[2)],Heikki　Vanhamaki[2)],塩川　和夫[1)],Virtanen　Ilkka[2)],Cai　Lei[7)],Workayehu　Abiyot[2)],Pedersen　Marcus[2)],Kauristie　Kirsti[4)],津田　卓雄[8)],Kozelov　Boris[9)],Demekhov　Andrei[9)],Yahnin　Alexander[9)],土屋　史紀[10)],熊本　篤志[10)],笠原　禎也[11)],松岡　彩子[12)],小路　真史[1)],寺本　万里子[13)]
[1)]名大 ISEE,[2)]オウル大学,[3)]国立極地研究所,[4)]フィンランド気象研究所,[5)]オウル大学ソダンキラ地球物理観測所,[6)]欧州非干渉散乱レーダー協会,[7)]スウェーデン王立工科大学,[8)]電気通信大学,[9)]ロシア極地地球物理学研究所,[10)]東北大学,[11)]金沢大学,[12)]京都大学,[13)]九州工業大学

## An event study of the thermospheric response at a pseudo breakup during geomagnetically quiet conditions

#Shin-ichiro Oyama[1),2),3)], Atsuki Shinbori[1)], Yasunobu Ogawa[3)], Mirjam Kellinsalmi[4)], Tero Raita[5)], Michael Rietveld[6)], Aikio Anita[2)], Heikki Vanhamaki[2)], Kazuo Shiokawa[1)], Ilkka Virtanen[2)], Lei Cai[7)], Abiyot Workayehu[2)], Marcus Pedersen[2)], Kirsti Kauristie[4)], Takuo Tsuda[8)], Boris Kozelov[9)], Andrei Demekhov[9)], Alexander Yahnin[9)], Fuminori Tsuchiya[10)], Atsushi Kumamoto[10)], Yoshiya Kasahara[11)], Ayako Matsuoka[12)], Masafumi Shoji[1)], Mariko Teramoto[13)]
[1)]ISEE, Nagoya Univ.,[2)]Space Physics and Astronomy Research Unit, University of Oulu,[3)]National Institute of Polar Research,[4)]Finnish Meteorological Institute,[5)]Sodankyla Geophysical Observatory, University of Oulu,[6)]EISCAT,[7)]KTH Royal Institute of Technology,[8)]The University of Electro-Communications,[9)]Polar Geophysical Institute,[10)]Tohoku University,[11)]Kanazawa University,[12)]Kyoto University,[13)]Kyushu Institute of Technology

A geomagnetically quiet-time (Kp=0+) pseudo breakup event on 20 February 2018 was investigated to examine the Magnetosphere-Ionosphere-Thermosphere coupling at auroral to subauroral latitudes in the Scandinavian sector using multiple ground-based instruments and spacecraft. Coinciding with appearance of the pseudo breakup at 71-73 MLat at approximately 21 MLT, a red arc emerged at the ionospheric trough minimum located at 68 MLat (L?7.1). The ionospheric trough was scanned meridionally by the Swarm A and C spacecraft, and the measurements clearly showed an electron temperature peak (~15,000 K) at the trough minimum. We concluded that causality to produce the red arc was the heat flux transferred from the plasmapause similar to generation of the stable auroral red (SAR) arc. Different from the SAR arc, the red arc was found at the onset time. The red arc may represent a moment of SAR arc birth, which is generally masked by bright dynamic aurorae. The new feature is named the ephemeral auroral red (EAR) arc. Ion velocity measured by the Swarm A showed westward flow of about 1700 m/s in the trough but at the equator side slope and the flow speed at the trough minimum was almost 0 m/s. This suggests that the polarization electric field may not have been spatially uniform throughout the trough. A Dynasonde deployed at Tromsoe (67 MLat, which is located near the equatorward trough edge) measured westward turning of the F-region ion velocity at the pseudo breakup. The collocated Fabry-Perot interferometer (FPI, 630.0 nm) also detected westward wind acceleration following the ion velocity change with almost no delay but with some relative speed. For an approximately 20-min interval after the pseudo breakup, **Un**?**Vi** was negative, which suggests that the mechanical energy of the neutral particles was transferred to the plasma in the ionosphere, contributing to the Joule heating rate at a moment of sudden magnetospheric electric field change at the pseudo breakup. Here **Un** and **Vi** are the neutral wind and ion velocity, respectively. However, after this interval, **Un**?**Vi** turned to be positive. The Dynasonde-FPI comparison suggests that the thermospheric wind was prompt to respond to the substorm-induced ion velocity change even in the low plasma density trough, and that inertia of the neutral particle plays a partial role to generate the thermal energy.

R005-54
Zoom meeting C ：11/3　AM2　(10:45-12:30)
10:45-11:00

## 地上光学およびレーダー観測データを用いたトモグラフィ解析による脈動オーロラ発光強度3次元分布の再構成

#吹澤　瑞貴[1)],坂野井　健[2)],田中　良昌[3)],小川　泰信[4)]
[1)]東北大・理,[2)]東北大・理,[3)]国立極地研究所/ROIS-DS/総研大,[4)]極地研,[5)]ノルウェー北極大学 - トロムソ大学,[6)]フィンランド気象研究所,[7)]欧州非干渉散乱レーダー科学協会,[8)]オウル大学ソダンキラ地球物理観測所,[9)]スウェーデン宇宙物理学研究所

## 3D tomography reconstruction of pulsating auroral emission intensity from ground imaging and radar data

#Mizuki Fukizawa[1)], Takeshi Sakanoi[2)], Yoshimasa Tanaka[3)], Yasunobu Ogawa[4)], Bjorn Gustavsson[5)], Kirsti Kauristie[6)], Carl-Fredrik Enell[7)], Alexander Kozlovsky[8)], Tero Raita[8)], Urban Brandstrom[9)], Tima Sergienko[9)]
[1)]Graduate School of Science, Tohoku University,[2)]Grad. School of Science, Tohoku Univ.,[3)]NIPR/ROIS-DS/SOKENDAI,[4)]NIPR,[5)]UiT - The Arctic University of Norway,[6)]Finnish Meteorological Institute,[7)]EISCAT Scientific Association,[8)]Sodankyla Geophysical Observatory, University of Oulu,[9)]Swedish Institute of Space Physics

Pulsating aurora, which has a quasi-periodic modulation in its emission intensity, is commonly observed in the broad magnetic local time period from just after a substorm onset near the midnight to noon sector. Observational and theoretical studies showed that pulsating aurora is caused by precipitating electrons which scattered into a loss cone due to the cyclotron resonance with chorus waves. The precipitating electrons caused by chorus waves mainly cause ionizations in the ionospheric E region since their typical resonance energy is from a few to tens of keV. Theoretically, it is also expected that chorus waves can resonate with sub-relativistic (>~1 MeV) electrons. Miyoshi et al. (2015) reported that electron density enhancements were clearly identified even at an altitude of 68 km in association with a pulsating aurora. Hosokawa & Ogawa (2010) presented that an appearance of Pedersen current layer carried by electrons in the ionospheric D region during a pulsating aurora and Gillies et al. (2015) showed the existence of field-aligned current during pulsating auroral patches.
In this study, we aim to reconstruct the current structure associated with pulsating auroras by mainly using “generalized-aurora computed tomography (G-ACT, Tanaka et al., 2011)" method. First, we applied “the aurora computed tomography (ACT, Aso et al., 1998) method" to reconstruct the three-dimensional (3D) structure of pulsating aurora patches from multiple monochromatic auroral images. The ACT method has been applied to reconstruct the 3D structure of discrete auroras (e.g., Aso et al., 1998) but it is difficult to reconstruct that of pulsating auroras because their shape is ambiguous and they appear at close distances with each other. Here, we give the first result of the 3D structure of pulsating auroral emission by the ACT method. We analyzed an event in which relatively bright and isolated pulsating auroral patches were simultaneously observed by all-sky imagers at Skibotn, Kilpisjarvi and Abisko during a substorm recovery phase during the period of 0?2 UT on 18 February 2018. The observation wavelength and temporal resolution of the all-sky imagers were 427.8 nm and 2 s, respectively. We set the origin as the geographic latitude and longitude at the ground of the center of target auroral patch, the x-axis as antiparallel to the horizontal component of the geomagnetic field, the y-axis as eastward, and the z-axis as anti-parallel to the geomagnetic field. The simulation region was －50 to 50 or －75 to 75 km for the x-axis, －100 to100 km for the y-axis, and 80 to 180 km for the z-axis to include the target patch. The 3D structures of three pulsating auroral patches were precisely reconstructed by solving a problem of minimization of posterior probability with the Gauss-Newton method based on the Bayesian model. The reconstructed emission altitudes are 88?102 km and the thickness was 2?14 km. The accuracy of reconstruction will be evaluated by computer simulation using model aurora, and by simultaneous EISCAT radar data. In the future, we will examine the current structure associated with pulsating aurora patches by reconstructing energy and spatial distributions of precipitating electrons from electron density data obtained with EISCAT radar and using the IMAGE magnetometer network and neutral atmospheric model MSIS.

脈動オーロラは真夜中付近においてサブストームが起きた直後から昼間側まで広い磁気地方時範囲でごく一般的に発生するオーロラであり、明るさが約 10 秒の周期をもって明滅を繰り返すという特徴をもつ。これまでの観測と理論研究から、脈動オーロラは主にコーラス波とのサイクロトロン共鳴によってロスコーン内に散乱された電子が地球大気中に降下することで引き起こされることが明らかになった。コーラス波の典型的な共鳴エネルギーは数 keV から数十 keV であるため、コーラス波により生成された降下電子は主に電離圏 E 領域で電離を引き起こす。また、理論からコーラス波は準相対論的電子（>~1 MeV）とも相互作用することが期待される。この間接的証明として、先行研究では脈動オーロラに伴う電離が高度 68 km まで達するという報告がされている(Miyoshi et al., 2015)。さらに、Hosokawa & Ogawa (2010)では脈動オーロラに伴う D 領域の電子密度増加によりペダーセン電流が流れることが示唆され、Gillies et al. (2015) では脈動オーロラパッチ上で沿磁力線電流が流れていることが報告された。
そこで本研究では「一般化オーロラトモグラフィ（Tanaka et al., 2011)」解析手法を中心に用いて脈動オーロラ中の電流構造を再構成することを最終目標に、まず多地点単波長で観測されたオーロラ画像から「オーロラトモグラフィ

(Aso et al., 1998)」解析手法を用いて脈動オーロラパッチの 3 次元発光構造の再構成を試みた。これまでオーロラトモグラフィはディスクリートオーロラに対して適用されてきたが(e.g., Aso et al., 1998)、形状がはっきりせず複数のパッチが近接して発光する脈動オーロラでは再構成が難しく、これまで報告例がない。本研究では、2018 年 2 月 18 日 0－2UT のサブストーム回復相に比較的明るく孤立した脈動オーロラパッチが、北欧 3 地点（Skibotn、Kilpisj?rvi、Abisko）に設置されている全天カメラで同時に観測されているイベントを解析することで、脈動オーロラパッチの 3 次元空間構造と時間変化を初めて明らかにした。全天カメラの観測波長は 427.8 nm で時間分解能は 2 秒である。再構成領域は対象とするオーロラの地表における緯度と経度を原点、地磁気水平成分に反平行方向を x 軸、東方向を y 軸、地磁気反平行方向を z 軸とし、対象とするオーロラを含むように x 軸方向に－50 から 50 km または－75 から 75 km、y 軸方向に－100 から 100 km、z 軸方向に 80 から 180 km の空間を用意し、空間分解能は 2 km とした。この期間の内、 3 つの脈動オーロラパッチに対してベイズモデルに基づいて事後確率の最小化問題を Gauss-Newton 法により解くことによりオーロラ発光強度の 3 次元構造を再構成することができた。再構成した脈動オーロラパッチの発光高度は 88?102 km で、発光層の厚さは 2?14 km であった。再構成結果の精度についてはモデルオーロラを用いたシミュレーションや、同時の EISCAT レーダーデータにより検証していく予定である。今後は、EISCAT レーダーによって観測された電子密度高度分布の情報を加えて降下電子のエネルギー・空間分布を推定し、最終的には IMAGE 地磁気観測網データ、中性大気モデル MSIS などと組み合わせることで脈動オーロラに伴う電流構造の推定を目指す。

R005-55
Zoom meeting C ：11/3　AM2　(10:45-12:30)
11:00-11:15

## 南極昭和基地大型大気レーダーによる電離圏沿磁力線不規則構造のイメージング観測

#香川　大輔[1)],橋本　大志[2)],齊藤　昭則[1)],西村　耕司[2)],堤　雅基[2)],佐藤　亨[3)],佐藤　薫[4)]
[1)]京大・理・地惑,[2)]国立極地研究所,[3)]京大・情報学・通信情報システム,[4)]東大・理

## Imaging observation of Ionospheric Field Aligned Irregularities by the PANSY radar at Antarctic Syowa Station

#Daisuke Kagawa[1)], Taishi Hashimoto[2)], Akinori Saito[1)], Koji Nishimura[2)], Masaki Tsutsumi[2)], Toru Sato[3)], Kaoru Sato[4)]
[1)]Earth and Planetary Sciences, Kyoto Univ.,[2)]National Institute of Polar Research,[3)]Communications and Computer Eng., Kyoto Univ.,[4)]Graduate School of Science, Univ. of Tokyo

Program of Antarctic Syowa MST/IS radar (PANSY radar) is the large atmospheric and VHF-band radar located at the Antarctic Syowa Station. This radar has the capability of observing plasma quantities at altitudes of 100-500km using the ionospheric incoherent scatter (IS). In 2015, the PANSY radar performed the first ionospheric IS observation in the Antarctica.
This has a frequency of 47MHz, so it is capable of observing the echoes of field aligned irregularities (FAI) in E-region. If FAI has a space scale of half wavelength of radio waves, they are coherently backscattered, so the PANSY radar observes the coherent echoes from 3-meter-scale FAI in E-region. In order to suppress contamination from the FAI echoes during the IS observation by the PASNY radar, Hashimoto et al. (2019) developed a signal processing using adaptive beamforming. The PANSY radar has the FAI array in addition to the main array, and it can separate the signal from various angles using the method based on directionally-constrained minimization of power (DCMP) algorithm. In fact, using this method we can observe E-region FAI and its motion.
In December 2017, FAI imaging observation was performed, and periodic-like echoes were detected with global Pc5 pulsations. Studies and observations of Pc5 and FAI are performed before. For example, Wang et al. (2019) provided measurements of 2-dimensional structures of dayside Pc5 waves utilizing?coordinated observations by the THEMIS satellites and the all-sky imager at South Pole, and F-region FAI observation by the SuperDARN also detected?periodic echoes for the same period as one by the PANSY radar. The former, however, reported the events only at nighttime and the latter cannot measure detailed spatial structures because of its HF frequency. Therefore, utilizing the PANSY radar, it is expected that we can provide observations also at daytime and measurements of spatial structures of the FAI occurring with Pc5 pulsations.
However, it is found that FAI imaging using the Capon method cannot measure the spatial structures accurately. FAI echoes are generally observed if the conditions that radio waves are perpendicular to FAI are satisfied, but the imaging also shows the "ghosts" which were?mistakenly observed as?FAI in?the non-echoing region. This problem occurs probably because objects?in the grating lobes which are in the FAI array radiation pattern are not identified. So, we should develop the new imaging method which removes the effects of them and provides accurate spatial structures. The new method is based on the CLEAN algorithm, and in the iteration the responses of the non-mainlobe region in the radiation pattern of the FAI array, such as grating lobes and sidelobes, are suppressed, which gives the imaging of FAI detected by the mainlobe without contamination of noises.
In the presentation, we will show the new FAI imaging method which removes the effects of antenna radiation pattern, and gives accurate and high-resolution spatial structures of FAI. Moreover, performing the imaging using this method we try to find out physical processes of FAI generation.

南極昭和基地大型大気レーダー（PANSY レーダー）は南極の昭和基地に設置されている大型 VHF 帯大気レーダーである。本レーダーは電離圏非干渉性散乱（IS）を用いて地表 100km から 500km におけるプラズマ物理量を観測することが可能であり、2015 年には南極で初となる電離圏 IS 観測が開始された。また、47MHz の周波数を用いており、E 領域における沿磁力線不規則構造（Field Aligned Irregularity; FAI）エコーの観測も可能である。FAI がレーダー電波の半波長の空間スケールを持つとき電波はコヒーレント散乱を起こすため、PANSY レーダーでは約 3m スケールの E 領域 FAI からのコヒーレント・エコーの観測が行われる。この FAI エコーの混入による PANSY レーダーの IS 観測への影響に対処するため、Hashimoto et al. (2019）では適応的ビーム形成技術を用いた信号処理法が開発された。PANSY レーダーにはメインアレイに加え FAI アレイが導入されており、方向拘束付き出力電力最小化法に基づいた手法を用いて異なる角度からの信号を分離できる。つまり、この手法を用いることにより E 領域 FAI やその運動を観測することが可能である。
2017 年 12 月に行われた FAI のイメージング観測において、グローバルな Pc5 地磁気脈動イベントに伴って周期的に発生する FAI エコーが確認された。これまでにも、南極域における Pc5 や FAI に関する研究・観測は行われてきた。例えば、Wang et al. (2019）では、THEMIS 衛星と全天イメージャーの協同観測により昼側 Pc5 の二次元構造の推定が行われた。また、昭和基地に設置されている SuperDARN による F 領域 FAI の観測では、PANSY レーダーによる観測と同じ時間帯において同様の周期的なエコーが検出された。しかし、前者は夜間のみの観測にと

どまり、後者は HF 帯の周波数を用いているために FAI の詳細な空間構造を測定するには至っていない。そこで、PANSY レーダーを用いることで、夜間だけでなく昼間においても観測を行うことができ、周期的に発生する FAI の詳細な構造を測定することができると期待される。
しかしながら、現在の Capon 法を用いた FAI イメージングでは、空間構造の測定に不確定性があることがわかった。FAI は、本来レーダー電波と地磁気の磁力線が直交するところで観測されるはずであるが、それ以外のところにおいても FAI エコーとして観測が行われている。これは、PANSY レーダーの FAI 観測の視野内に現れるグレーティングローブが原因であると考えられる。そのため、その影響を除去し真の空間構造を推定する新しいイメージング手法の開発が必要である。新手法では CLEAN アルゴリズムに基づき、イタレーションを行う中で、グレーティングローブやサイドローブといった、FAI アレイの放射パターンにおけるメインローブ以外の領域の応答値を小さくしていく。これにより、ノイズの影響をほとんど受けることなく、メインローブで検出された FAI のイメージングを得ることができる。
本発表では、アンテナの放射パターンの影響を除去し、FAI の正確かつ高分解能な空間構造を得るための新しいイメージング手法を紹介する。また、その手法を用いて行われるイメージングから、FAI 発生の物理過程の解明を試みる。

R005-56
Zoom meeting C ：11/3　AM2　(10:45-12:30)
11:15-11:30

# 電離圏 F 領域の衝突周波数モデル

#家田　章正
名大宇宙地球研

# Ion?Neutral Collision Frequency Models for the F-region Ionosphere

#Akimasa Ieda
ISEE, Nagoya Univ.

The Earth's F region ionosphere is dominated by the collision between atomic oxygen and its first positive ion. An accurate corresponding collision frequency model is necessary to understand the ionosphere. However, the widely used classic Banks theoretical model typically provides a collision frequency that is 30% lower than the expectation from ionospheric observations. Accordingly, the classic collision frequency is often adjusted by multiplying it by a constant known as the Burnside factor. This correction-factor model adopted the classic model as its basis due to a misunderstanding that the classic model was based on a laboratory experiment; that is, the correction factor was originally meant to compensate for laboratory contamination.
In this study, we construct a collision frequency model based on the laboratory experiment. We find that the resultant laboratory-based model is consistent with ionospheric observations. In this construction, we have determined that the impact of laboratory contamination is small (7%) and is mostly canceled by a misinterpretation regarding the conventional definitions of energy. Thus, the 30% difference is mainly caused by a theoretical error in the classic model itself. This error is energy-dependent and corrected by the later wide-energy theoretical model. Thus, the classic model cannot be corrected by a constant and should be replaced by the later model.

地球電離圏 F 領域は、酸素原子と酸素原子イオンの衝突に支配されている。その衝突周波数の正確なモデルが電離圏を定量的に理解するために必要である。しかし、Banks などの古典モデルは約 30%過小評価であることが、電離圏観測から示唆されている。また、この古典モデルを用いると、電離圏シミュレーションの結果は観測と整合しない。このために、補正定数（Burnside factor）を古典モデルに掛けた、補正モデルがシミュレーションでは一般的に用いられる。この補正モデルの形式は、古典モデルが実験結果であるという誤解に基づいている。つまり、補正定数は、未知の実験コンタミを想定している。しかし、古典モデルは理論であって実験結果ではないため、実験のコンタミとは無関係である。従って、補正モデルを使用する物理的根拠はない。
　本研究では、実験室測定結果から衝突周波数モデルを初めて作成した。このモデル作成において、初めて実験室コンタミを補正した。また、エネルギーの定義が過去の研究において実験と理論で同じであると誤解されていることを指摘し修正を行った。その結果、作成した実験室モデルは電離圏観測と整合していることを見いだした。したがって、古典モデルが約 30%低いのは、古典理論が不正確なためである。この間違いを修正した新理論は既存であるが、これまで採用されてこなかった。これは、古典理論は実験に基づく、あるいは実験結果と整合していると、広く誤解されてきたためである。本研究では、修正理論・実験室結果・電離圏観測が整合していることを示した。また、古典理論の間違いは、温度依存性があるために定数では補正できない。したがって、古典理論でなく修正理論を採用すべきであり、その結果、補正定数は不要である。

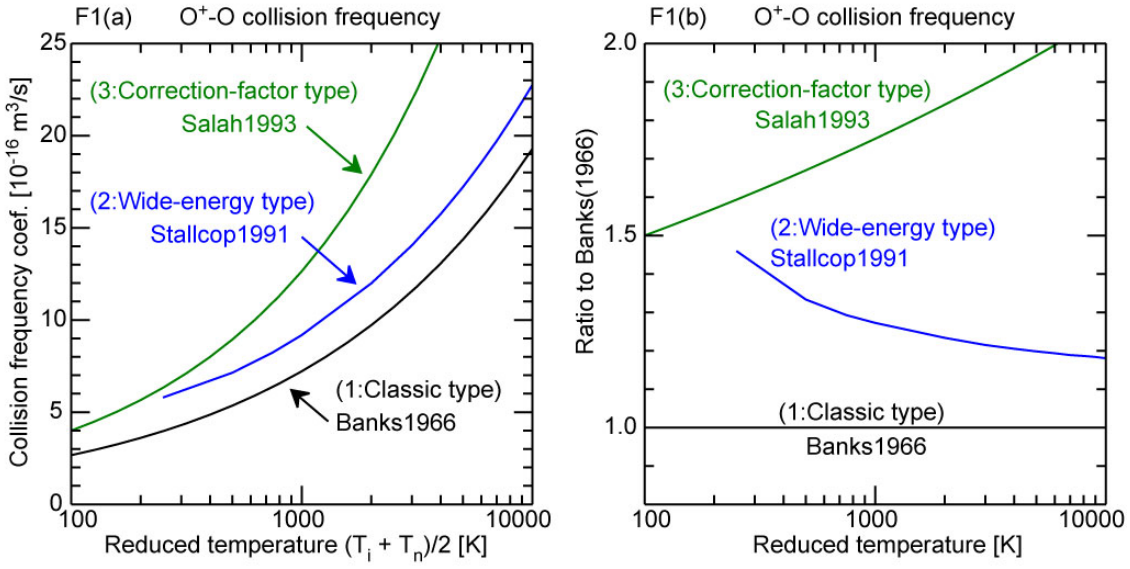

R005-57
Zoom meeting C ：11/3 AM2 (10:45-12:30)
11:30-11:45

# Statistical properties of ion upflows in the low-altitude ionosphere observed by the EISCAT radar

#Masayoshi Takada[1)], Kanako Seki[2)], Yasunobu Ogawa[3)]
[1)]Earth and Planetary Science, Tokyo Univ.,[2)]Dept. Earth & Planetary Sci., Science, Univ. Tokyo,[3)]NIPR

Molecular ions ($O_2^+$/$NO^+$/$N_2^+$) in the ring current of the terrestrial magnetosphere have been observed during the magnetic storms [e.g., Klecker et al., 1986; Seki et al., 2019]. Since the molecular ions usually exist in the low-altitude (< 300 km) ionosphere, an efficient upward ion transport (upflow) overcoming the loss by dissociative recombination is needed to supply them to the magnetosphere. However, the mechanisms that cause such an ion upflow at low-altitude are not clearly understood. As candidate mechanisms, some heating and acceleration processes such as ion frictional heating and small scale instabilities by soft particle precipitations have been investigated. Previous study showed that none of them was efficient enough [Peterson et al., 1994]. The purpose of this study is to understand properties of the ion upflows in the low-altitude ionosphere and their generation mechanisms based on long-term observational results of the EISCAT radars.

We used data from the EISCAT Svalbard radar at Longyearbyen from January 1, 2006 to January 1, 2016 and surveyed statistical properties of ion upflows in the low-altitude ionosphere. We selected data obtained at altitudes between 200 and 400 km, when the radar was looking along the local magnetic field line. Then, an ion upflow event was defined based on the following criteria: (1) Above the lowest altitude where the upward velocity becomes > 50 m/s, the flow velocity continues to be upward (> 0 m/s) up to 400 km altitude. (2) The average velocity between the lowest to 400 km altitudes is > 50 m/s. (3) An ion upflow event must continue for 2 minutes or more. The ion upflow events were identified in ~5 % of the selected field-aligned data in the 200-400 km altitude. The statistical results show that the ion upflows were observed during periods of relatively high AE index (> 200 nT), which means that geomagnetic activities affected the occurrence rate of ion upflows in the low-altitude ionosphere. On the other hand, the ion upflows were observed in the positive and negative SYM_H conditions. The result indicates that ion upflows were occurred both during the magnetic storms and non-storm periods. The most of the ion upflow events were observed when the average electron temperature exceeds 2000 K in the 200-400 km altitude. The detection probability of the ion upflow events become high when the average ion temperature was enhanced to more than 1500K in the 200-400 km altitude. It suggests that the electron temperature enhancement is a necessary condition for the ion upflow from the low-altitude ionosphere, while the ion temperature increase is also important to cause the upflows in many cases. In the presentation, we will also report on dependence of the ion upflows on the solar activities.

**References:**

[1] B. Klecker et al., Discovery of energetic molecular ions ($NO^+$ and $O_2^+$) in the storm time ring current, Geophys. Res. Lett., 13, 632-635, 1986
[2] K. Seki et al., Statistical Properties of Molecular Ions in the Ring Current Observed by the Arase (ERG) Satellite, Geophys. Res. Lett., 46, 8643?8651, 2019
[3] W. K. Peterson et al., On the sources of energization of molecular ions at ionospheric altitudes, J. Geophys. Res., 99(A12), 23,257-23,274, 1994

R005-58
Zoom meeting C ：11/3 AM2 (10:45-12:30)
11:45-12:00

## Modeling of EUV light scattered by oxygen ions and comparison with observation

#Shin'ya Nakano[1)], Yuta Hozumi[2)], Akinori Saito[3)]
[1)]The Institute of Statistical Mathematics,[2)]UEC,[3)]Dept. of Geophysics, Kyoto Univ.

An imager of ISS-IMAP observed extreme ultraviolet (EUV) at 83.4 nm, which is scattered by oxygen ions (O+), even in the umbra of the Earth. However, the single scattering of solar EUV radiation in the upper atmosphere does not well explain the observation. We are developing a computational model for simulating multiple scattering of EUV by O+ ions. This model simulates EUV flux using a Monte Carlo method in which trajectories of a large number of EUV photons are computed. The scattering cross section is determined according to the O+ distribution and ion temperature which are given by the IRI model. The change in the EUV frequency of a photon is assumed to obey a Gaussian distribution which is derived from thermal motion of O+ ions. For simplicity, the mean of this Gaussian distribution is assumed to be independent of the EUV frequency before the scattering.
We have simulated EUV flux in the ionosphere using our Monte Carlo model and compared with some observational results. At present, EUV flux is not necessarily well reproduced. However, some features of EUV flux on the nightside, which were observed by the EUV imager of ISS-IMAP, are reproduced by assuming a large scattering cross section. The prospect for estimating O+ density distribution will also be discussed.